

Distribution Agreement

In presenting this dissertation as a partial fulfillment of the requirements for an advanced degree from Emory University, I hereby grant to Emory University and its agents the non-exclusive license to archive, make accessible, and display my dissertation in whole or in part in all forms of media, now or hereafter known, including display on the world wide web. I understand that I may select some access restrictions as part of the online submission of this dissertation. I retain all ownership rights to the copyright of the dissertation. I also retain the right to use in future works (such as articles or books) all or part of this dissertation.

Betül Kacar

Aug 26th, 2009

Expression and Functional Characterization of Monoamine Oxidase from the
Zebrafish (*Danio Rerio*): Comparisons with Human Monoamine Oxidases A and B

By

Betül Kacar
Doctor of Philosophy
Department of Chemistry

Dale E. Edmondson, Ph.D.
Advisor

David Lynn, Ph.D.
Committee member

Stefan Lutz, Ph.D.
Committee member

Accepted:

Lisa A. Tedesco, Ph.D.
Dean of the Graduate School

2009

Expression and Functional Characterization of Monoamine Oxidase from the
Zebrafish (*Danio Rerio*): Comparisons with Human Monoamine Oxidases A and B

By

Betül Kacar
B.S., Marmara University, 2004

Advisor: Dale E. Edmondson, Ph.D.

An Abstract of
A dissertation submitted to the Faculty of the Graduate School of Emory University in
partial fulfillment of the requirements for the degree of
Doctor of Philosophy
in Chemistry

2009

Abstract

Expression and Functional Characterization of Monoamine Oxidase from the Zebrafish (*Danio Rerio*): Comparisons with Human Monoamine Oxidases A and B

By Betül Kacar

Monoamine Oxidases (MAO) are flavin containing enzymes located in the outer mitochondrial membrane. Mammals, including humans are shown to contain two forms of this enzyme as MAO A and MAO B. However, not all organisms contain two separate genes expressing these enzymes. Recent studies have shown that zebrafish, a popular teleost organism suitable for various pharmacological applications, contains a single MAO gene. It was proposed that human and teleost MAOs are co-orthologs and share a single common ancestor that underwent a gene duplication event. In addition, studies with whole zebrafish neural tissues have shown that zebrafish MAO exhibit properties closer to human MAO A. To test this hypothesis and to provide the first detailed characterization of zebrafish MAO (zMAO), we developed a high-level expression and purification system for zMAO where we could obtain 235 mg of protein from 0.5 L culture of *Pichia pastoris*. Then we performed the first detailed functional analysis of the protein with various MAO A and MAO B specific substrates and inhibitors. Here, we also present a comprehensive analysis of quantitative structure relationship of zMAO catalysis in comparison with the human MAO isoforms. Overall data suggest that zMAO contains the properties of both human MAO A and MAO B with properties closer to those of MAO A. The studies from this dissertation provide extensive analysis of this single form of the enzyme and are aimed to be helpful in the pharmacological studies that target designing better drugs targeting MAO using this zebrafish as a system.

Expression and Functional Characterization of Monoamine Oxidase from the
Zebrafish (*Danio Rerio*): Comparisons with Human Monoamine Oxidases A and B

By

Betül Kacar
B.S., Marmara University, 2004

Advisor: Dale E. Edmondson, Ph.D.

A dissertation submitted to the Faculty of the Graduate School of Emory University in
partial fulfillment of the requirements for the degree of
Doctor of Philosophy
in Chemistry

2009

*Isn't it strange how princes and kings,
and clowns that caper in sawdust rings,
and common people, like you and me,
are builders for eternity?*

*Each is given a list of rules;
a shapeless mass; a bag of tools.
And each must fashion, ere life is flown,
a stumbling block, or a Stepping-Stone.*

R.L. Sharpe

Acknowledgements

I have spent the last five years thinking of the day I start writing this thesis. During these years I faced many failures, many of which are not included here. Now I realize that those failures made the story told here, possible. So many people walked through with me in this journey, but out of these people, the one person I can't overstate my gratitude to is my Ph.D. advisor, Dr. Dale E. Edmondson. I am happy that I had you by my side over these years. Through your full optimism, encouragement and broad knowledge in chemistry and enzymology, I always knew that I am in safe hands. Thank you for believing in me, even when I did not believe in myself. I will forever be grateful for the opportunity you've given me and the way you changed my life.

I would like to thank Drs. David Lynn and Stefan Lutz, my committee members, for their good teaching and good company. Thanks to you, my committee meetings were always very constructive, enjoyable and motivational. Dave, talking to you even for five minutes charges me with so much inspiration. I will utterly miss talking about crazy and wild scientific ideas with you. Stefan, your energy, innovative suggestions and your sense of humor added colors to my graduate school life. Thank you for being very supportive at all times. I also wish to thank Dr. Patricia Marsteller. She has been my secret power source during graduate school years. Pat, you know what you mean to me. Thank you for revolutionizing my perception on science as a scientist and an educator.

I am thankful to all Edmondson lab members, for their friendship and support during the past five years. I would like to thank Jin Wang, Milagros Aldeco and Min Li for their technical help and friendship. My friends in graduate school; Hasan & Lorraine

Irier, Seth Childers, Lingfeng Liu, Anil Mehta, Zhanetta Astakhova, Karen Ventii, Michelle Miles and Yue Liu were always there for me, truly supported and encouraged me to push it harder, especially at times when I wanted to quit. I am only lucky to have friends like you. Thank you.

Finally, I would like to thank my family, especially my father Hayrettin and my mother Emine. This thesis is my gift to you. Thank you for trusting my decisions and for giving me the best that you could.

Lastly, and most importantly, to Murat; you supported me, you listened to me and you loved me. And I love you. Thank you.

Table of Contents

CHAPTER 1 – Introduction to Monoamine Oxidases

PART I: Human MAO A and MAO B.....	1
<i>1.1 Pharmacological Importance of MAO.....</i>	<i>1</i>
<i>1.1.1 Molecular Characteristics of Human MAO A and Human MAO B.....</i>	<i>2</i>
<i>1.1.2 Structural Analysis of Human MAO Isoforms.....</i>	<i>4</i>
<i>1.1.2.1 Flavin Binding Domain.....</i>	<i>10</i>
<i>1.1.2.2 Substrate Binding Domain.....</i>	<i>15</i>
<i>1.1.2.3 Membrane Binding Domain.....</i>	<i>19</i>
<i>1.1.3 MAO Substrates and the Amine Mechanism.....</i>	<i>21</i>
<i>1.1.4 Properties and Importance of MAO Inhibitors.....</i>	<i>26</i>
<i>1.1.4.1 Irreversible Inhibitors.....</i>	<i>27</i>
<i>1.1.4.2 Reversible Inhibitors.....</i>	<i>29</i>
PART II: Zebrafish MAO.....	34
<i>1.2 What makes Zebrafish MAO important?.....</i>	<i>34</i>
<i>1.2.1 Molecular Properties.....</i>	<i>34</i>
<i>1.2.2 Comparison to Human MAO A and MAO B.....</i>	<i>37</i>
<i>1.2.3 Importance of Zebrafish in Drug Development.....</i>	<i>43</i>
<i>1.3 Dissertation Objectives.....</i>	<i>44</i>

1.4 References.....	46
---------------------	----

CHAPTER 2 – High-level expression and purification of zebrafish monoamine oxidase in *Pichia pastoris*

2.1 Introduction.....	54
-----------------------	----

2.2 Materials and Methods.....	55
--------------------------------	----

2.2.1 Materials.....	55
----------------------	----

2.2.2 Cloning of zebrafish MAO.....	56
-------------------------------------	----

2.2.3 Transformation of zebrafish MAO gene into <i>P. Pastoris</i>	57
--	----

2.2.4 Expression of zebrafish MAO.....	57
--	----

2.2.5 Purification of zebrafish MAO.....	58
--	----

2.2.6 Determination of the Protein Content.....	61
---	----

2.2.7 Steady-State Kinetics.....	61
----------------------------------	----

2.2.8 Mass Spectroscopy.....	62
------------------------------	----

2.2.9 HPLC Separation.....	63
----------------------------	----

2.2.10 Fluorescence Studies.....	64
----------------------------------	----

2.2.11 Thermal Stability.....	64
-------------------------------	----

2.2.12 Oxygen Affinity.....	65
-----------------------------	----

2.2.13 Data Analysis.....	65
---------------------------	----

2.3 Results.....	65
------------------	----

2.3.1 Enzyme expression and purification.....	65
2.3.2 Characterization of Zebrafish MAO.....	67
2.3.3 Spectral Properties.....	68
2.3.4 Determination of the nature of the covalent linkage.....	71
2.3.5 Identification of the Flavin.....	75
2.3.6 Protein Sequence Analysis.....	76
2.3.7 Thermal Stability.....	78
2.3.8 Catalytic Properties.....	80
2.4 Discussion.....	83
2.5 References.....	87
CHAPTER 3 – Functional Analysis of Zebrafish MAO.....	91
3.1 Introduction.....	91
3.2 Materials and Methods.....	91
3.2.1 Materials.....	91
3.2.2 Preparation of Enzyme.....	92
3.2.3 Steady-state Kinetics Experiments.....	93
3.2.4 Competitive Inhibition.....	95
3.2.5 Data Analysis.....	95
3.2.6 Enzyme Functionality.....	95

3.3 Results.....	96
3.3.1 Steady-State Kinetic Properties for the zMAO.....	96
3.3.2 Competitive Inhibition.....	98
3.3 Summary.....	107
3.4 References.....	112
 CHAPTER 4 – Comparative Structure-Activity Relationships of Zebrafish Monoamine Oxidase	
4.1 Introduction.....	116
4.2 Materials & Methods.....	119
4.2.1 Materials.....	119
4.2.2 Preparation of the enzymes.....	120
4.2.3 Determination of kinetic parameters: k_{cat} , K_m and K_d	120
4.2.4 Steady state kinetic measurements of para- and meta- substituted benzylamine analogue oxidation.....	121
4.2.5 Steady state kinetic measurements of para- and meta- substituted phenylethylamine analogue oxidation.....	123
4.2.6 Data analysis.....	123
4.3 Results.....	124
4.3.1 Steady state kinetic measurements with para-substituted benzylamine analogues and the effects of isotopic substitution.....	124

4.3.5	<i>Steady state kinetic measurements with meta-substituted benzylamine analogues and the effects of isotopic substitution.....</i>	<i>126</i>
4.3.7	<i>Steady state kinetic measurements of para-substituted phenylethylamine analogues.....</i>	<i>129</i>
4.3.9	<i>Steady state kinetic measurements with meta-substituted phenylethylamine analogues.....</i>	<i>132</i>
4.3.	<i>Quantitative Structural Activity Relationships Describing zMAO Catalysis.....</i>	<i>134</i>
4.3.1	<i>QSAR in para- and meta- substituted benzylamine analogues binding to zMAO.....</i>	<i>138</i>
4.3.2	<i>QSAR in meta- and para- substituted phenylethylamine analogues binding to zMAO.....</i>	<i>144</i>
4.4	<i>Discussion.....</i>	<i>156</i>
4.4.1	<i>Overview of the QSAR Data.....</i>	<i>156</i>
4.4.1	<i>Mechanistic and Structural Interpretation.....</i>	<i>161</i>
4.5	<i>References.....</i>	<i>167</i>
	Chapter 5 – Conclusion & Future Work.....	170
5.1	<i>Summary of the Results.....</i>	<i>170</i>
5.2	<i>Reflections and Future Work.....</i>	<i>174</i>
5.3	<i>References.....</i>	<i>177</i>

List of Figures

Figure 1.1: <i>Monomeric structure of recombinant human liver MAO A</i>	6
Figure 1.2: <i>Structure of recombinant human liver MAO B</i>	7
Figure 1.3: <i>Recently solved crystal structure of MAO A</i>	8
Figure 1.4: <i>Dimeric structure of recombinant human liver MAO B</i>	9
Figure 1.5: <i>Structure of the two commonly found flavin cofactors</i>	12
Figure 1.6: <i>Characteristic UV-Vis absorption spectra for flavin cofactor</i>	13
Figure 1.7: <i>LIPLOT representation of the FAD binding site and the surrounding residues of MAO B</i>	14
Figure 1.8: <i>Structure of the Ile199 gate in human MAO A and MAO B</i>	16
Figure 1.9: <i>Schematic representation of the binding site in human MAO B with the irreversible inhibitor Pargyline</i>	17
Figure 1.10: <i>Detailed view of the MAO A binding site with the inhibitor Harmine</i>	18
Figure 1.11: <i>C-terminal membrane-binding domain of human MAO A and human MAO B</i>	20
Figure 1.12: <i>Concerted-Nucleophilic Attack Mechanism</i>	25
Figure 1.13: <i>Structures of Acetylenic MAO Inhibitors</i>	26
Figure 1.14: <i>Structures of N-propargyl-aminoindan analogues</i>	28
Figure 1.15: <i>Structures of Hydrazine Inhibitors</i>	29

Figure 1.16: Structures of reversible MAO inhibitors used in this study.....	31
Figure 1.17: Structure of Human MAO B in complex with 1,4-diphenyl-2-butene.....	32
Figure 1.18: Phylogenic tree showing evolutionary history of MAO.....	35
Figure 1.19: Phylogenetic tree of Monoamine Oxidases showing the separation of mammals from teleosts.....	36
Figure 1.20: Multiple sequence alignment of zMAO, human MAO A and B.....	38
Figure 2.1 Representation of the zMAO gene before incorporation into the TOPO plasmid.....	56
Figure 2.2 SDS-polyacrylamide gel electrophoresis of purified zMAO and hMAO A.....	68
Figure 2.3: (A) UV-Vis spectra of purified zMAO before and after the addition of 10-fold molar excess of MAO B specific deprenyl (B) Time course inhibition of zMAO with deprenyl.....	69
Figure 2.4: (A) UV-Vis spectra of purified zMAO before and after the addition of 10-fold molar excess of clorgyline (B) Time course inhibition of zMAO by MAO A specific clorgyline.....	70
Figure 2.5: Fluorescence emission spectrum of liberated zMAO flavin peptide and HPLC elution profile of the flavinylated peptide at 350 nm.....	74
Figure 2.6: Comparision of thermal stability of human MAO A and zebrafish MAO.....	79
Figure 2.7: Lineweaver-Burk plot of the effect of [O ₂] on rate of zMAO oxidation of benzylamine.....	81
Figure 3.1: Chemical structures of MAO A specific inhibitors.....	102

Figure 3.2: <i>Ultraviolet-visible absorption spectra of Zebrafish MAO before and after the addition of rasagiline</i>	106
Figure 3.6: <i>(A) Comparison of the UV-Visible absorption spectra of human MAO A, human MAO B (B) and zMAO phenylethylhydrazine inhibition</i>	108
Figure 4.1: <i>Chemical structures of MAO substrates benzylamine and phenylethylamine</i>	120
Figure 4.2: <i>Correlation of steady state rates of zMAO and human MAO A k_{cat} values with the substituent electronic parameter (σ)</i>	135
Figure 4.3: <i>Correlation of calculated binding affinities of p-benzylamine analogues for zMAO and the substituent electronic parameter (σ)</i>	137
Figure 4.4: <i>Quantitative structure activity relationships describing the turnover rate of para-substituted benzylamine analogues under saturated oxygen</i>	139
Figure 4.5: <i>Quantitative structure activity relationships describing the binding of para-substituted benzylamine analogues and the effects of isotopic substitution under saturated oxygen</i>	139
Figure 4.6: <i>Quantitative structure activity relationships describing the binding of meta-substituted benzylamine analogues are shown for human MAO B</i>	143
Figure 4.7: <i>Quantitative structure activity relationships describing the steady state turnover rates of para-substituted phenylethylamine analogues with zebrafish MAO</i>	145
Figure 4.8: <i>Quantitative structure activity relationships describing the binding of para-substituted phenylethylamine analogues to zebrafish MAO</i>	146
Figure 4.9: <i>Quantitative structure activity relationships describing the binding of para-substituted phenylethylamine analogues to human MAO B</i>	148

Figure 4.10: *Quantitative structure activity relationships describing the binding of meta-substituted phenylethylamine analogues to zebrafish MAO.....151*

Figure 4.11: *Quantitative structure activity relationships describing the binding of meta-substituted phenylethylamine analogues to human MAO A.....155*

Figure 4.12: *Quantitative structure activity relationships describing the binding of meta-substituted phenylethylamine analogues to human MAO B.....158*

Figure 4.13 *Model representation of the relative conformations of para-substituted benzylamine analogues bound to MAO A and MAO B.....163*

List of Tables

Table 1.1: <i>Chemical structures of the MAO substrates</i>	24
Table 1.2: <i>Summary of MAO Inhibitors and their K_i values</i>	33
Table 1.3: <i>An overview analysis zebrafish MAO</i>	39
Table 1.4: <i>MAO A residues in contact with ligand flavin</i>	41
Table 1.5: <i>Comparative sequence analysis of zebrafish MAO with human MAO isoforms</i>	42
Table 2.1: <i>Purification Scheme for zebrafish MAO expressed in Pichia pastoris</i>	67
Table 2.2: <i>Reconstitution of the apo-glucose oxidase activity</i>	76
Table 2.3: <i>Mass profile of the recovered peptide for tryptic-digested zMAO</i>	77
Table 2.4: <i>Representation of the identified peptides of zMAO</i>	77
Table 2.5: <i>Steady state kinetic parameters of zebrafish MAO measured under air saturation and saturated oxygen</i>	82
Table 3.1 <i>Wavelength and the extinction coefficient values of the substrates</i>	93
Table 3.2 <i>Comparison of steady-state kinetics values for zMAO, human MAO A, and human MAO B</i>	97
Table 3.3 <i>Comparison of zMAO with human MAO A specific inhibitors</i>	98
Table 3.4: <i>Comparison of zMAO with MAO B inhibitors</i>	99
Table 3.5: <i>K_i values and the structures of the aminoindan (AI) analogues tested with zMAO, in comparison to human isoforms</i>	101

Table 3.6: <i>Inhibition values for MAO B specific rasagiline.....</i>	<i>102</i>
Table 3.7: <i>Comparison of zMAO inhibition by arylalkylhydrazines with human MAO A and B.....</i>	<i>104</i>
Table 3.8: <i>Inhibition profile of zMAO with amphetamine.....</i>	<i>107</i>
Table 3.9: <i>Comparison of $\ln(k_{cat}/K_m)$ ($\text{min}^{-1} \text{mM}^{-1}$) for zMAO and human MAO isoforms using various substrates.....</i>	<i>108</i>
Table 3.10: <i>K_i (μM) inhibition ratio values zMAO with MAO A, MAO B and non-specific inhibitors.....</i>	<i>111</i>
Table 4.1 <i>Overall view of the equations used in QSAR studies.....</i>	<i>118</i>
Table 4.2 <i>Explanation of the parameters in Hansch equation used in QSAR studies....</i>	<i>118</i>
Table 4.3 <i>Extinction coefficients for para- and meta- substituted benzylamine substrates.....</i>	<i>122</i>
Table 4.4 <i>Effect of para-substitution on the kinetic properties of zMAO oxidation by various benzylamine analogues.....</i>	<i>127</i>
Table 4.5: <i>Comparison of the steady-state rates of hMAO A, hMAO B and zMAO catalyzed α, α-^1H-m-substituted benzylamines.....</i>	<i>128</i>
Table 4.6: <i>Steady-state kinetic constants for the human MAO B catalyzed oxidation of m-substituted benzylamine analogues.....</i>	<i>128</i>
Table 4.7: <i>Steady-state kinetic constants for the zMAO catalyzed oxidation of p-substituted phenylethylamine analogues.....</i>	<i>130</i>
Table 4.8: <i>Steady-state kinetic constants for the human MAO B catalyzed oxidation of p-substituted phenylethylamine analogues.....</i>	<i>131</i>

Table 4.10: <i>Steady-state kinetic constants for the zMAO catalyzed oxidation of m-substituted phenylethylamine analogues</i>	133
Table 4.11: <i>Steady-state kinetic constants for the hMAO A catalyzed oxidation of m-substituted phenylethylamine analogues</i>	133
Table 4.12: <i>Steady-state kinetic constants for the hMAO B catalyzed oxidation of m-substituted phenylethylamine analogues</i>	134
Table 4.13: <i>Effects of para-substitution on the kinetic properties of zMAO oxidation by various benzylamine analogues under saturated oxygen</i>	138
Table 4.14: <i>Correlation Analysis of $\log k_{cat}$ with Hydrophobic, Steric and Electronic Parameters in the Interaction of meta-substituted benzylamine analogues with zebrafish MAO</i>	140
Table 4.15: <i>Correlation Analysis of $\log k_{cat}$ with Hydrophobic, Steric and Electronic Parameters in the Interaction of meta-substituted benzylamine analogues with human MAO A</i>	141
Table 4.16: <i>Correlation Analysis of $\log k_{cat}$ with Hydrophobic, Steric and Electronic Parameters in the Interaction of meta-substituted benzylamine analogues with human MAO B</i>	142
Table 4.17: <i>Correlation Analysis of $\log K_d$ with Hydrophobic, Steric and Electronic Parameters in the Interaction of meta-substituted benzylamine analogues with human MAO B</i>	142
Table 4.18: <i>Correlation Analysis of $\log k_{cat}$ with Hydrophobic, Steric and Electronic Parameters in the Interaction of para-substituted phenylethylamine analogues with zebrafish MAO</i>	144

Table 4.19: <i>Correlation Analysis of $\log K_d$ with Hydrophobic, Steric and Electronic Parameters in the Interaction of para-substituted phenylethylamine analogues with zebrafish MAO</i>	146
Table 4.20: <i>Correlation Analysis of $\log k_{cat}$ with Hydrophobic, Steric and Electronic Parameters in the Interaction of para-substituted phenylethylamine analogues with human MAO B</i>	147
Table 4.21: <i>Correlation Analysis of $\log K_d$ with Hydrophobic, Steric and Electronic Parameters in the Interaction of para-substituted phenylethylamine analogues with human MAO B</i>	149
Table 4.22: <i>Correlation analysis of $\log k_{cat}$ with hydrophobic, steric and electronic parameters in the interaction of meta-substituent phenylethylamine analogues with zebrafish MAO</i>	150
Table 4.23: <i>Correlation analysis of $\log k_{cat}$ with hydrophobic, steric and electronic parameters in the interaction of meta-substituted phenylethylamine analogues with human MAO A</i>	152
Table 4.24: <i>Correlation analysis of $\log K_d$ with hydrophobic, steric and electronic parameters in the interaction of meta-substituted phenylethylamine analogues with human MAO A</i>	152
Table 4.25: <i>Correlation analysis of $\log k_{cat}$ with hydrophobic, steric and electronic parameters in the interaction of meta-substituted phenylethylamine analogues with human MAO B</i>	154
Table 4.26: <i>Correlation analysis of $\log K_d$ with hydrophobic, steric and electronic parameters in the interaction of meta-substituted phenylethylamine analogues with human MAO B</i>	155
Table 4.27: <i>Summary of QSAR parameters effective on zMAO, hMAO A and hMAO B</i>	157

Table 4.28: *Correlation of QSAR parameters and their constants for zebrafish MAO and human MAO isoforms to k_{cat}160*

Table 4.29: *Correlation of QSAR parameters and their constants for zebrafish MAO and human MAO isoforms to binding constant.....160*

List of Schemes

Scheme 1.1: <i>General reaction scheme of MAO</i>	21
Scheme 1.2: <i>Reaction pathway for MAO B catalysis</i>	23
Scheme 1.3: <i>Reaction pathway for MAO A catalysis</i>	23
Scheme 1.4: <i>Equation used for the QSAR studies</i>	26
Scheme 2.1 <i>Representation of the system that is maintained during column purification of zMAO</i>	59
Scheme 2.2 <i>Proposed mechanism for elimination of the 8α-cysteinylsulfone to form unsubstituted flavin</i>	73
Scheme 2.3: <i>Incubation of FAD with inactive apo-Glucose Oxidase (apoGO) results as the active holo-Glucose Oxidase</i>	75

List of Equations

Equation 4.1.....	135
Equation 4.2.....	136
Equation 4.3.....	140
Equation 4.5.....	144
Equation 4.6.....	145
Equation 4.7.....	147
Equation 4.8.....	147
Equation 4.9.....	149
Equation 4.10.....	149
Equation 4.11.....	151
Equation 4.12.....	151
Equation 4.13.....	154
Equation 4.14.....	154
Equation 4.15.....	154

CHAPTER 1

INTRODUCTION

“When a mystery is too overpowering, one dare not disobey.”

Antoine de Saint Exupéry, The Little Prince

PART I: Human MAO A and MAO B

1.2 Pharmacological Importance of MAO

In 1928, Dr. Mary Hare discovered an enzyme in the liver that catalyzes the deamination of tyramines which she subsequently named Tyramine Oxidase (Hare 1928). Hare eventually discovered that this enzyme could deaminate not only tyramines but also a variety of primary amines; and renamed the enzyme as monoamine oxidase (MAO) (E.C. 1.4.3.4). Shortly afterwards, it was found that MAO plays an important role in mood regulation, and in 1975, the CIBA foundation honored Dr. Mary Hare's discovery, as "one of the seminal discoveries in twentieth century neurobiology." (Bernheim 1984)

In 1988, two forms of MAO were found in mammals and were named MAO A and MAO B, respectively (Bach, Lan et al. 1988) . MAO A and B are located on the outer mitochondrial membrane and they belong to a protein family of flavin-containing amine oxidoreductases (Akopyan, Veryovkina et al. 1971). Despite their ~70% sequence identity, the enzymes differ in substrate and inhibitor selectivity. Both enzymes contain a covalently attached flavin cofactor that is linked via an 8 α -S-cystenyl linkage (Weyler 1989) (Figure 4). MAO enzymes catalyze the oxidative deamination of several monoamines, which leads to production of hydrogen peroxide, the corresponding aldehyde and either ammonia (from primary amines) or a substituted amine (from

secondary amines) (Scheme 1). Because of the crucial role that MAO enzymes play in the degradation of neurotransmitters, MAO dysfunction is proposed to be responsible for a number of neurological disorders, making these enzymes pharmacologically important (Fowler 1998) (Edmondson 2009)

1.2.1 Molecular Characteristics of Human MAO A and MAO B

Two genes with ~70% sequence similarity encode human MAO A and MAO B and are located side-by-side on the short arm of the X chromosome (Xp 11.23 – 11.4) (Lan, Chen et al. 1989). A single mutation on MAO A gene leads to impulsive behavior and mental retardation, known as Brunner Syndrome (Mc Dermott Rose 2009). Higher or lower MAO A expression and activity have been associated with depression, substance abuse, attention deficit disorder, aggressive behavior and irregular sexual maturation. A study reported in *Science* magazine in August 2002 demonstrated that maltreated children with a low-activity polymorphism in the promoter region of the MAO A gene are more likely to develop antisocial behavior than maltreated children with the high-activity MAO A variant (Caspi A 2002). A particular MAO A genotype (named as warrior gene) causing violent and dominant behavior is over-represented in Māori society of New Zealand (Lea 2007) and males with low levels of MAO A tend to be more revengeful (Mc Dermott Rose 2009). In these studies, maltreatment was found to cause a stronger propensity for antisocial behavior together with the low MAO A activity. This is a rare example of environmental affects on gene expression and human behavior.

Another interesting aspect of MAO A comes from cardiac research (Bianchi 2005). It has been found that the hearts of aged rats contain high-levels of MAO A (~9 fold), similar to

humans who have increased MAO A levels with age (Maurel 2003). Increased MAO levels produce increased levels of reactive oxygen species, which leads to cell apoptosis and necrosis of cardiac cells (Bianchi 2005). Therefore, clarification of the role of MAO A in cardiac cell degeneration is pharmacologically important and remains to be determined.

MAO B, on the other hand, is thought to play significant roles in neurological diseases such as Parkinson's and Alzheimer's. It has been shown that human brain MAO B activity increases 4-5 fold with age, leading to the increase of its by-product hydrogen peroxide and consequent cell apoptosis (Fowler 1980) (Wolf. 1991). Additionally in 1998, a population-based case study showed the association of cigarette smoking in relation to lower MAO B activity (Checkoway 1998).

MAO B expression is associated with specific human disorders as well. Earlier studies have shown gender-based differences in MAO B activity, women have approximately 30% higher MAO B platelet activity than men, possibly due to MAO B acting as an X-chromosome linked predisposing factor (Sandler 1981). Gender-related differences of MAO activity is seen in alcoholic men who have lower MAO (~40%) activity than alcoholic women (Coccini 2002). Furthermore, studies have shown that estrogen-related receptor alpha (ERR) up-regulates MAO B gene expression in breast cancer cells (Zhang 2006).

Overall, these findings validate the requirement for MAO regulation for human health and the importance of monoamine oxidase inhibitors (MAOI). MAOIs have been developed for the regulation of MAO and are prescribed as one of the major classes of

drug used for the treatment of depression. Initially developed irreversible MAOIs were shown to have a variety of side effects, such as the “cheese effect”. A first generation MAOI (specifically a MAO A inhibitor) was found to cause a substantial increase of tyramine in the blood. In return, patients using this MAOI together with tyramine rich food (like cheese and/or wine) were faced with hypertension (Youdim 2004). Eventually, the case was named as the “cheese effect” and is still a good example of the dietary restrictions of MAOIs. To date, due to the requirement of strict dietary regulations and the potency of drug-drug interactions, MAOIs are used as a last-line treatment. Therefore, it is of interest to develop the MAO research field to provide better and improved drugs.

1.1.2 Structural Analysis of Human MAO Isoforms

The lack of structural information on the human MAO enzymes resulted in difficulties in designing effective and specific MAOIs for decades (Edmondson, Mattevi et al. 2004). The main obstacles behind this lack of progress were the membrane bound nature of these two proteins and difficulties in separating the two forms from natural state. Therefore, the high-level expression and purification system developed in the Edmondson Lab in the beginning of 2000s was revolutionary (Newton-Vinson 2000; Li 2002) and led to the establishment of purified protein with higher solubility and stability in detergent. Together with a collaboration with Mattevi Lab in Pavia, Italy, the crystal structures of human MAO A (3.0 Å³) (De Colibus 2005) and human MAO B (3.0 Å³) (Binda 2002) were first reported. Subsequent work led to a 1.65 Å³ structure for MAO B and a 2.2 Å³ structure for human MAO A (Son 2008). Availability of these high-resolution crystal structures has provided an increased understanding of the functions,

similarities and differences of these outer mitochondrial membrane enzymes. At first glance, one main difference between human MAO A and MAO B is their oligomeric states. While human MAO A crystallizes as a monomer (Figure 1.1,1.3) (De Colibus 2005), human MAO B crystallizes as a dimer (Figure 1.2,1.4) (Binda 2004) with each monomeric unit containing a flavin (FAD) binding domain, a substrate binding domain and a membrane anchoring domain (Figure 1.1, Figure 1.2). A recent study by Edmondson's Lab using pulsed EPR analysis demonstrated that both proteins are dimeric in their membrane bound forms (Upadhyay, Borbat et al. 2008). Overall, the distinctive conformations of the catalytic sides in each human MAO accounts for their discrete (and overlapping) substrate and inhibitor specificities.

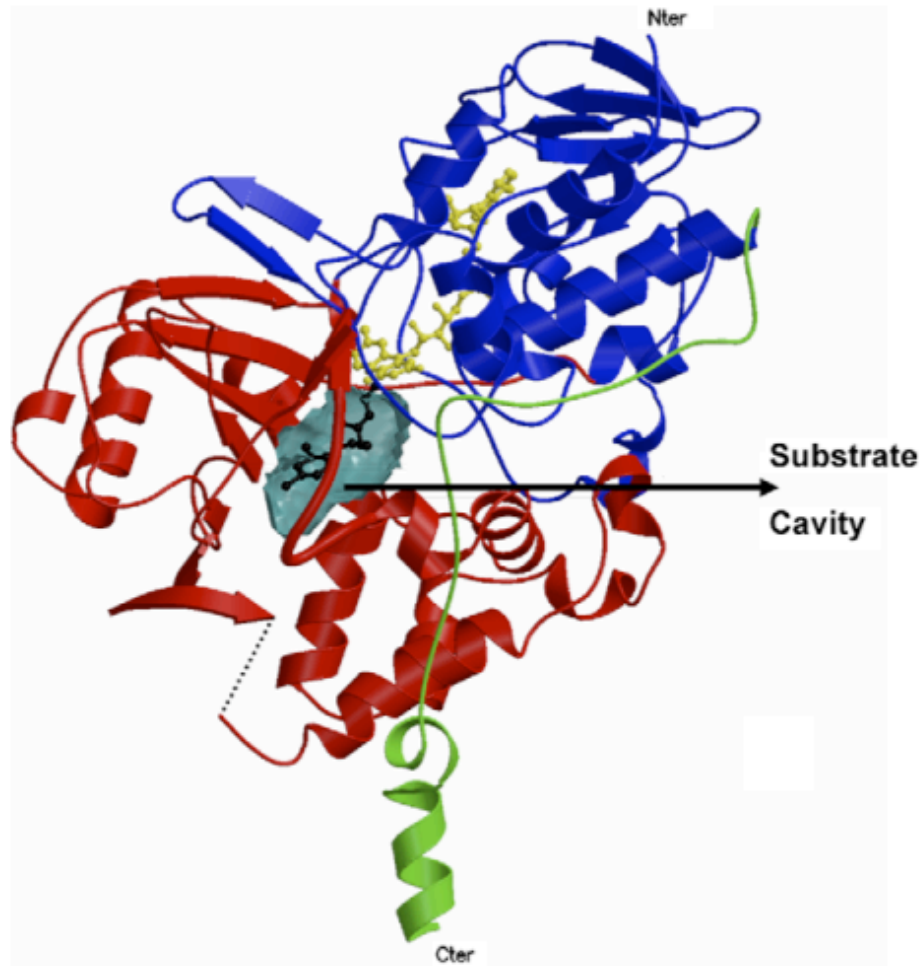


Figure 1.1: Monomeric structure of recombinant human liver MAO A

Figure adapted from (De Colibus 2005), Copyright (2005) National Academy of Sciences, U.S.A.

The color code is the same as Figure 1.2: FAD is shown in yellow; the FAD binding domain is in blue, substrate-binding domain is in red. Human MAO A contains a monopartite cavity, consisting of a single hydrophobic cavity in the active site. Cavity is shown in cyan in the figure (*PDB ID code 2BXR*).

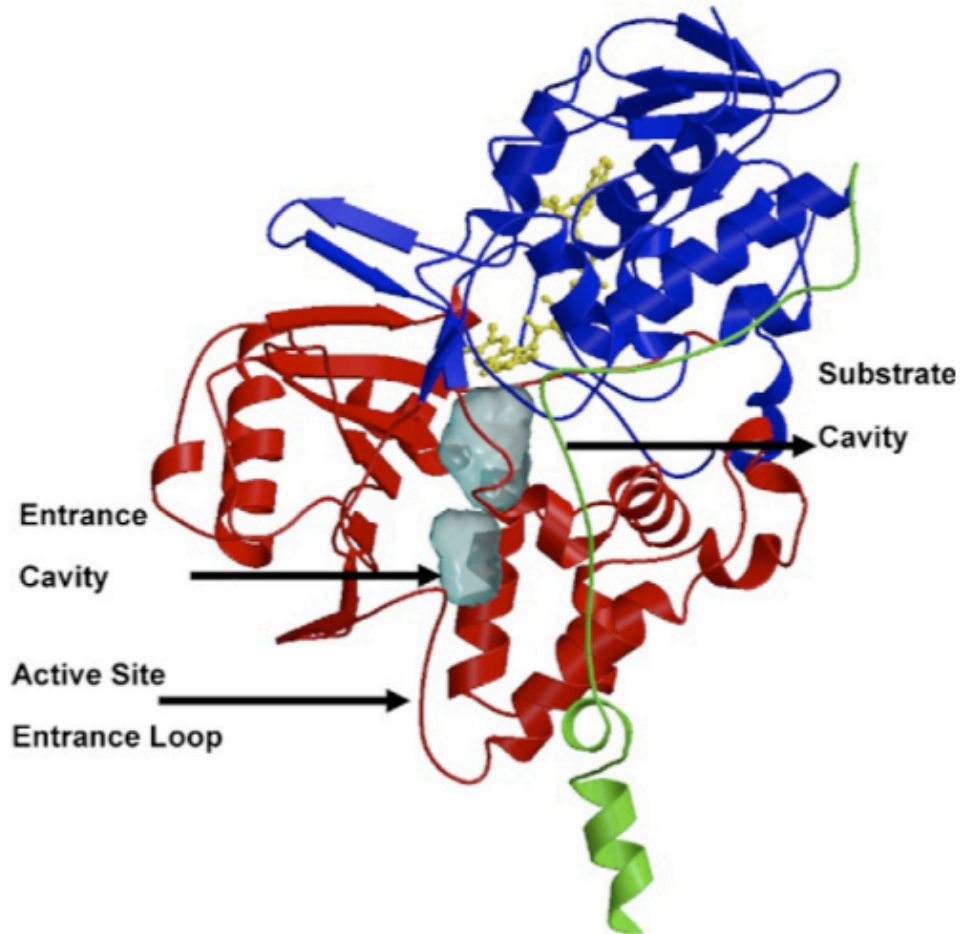


Figure 1.2: Structure of recombinant human liver MAO B.

Reprinted by permission from Macmillan Publishers Ltd: [Nature Structural Biology] (Binda 2002) Copyright 2001.

Adjacent to the active site cavity (cyan) is the “entrance” cavity (blue). MAO B contains two cavities as the “entrance cavity” and the “substrate cavity”. Color code is same as in the previous figure. The FAD is shown in yellow. The covalent pargyline inhibitor is in black. “N-ter” and “C-ter” indicate the observed N-terminal and C-terminal amino acids, respectively. The FAD-binding domain (residues 4-79, 211-285, 391-453) is in blue, the substrate-binding domain (residues 80-210, 286-390, 454-488) is in red, and the C-terminal membrane binding region (residues 489-500) is in green. Only one subunit of the dimeric structure is shown (*PDB ID Code 1GOS*).

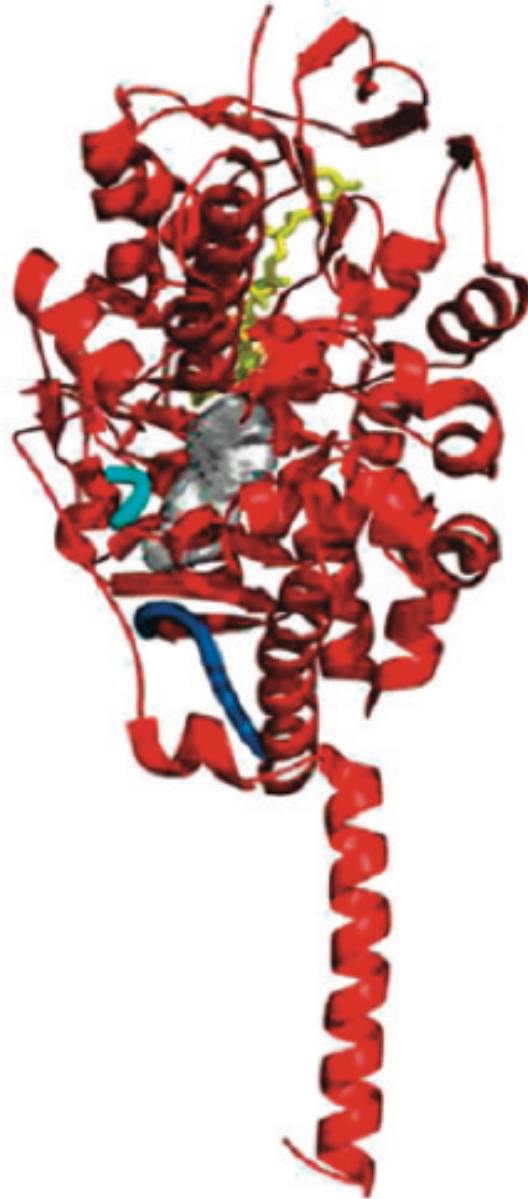


Figure 1.3: Recently solved crystal structure of human MAO A (Son 2008).
Copyright (2008) National Academy of Sciences, U.S.A.

Flavin is represented in yellow, active site pocket is in gray, and the cavity-shaping loop is shown in cyan. The C-terminal membrane helix is pointed downwards (*PDB ID Code 2Z5X*).

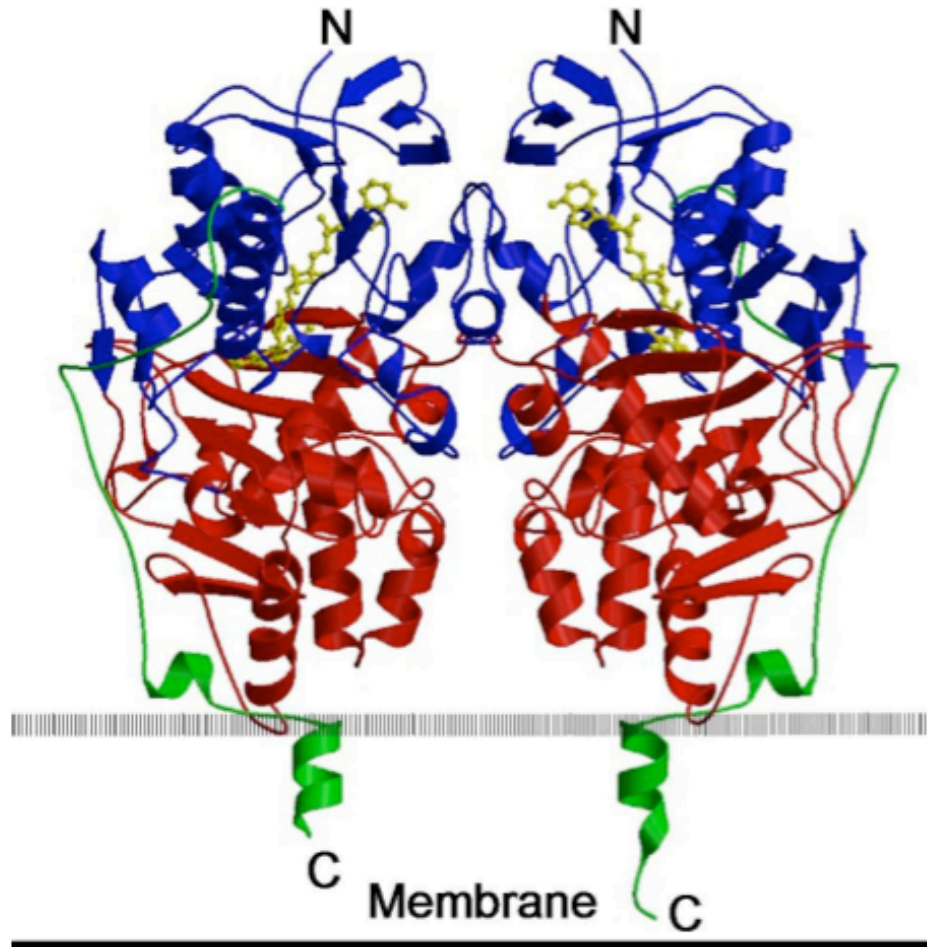


Figure 1.4: Dimeric structure of recombinant human liver MAO B.

*Reprinted by permission from Macmillan Publishers Ltd: [[Nature Structural Biology](#)] (Binda 2002)
Copyright 2001.*

The FAD is shown in yellow; the FAD-binding domain is in blue; the substrate-binding domain is in red and the C-terminal membrane-binding region is shown in green and is inserted into membrane (*PDB ID Code 1GOS*).

1.1.2.1 Flavin Binding Domain

Flavin refers to the yellow chromophores that are common in organisms ranging from bacteria to humans (Ghisla 1971). These chromophores are essential for a variety of metabolic processes and they undergo reversible one- or two-electron oxidation-reduction reactions (Ghisla 1989). There are two main flavin cofactors, FAD (flavin-adenine dinucleotide) and FMN (flavin mononucleotide) (Figure 1.5). FAD is the conjugation of FMN with an AMP (adenosine monophosphate) molecule. Monoamine Oxidases contain a covalently attached FAD cofactor, while many other flavoproteins may contain a non-covalently linked FAD or FMN (Edmondson 1999). Different flavin oxidation - reduction states lead to different UV-Vis absorption spectra (Figure 1.6).

As seen in the crystal structures of human MAOs, FAD is attached to the enzyme via a cysteine thio-ether (Cys-406 in MAO A and Cys-397 in MAO B), specifically through an 8α -S-Cysteinyl bound. The presence of the cysteine is crucial for the enzyme. A mutation of Cys-406 to an Ala in rat liver MAO A leads to non-covalent FAD and exhibits ~50% catalytic activity in comparison to the wild type (Hiro 1996). A Cys397Ser mutation in human liver MAO B leads to inactive enzyme (Zhou 1998). Similarly, human MAO A Cys406Ala and human MAO B Cys397Ala results as apo-enzyme, whose activity can be restored with FAD incorporation but not FMN or riboflavin (Nandigama and Edmondson 2000) (Miller and Edmondson 1999).

Another interesting feature of the FAD cofactor is its “bent” form. In the crystal structures of both oxidized and inhibitor bound forms of MAOs, the inhibitors bind to the N5 atom on the re-side of the cofactor (Binda 2002) (De Colibus 2005). This bent flavin ring found in both oxidized and N(5) alkyl and C(4a) alkyl forms of the enzyme is a unique property among flavoenzyme oxidases. The requirement for such a specific flavin conformation needs further investigation.

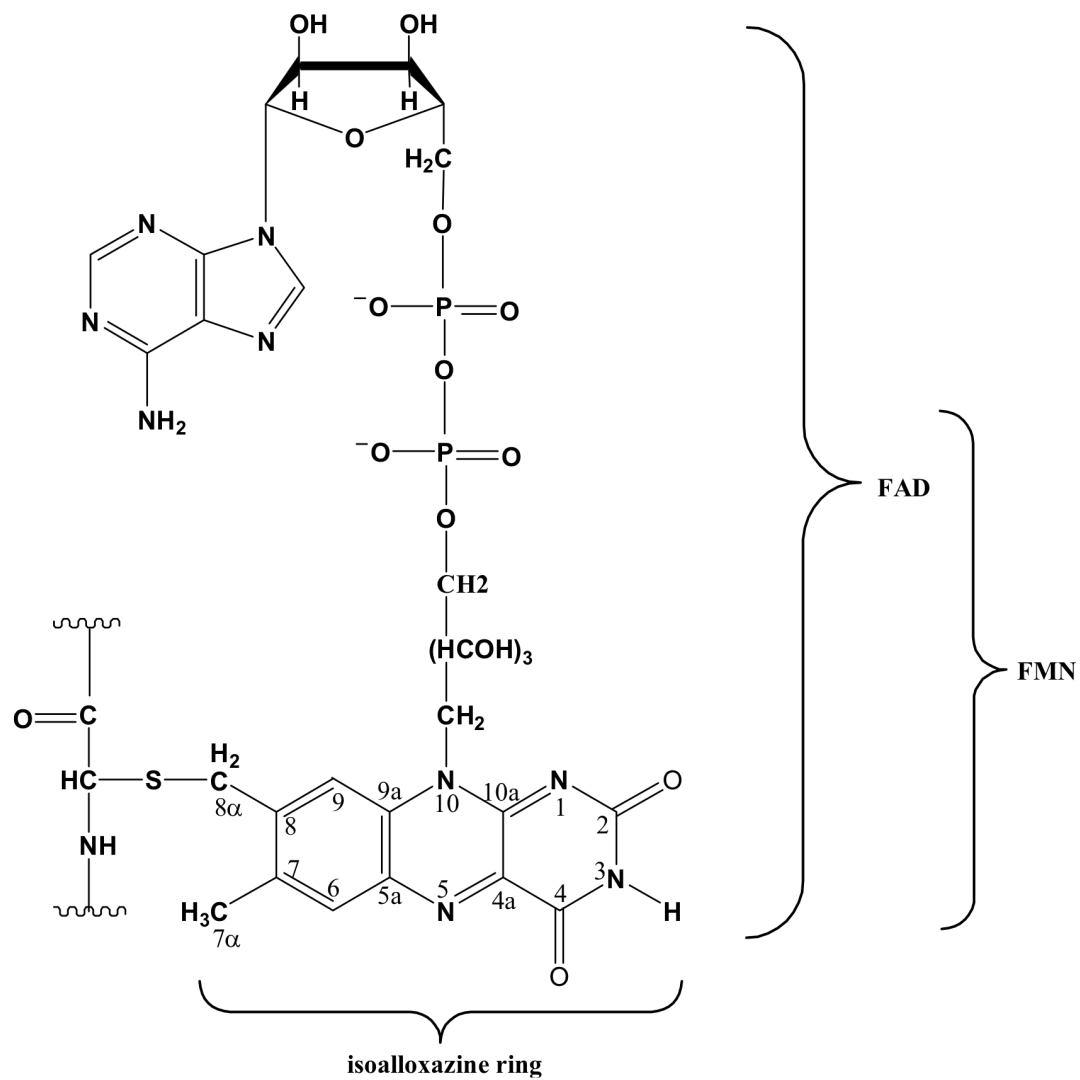


Figure 1.5: Structure of the two commonly found flavin cofactors in flavoproteins

Flavin cofactor, FAD is covalently attached to either MAO enzymes. Oxidation reaction is taking place on the isoalloxazine ring portion of the cofactor. In MAOs, FAD is linked to the enzyme via an 8α -S-Cysteinyl bond.

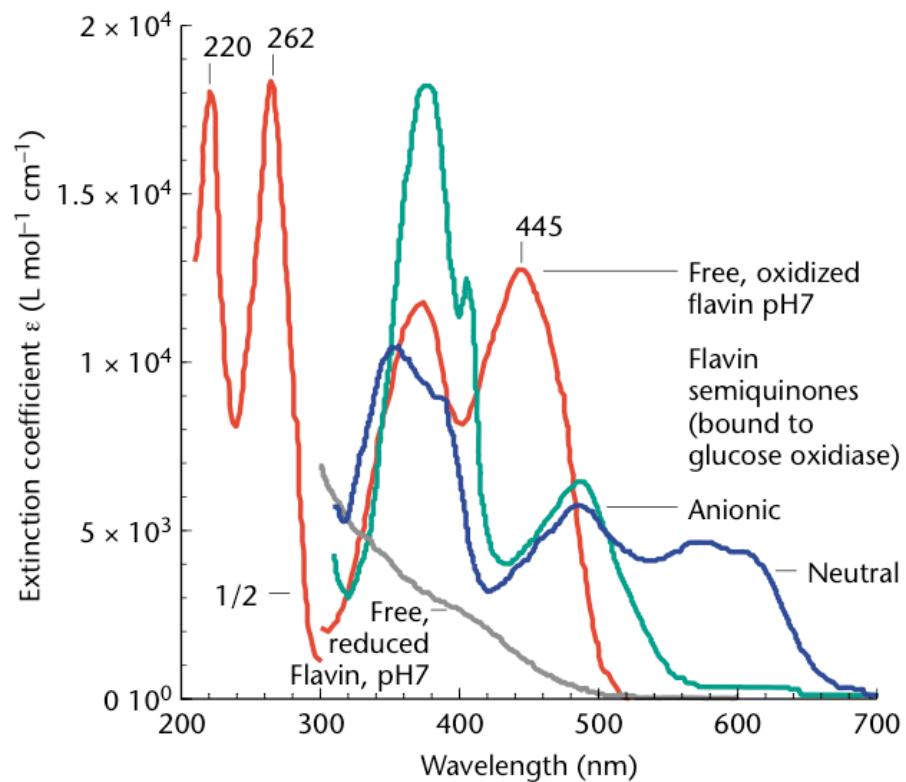


Figure 1.6: Characteristic UV-Vis absorption spectra for flavin cofactor (Edmondson 1999).
(with kind permission of Springer Science and Business Media).

MAOs exhibit an anionic flavin semiquinone. Upon MAO reaction with the substrate, the flavin gets reduced. For reoxidation, the reduced flavin donates electrons to the oxygen molecule

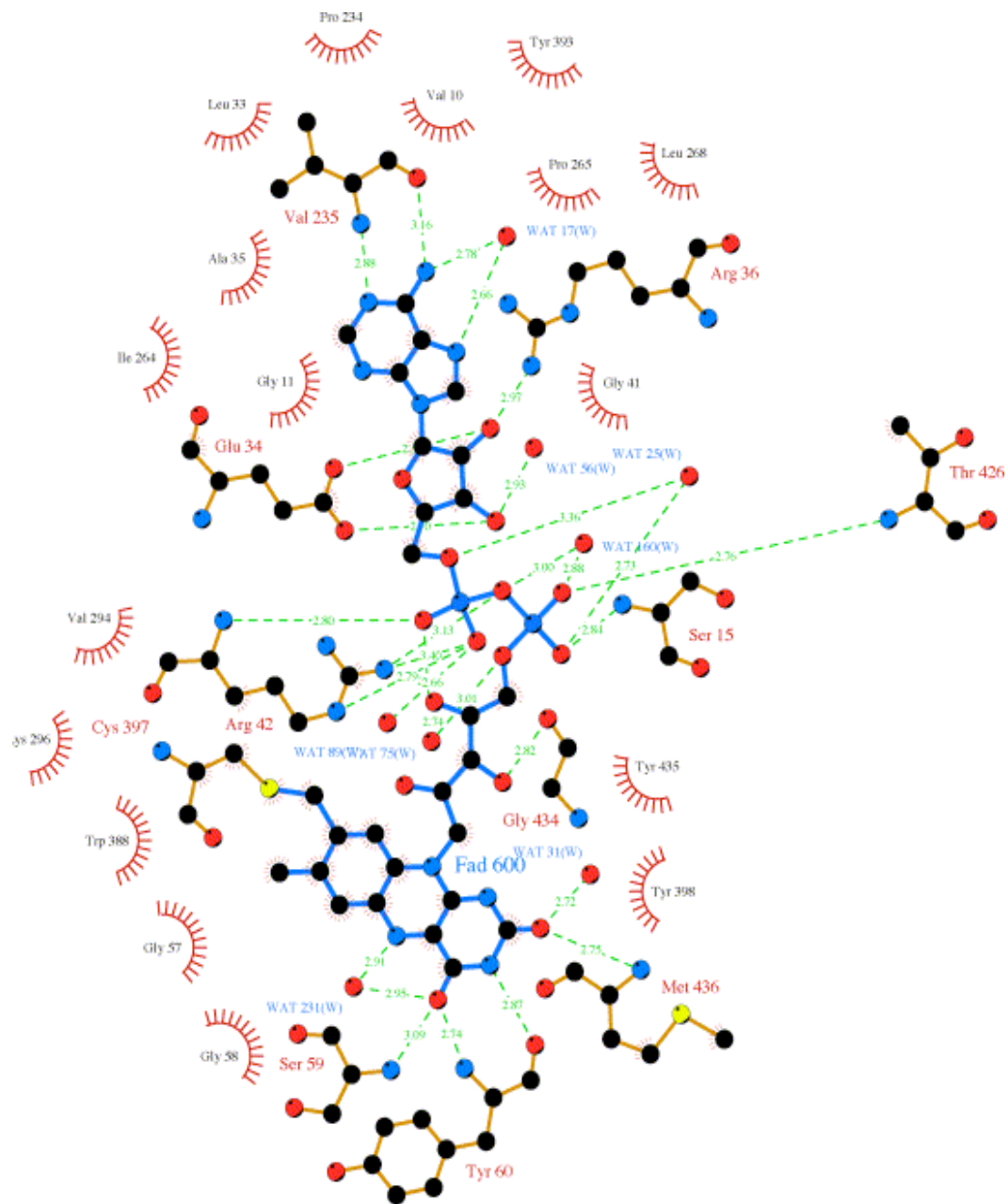


Figure 1.7: LIGPLOT representation of the FAD binding site and the surrounding residues of MAO B.

The dashed lines represent the hydrogen bonds, nitrogens in blue, oxygens in red, carbons are in black and sulfurs are cyan spheres. *This figure was published in (Edmondson 2004), Copyright (2004) Elsevier.*

1.1.2.2 Substrate Binding Domain

One interesting feature of the human MAO A and MAO B is their distinct substrate binding domains. While human MAO A consists of a single hydrophobic cavity (550 Å³); human MAO B contains a dipartite cavity as the substrate cavity (adjacent to the flavin cofactor, 420 Å³) and the entrance cavity (facing the membrane surface, 290 Å³). The hydrophobic cavity is shielded from solvent exposure by a cavity-shaping loop, region 210-216 for MAO A and 201-207 for MAO B respectively (Edmondson 2009) (Figure 1.8).

Residues Phe168, Leu171, Ile199 and Tyr326 serve as a “gate” between the two cavities of MAO B for the diffusion of the substrates, whereas there is no gate formation in human MAO A (Figure 1.8). Among these residues, Ile199 in human MAO B has shown to have a particular role on the selectivity of the enzyme’s substrate/inhibitors and was assigned as the “gate switch” as it changes its conformation from “closed” to “open” upon the inhibitor’s binding with the following bulky inhibitors: 8-(3-chlorostyryl) caffeine, 1,4-diphenyl-2-butene, safinamide and *trans,trans*-farnesol (Figure 1.16) (Hubalek 2005). In comparison, MAO A contains a Phe in the corresponding position of Ile199, an Ile in place of Tyr326, Asn in place of Cys172 and Ile in place of Leu171 (Figure 1.9).

Substrate Domain:

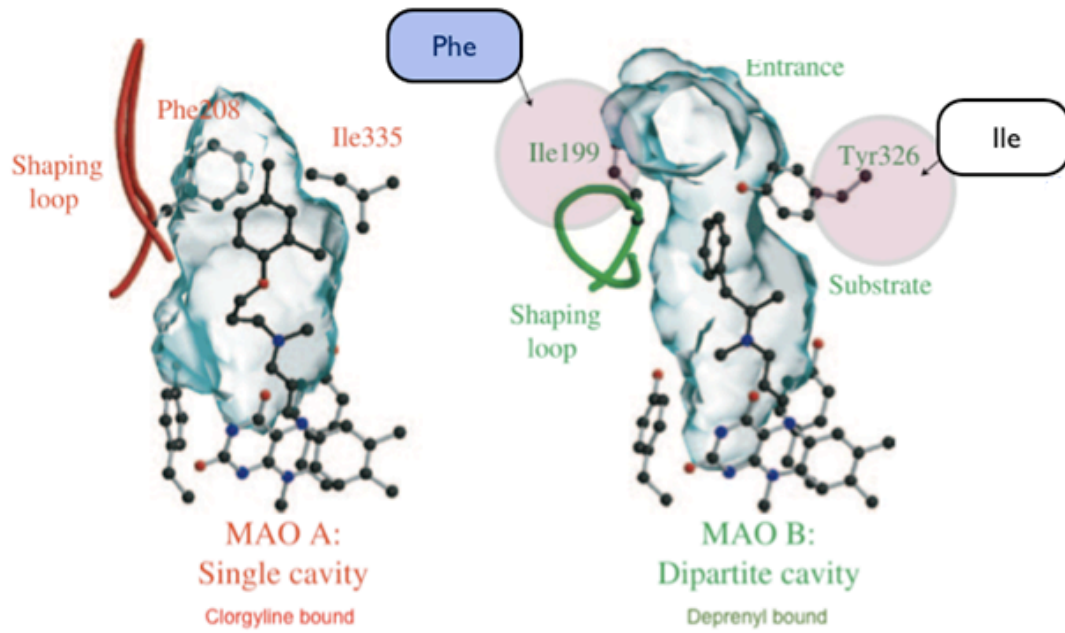


Figure 1.8: Structure of the respective active site cavities in human MAO A and MAO B

Ile199 acts as a “gate keeper” in the MAO B dipartite cavity, whereas MAO A has a Phe in that position which does not have such a role. Tyr326 is on the other side of the gatekeeper Ile, which is also absent in MAO A. This figure was published in (Edmondson 2004), Copyright (2004) Elsevier.

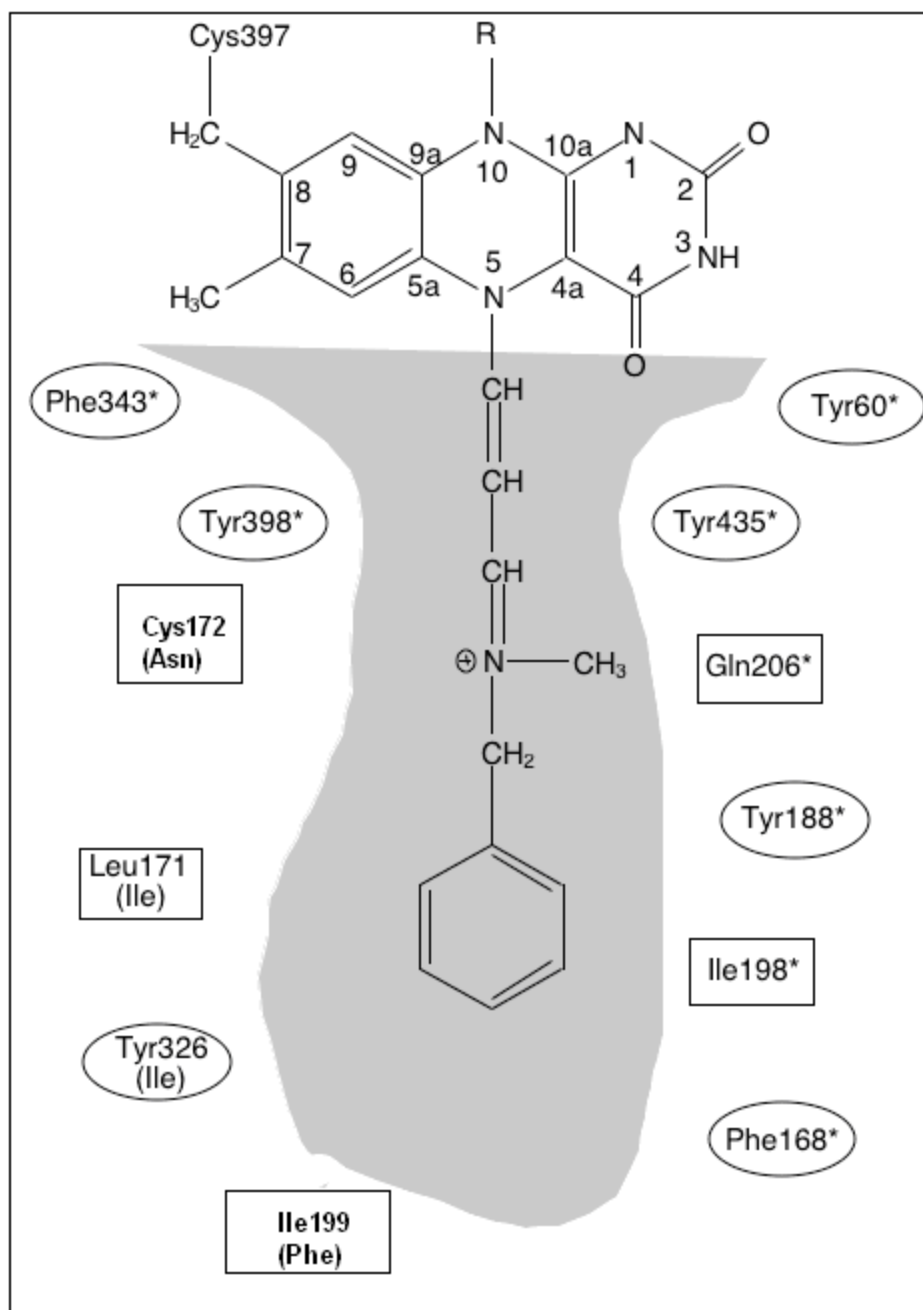


Figure 1.9: Schematic representation of the binding site in human MAO B with the irreversible inhibitor Pargyline.

Conserved amino acid in human MAO A, human MAO B and zebrafish MAO are shown with asterisk. Corresponding human MAO A residue for non-conserved amino acids are shown in parenthesis. *Reprinted by permission from Macmillan Publishers Ltd: [Nature Structural Biology] (Binda 2002) copyright 2001.*

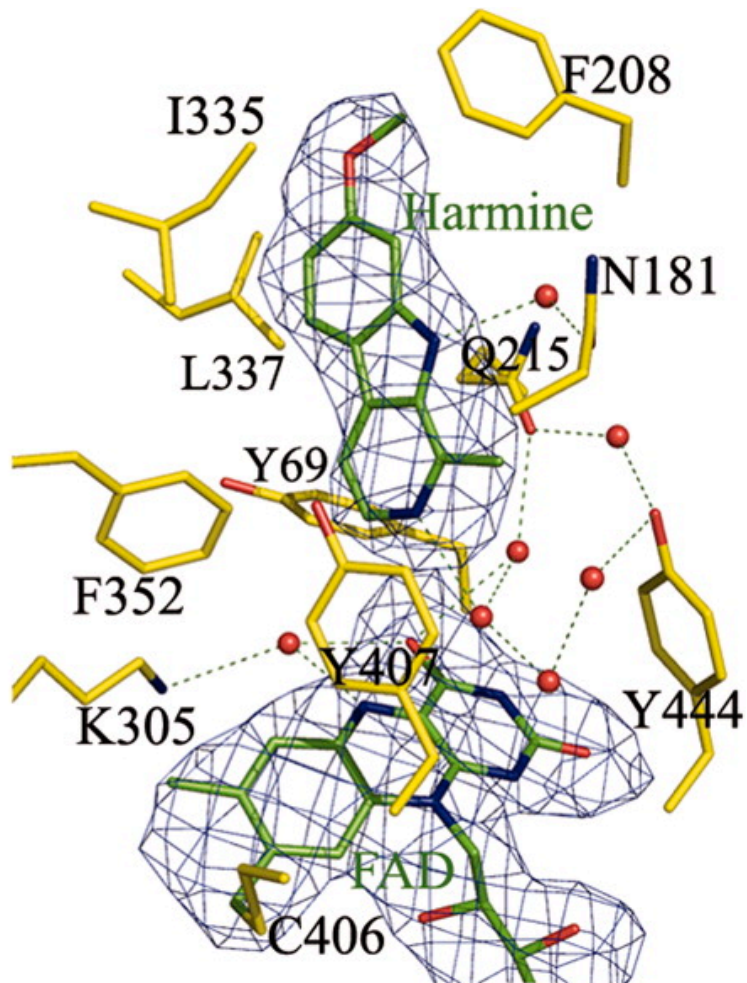


Figure 1.10: Detailed view of the MAO A binding site with the inhibitor Harmine.
Figure adapted from (Son 2008), Copyright (2005) National Academy of Sciences, U.S.A.

Human MAO A binding site is highly conserved with human MAO B yet the proteins have distinct substrate/inhibitor specificities.

1.1.2.3. Membrane Binding Domain

Both human MAO enzymes are integral membrane proteins and anchor the membrane via C-terminal helices. As shown in Figure 1.11, the C-terminal helix of human MAO B is missing the final ~20 residues in its crystal structure while the C-terminal helix of human MAO A is fully observed (Binda 2002 ; Son 2008). Various deletions in the C-terminal do not abolish the membrane-binding feature of MAO B and does not lead to inactive enzyme (Rebrin 2001) (Newton-Vinson and Edmondson, unpublished data). The protein retains ~50% on the membrane and ~50% free in solution as compared to the full-length protein, however, it is unstable during purification and requires additional glycerol in the medium to maintain activity.

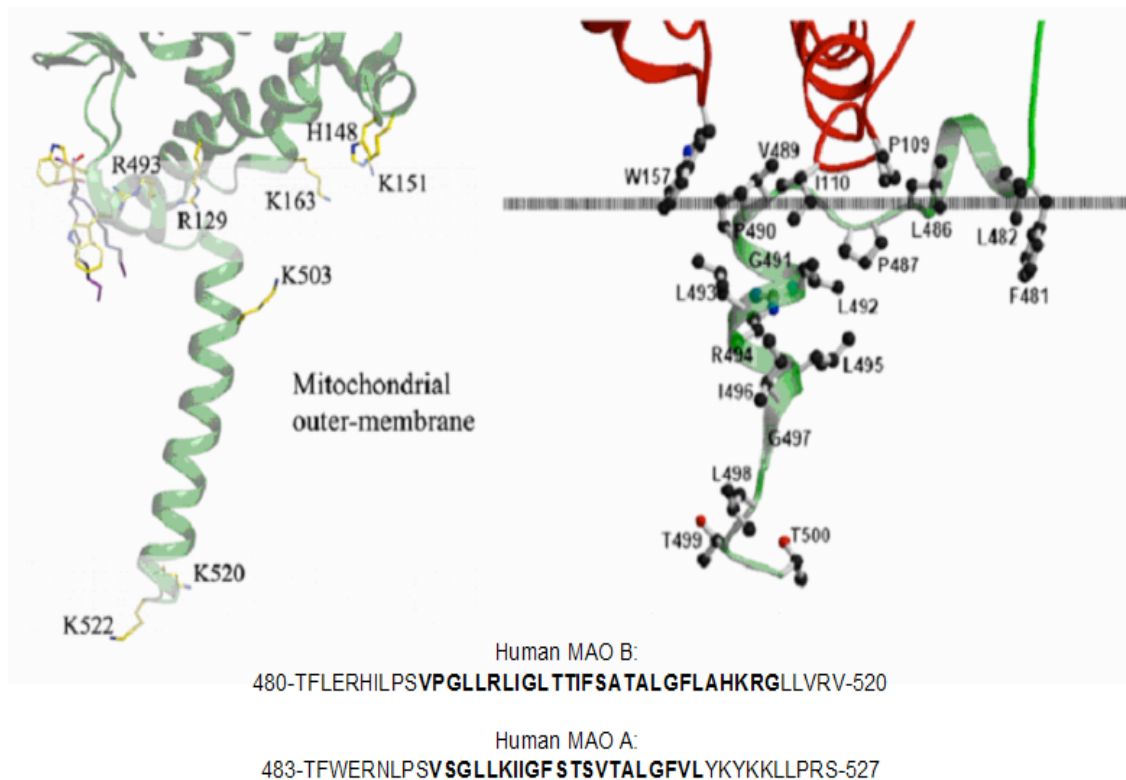
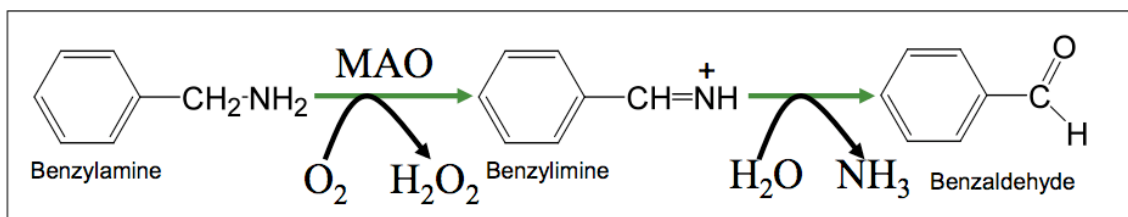


Figure 1.11: C-terminal membrane-binding domain of human MAO A (left) and MAO B (right).
 Reprinted by permission from Macmillan Publishers Ltd: [[Nature Structural Biology](#)] (Binda 2002)
 copyright 2001.

The positively charged residues of MAO A, Arg129, His148, Lys151, Lys163, Arg493, Lys503, Lys520, and Lys522 are shown on left. Residues 461-500 form the C-terminal tail and are shown in semi-green. Neighboring surface residues are in red. The amino acid sequence of MAO B and MAO A C-terminal residues are in shown in black, the residues that interact with the membrane are underlined. Figures are taken from (Son 2008) and (Binda 2002) respectively. C-terminal transmembrane helix of MAO A is rich in Lys residues.

1.1.3 MAO Substrates and the Amine Mechanism

General catalytic scheme of either MAO enzyme is based on the oxidative deamination of the primary amine substrate and then reoxidation by O₂ (Scheme 1.1). The MAO catalyzed reaction is initiated by oxidation of the amine substrates by the covalent flavin cofactor, resulting in a reduced flavin and an imine-product in the reductive half reaction. Molecular oxygen reoxidizes the reduced covalent flavin cofactor in oxidative half reaction, ultimately forming hydrogen peroxide. The corresponding aldehyde and either ammonia (from primary amines) or a substituted amine (from secondary amines) is hydrolyzed non-enzymatically (Edmondson, Mattevi et al. 2004)

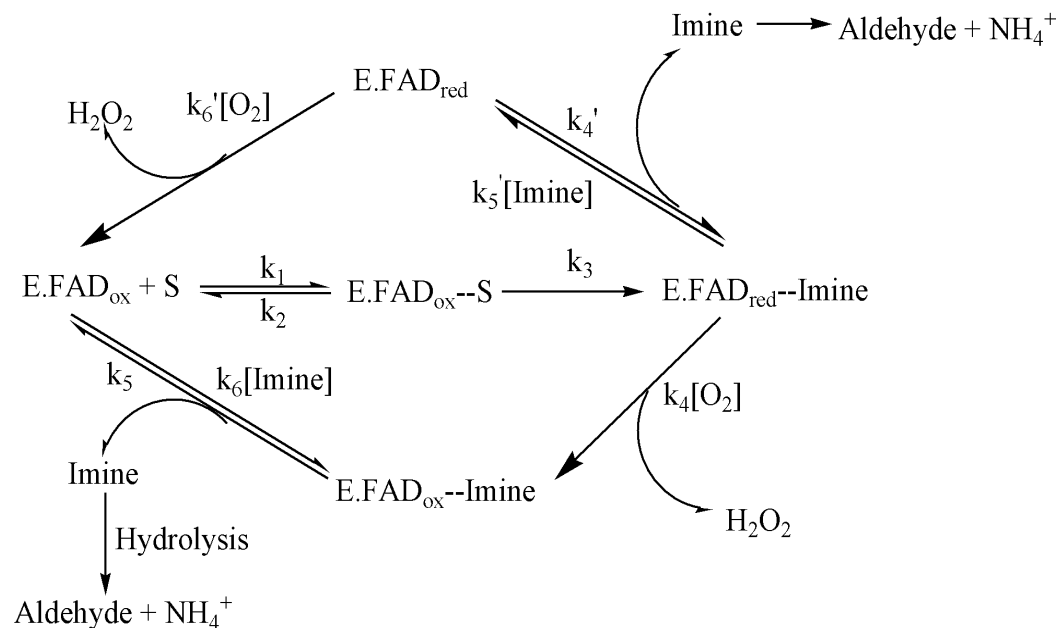


Scheme 1.1: General reaction scheme of MAO

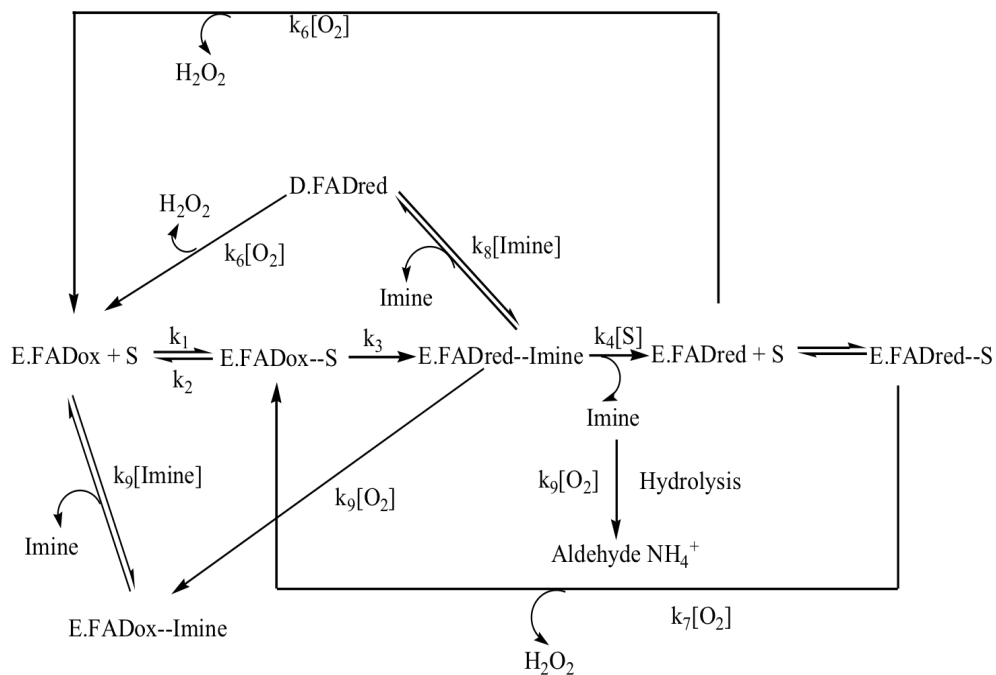
MAO oxidizes benzylamine via reducing the flavin (FAD) cofactor. Reacting with the O₂ molecule reoxidizes the enzyme. NH₃ and H₂O₂ are products of the overall reaction together with the corresponding product benzaldehyde.

Outlined in Scheme 1.2 and 1.3 are the differences between MAO A and MAO B reaction pathways. Depending on the substrate, MAO B might follow either the upper loop or the lower loop of the pathway shown in Scheme 1.2; MAO A on the other hand, always follows the lower loop (Miller and Edmondson 1999). The main determinant on this selectivity is the rate of imine release as compared to the rate of reaction to the

molecular oxygen (Husain, Edmondson et al. 1982). To complete the catalytic cycle, the reduced FAD cofactor has to react with O₂ to generate oxidized flavin. H₂O₂ is also released in this oxidative half reaction as well as the product imine (Edmondson 1993). For MAO A the K_m(O₂) value is 10μM (Ramsay 1994) and for MAO B it is 240μM (Walker and Edmondson 1994). Therefore, under normal air saturation conditions, where the molecular oxygen concentration is approximately 240 μM at 25°C, MAO B catalyzes the reaction at a rate one-half of its V_{max} while MAO A catalyzes the reactions at a maximum velocity. As a reminder, the reactive oxygen products (such as H₂O₂) released in the MAO-catalyzed reactions can lead to cell apoptosis and/or degeneration, which makes the regulation of MAO enzymes crucial.



Scheme 1.2: Reaction pathway for MAO B catalysis



Scheme 1.3: Reaction pathway for MAO A catalysis (Ramsay, Tan et al. 1994)

The rate of product imine release vs. rate of molecular oxygen oxidation of the reduced flavin-imine complex causes two different pathways for reaction catalysis.

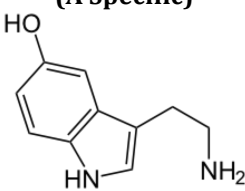
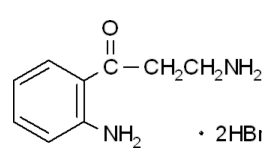
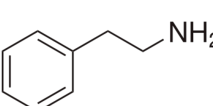
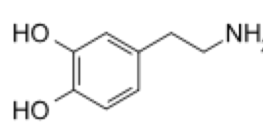
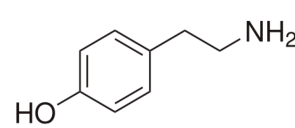
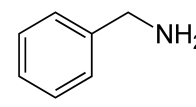
Human MAO A and B Substrates		
<p>Serotonin (A Specific)</p> 	<p>Kynuramine</p> 	<p>Phenylethylamine</p> 
<p>Dopamine</p> 	<p>Tyramine</p> 	<p>Benzylamine (B Specific)</p> 

Table 1.1: Chemical structures of the MAO substrates.

Serotonin is a MAO A specific and Benzylamine is a MAO B specific substrate. Kynuramine, Phenylethylamine, Dopamine and Tyramine are readily oxidized by MAO A as well as MAO B.

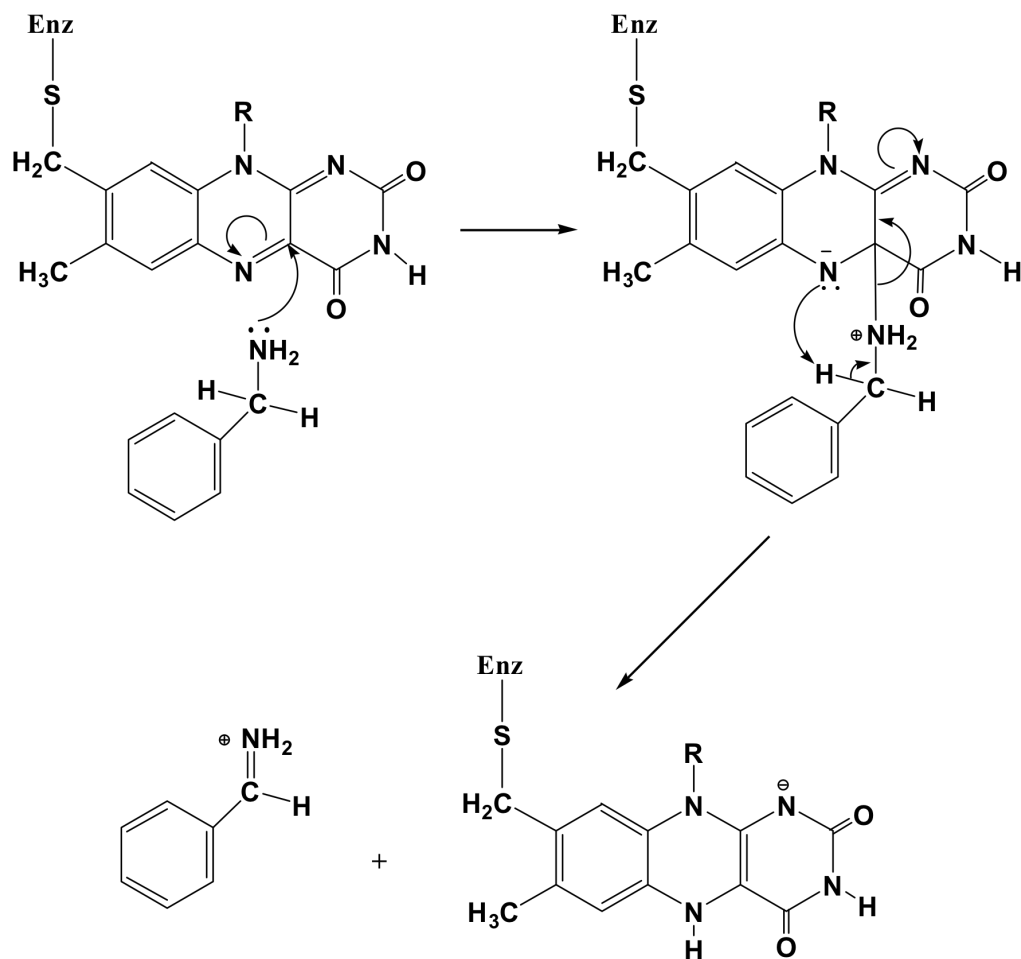


Figure 1.12: Concerted-Nucleophilic Attack Mechanism

The most widely accepted catalytic mechanism for overall MAO reaction is referred as “concerted-nucleophilic attack mechanism” (Miller and Edmondson 1999) (Figure 1.12). This mechanism is thought to be initiated by a nucleophilic attack of the substrate on the flavin with subsequent proton abstraction by flavin ring. Formation of the protonated imine intermediate is detected via UV-Vis absorption spectral data and is consistent with the mechanism (Edmondson 1993). Additional quantitative structure-activity relationship (QSAR) studies provide convincing evidence for this mechanism (Miller and Edmondson

1999). QSAR (Quantitative structure-activity relationship) studies played important roles in revealing the active site properties of MAO enzymes as well and are described in detail in Chapter 4.

$$\log k(\text{or}K_d) = \rho(\sigma) + A(\pi) + B(V_w)(\text{or}E_s) + C$$

σ -- electron donating or withdrawing properties of the substituent
 π -- lipophilicity of the substituent
 V_w -- van der Waals volume
 E_s -- Taft steric parameter

Scheme 1.4: Equation used for the QSAR studies

Correlation of the enzyme structure and activity via QSAR calculations helps to explain how structure influences the activity

1.1.4 Properties and Importance of MAO Inhibitors

Monoamine oxidase inhibitors (MAOIs) are a class of antidepressant drugs approved for the treatment of depression. MAOIs have been the targets of numerous studies due to their physiological importance in neurological disorders such as Parkinson and Alzheimer's Diseases (Edmondson 2009). It has been almost 50 years since the first MAO inhibitor; iproniazid was used clinically as an anti-depressant (Kline 1958). Since then, developing proper MAO inhibitors has been a challenge mainly because despite their 70% sequence identity, human MAO isoforms present significant differences in inhibitor selectivity. Therefore, to develop the finest inhibitor, the elements that gave rise to MAO-specificity have to be elucidated. Fortunately, the structures of both isoforms are now available and set a milestone to develop improved MAO inhibitors. The inhibitors that are referred in my studies can be categorized as (1) irreversible inhibitors and (2) reversible inhibitors (Table 1.1).

1.1.4.1 Irreversible Inhibitors

A) Acetylenic Inhibitors

The acetylenic inhibitors are administered as an adjustment for L-DOPA therapy in the treatment of Parkinson's disease and include MAO B specific inhibitors pargyline and rasagiline, and MAO A specific inhibitor clorgyline (De Colibus 2005) (Figure 1.9). These inhibitors stoichiometrically and irreversibly inhibit the enzymes through formation of an N(5) flavocyanine adduct that exhibits an absorption spectrum with a λ_{max} of 400-415 nm with an $\epsilon \sim 23,000 \text{ M}^{-1} \text{ cm}^{-1}$ with the FAD cofactor. The flavocyanine adduct bleaches the specific 450nm flavin peak in the UV-absorption spectrum (Chuang, 1974). The structures of the N(5) flavocyanine adducts were confirmed when the crystal structure of clorgyline and deprenyl inactivated MAO A (De Colibus 2005) and the pargyline-inactivated MAO B were solved (Binda, Newton-Vinson et al. 2002).

B) *N*-Propargyl-Aminoindans

Shown in Figure 1.13, rasagiline, a selective and irreversible MAO B inhibitor, falls under the category of *N*-propargyl-aminoindans. Rasagiline has recently been FDA approved for the treatment of Parkinson's patients (Chen 2007). It has been reported that a large number of rasagiline analogues also act as MAO inhibitors (Figure 1.14) (Sterling, Veinberg et al. 1998) (Kalir, Sabbagh et al. 1981). 6-Hydroxy-*N*-propargyl-1(*R*)-aminoindan (*R*-HPAI) is a non-selective inhibitor of either MAO A and MAO B. *N*-propargyl-1(*S*)-aminoindan (*S*-PAI) and *N*-methyl-*N*-propargyl-1(*R*)-aminoindan (*R*-MPAI) are other *N*-propargyl aminoindan analogues (Sterling, Veinberg et al. 1998). *S*-PAI is non-selective inhibitor, while methylation on the amino moiety of the propargyline

chain of this analogue makes the inhibitor (M-PAI) no longer MAO B specific (Hubalek, Binda et al. 2004).

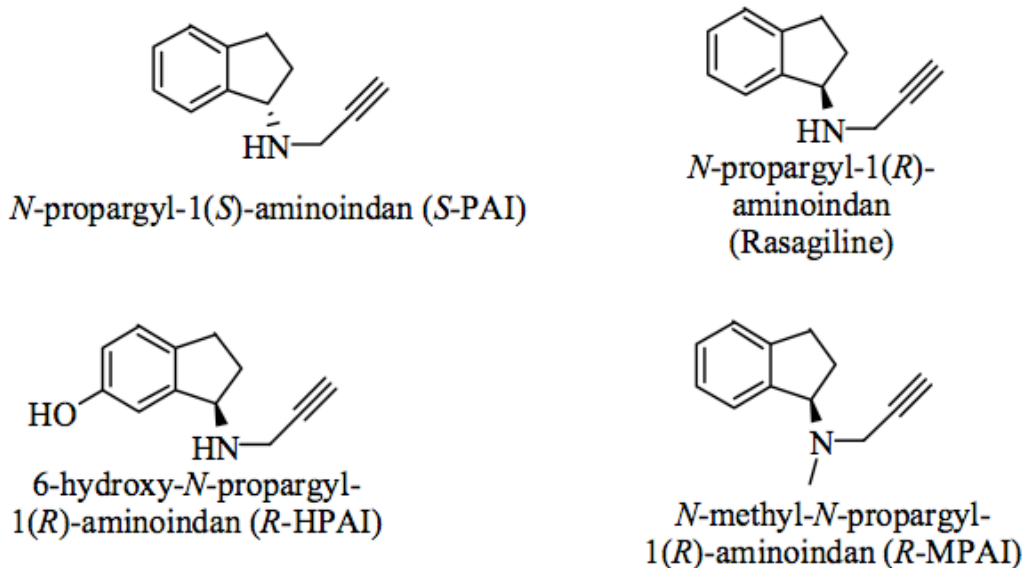


Figure 1.14: Structures of *N*-propargyl-aminoindan analogues.

Reprinted with permission from (Hubalek, Binda et al. 2004) . Copyright 2004 American Chemical Society

C) Hydrazine Inhibitors

Hydrazine inhibitors (Figure 1.15) were first discovered for their role in the treatment of mood elevation (Zeller 1974). Currently, phenylethylhydrazine is of the seven FDA approved MAO inhibitors, and it inhibits either MAO irreversibly (Binda 2008). Phenylhydrazine and benzylhydrazine also inhibit MAO non-specifically and irreversibly (Patek and Hellerman 1974). At first, it was presumed that the mechanism of hydrazine inhibition proceeds through formation of a C4(a)-phenyl adduct with FAD (Nagy, Kenney et al. 1979).

However, recent crystal structural data shows that the inhibition is covalent and involves N(5) product formation (Binda 2008) and either form of MAO can readily oxidize arylalkylhydrazines to form diazenes (Binda 2008).

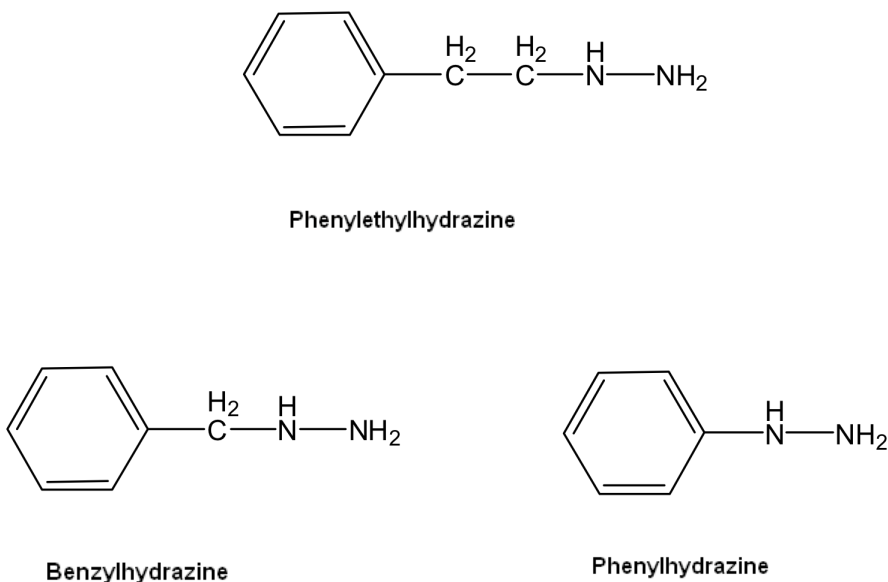


Figure 1.15: Structures of Hydrazine Inhibitors

1.1.4.2. Reversible Inhibitors

Despite their high sequence identity and similarities, MAO A and MAO B show significant functional differences when it comes to reversible inhibition, as well. Reversible MAO inhibitors are pharmacologically important because their action is ephemeral and selective (Lotufo-Neto F 1999). Besides, the side effects of older irreversible MAO drugs are avoided with the development of reversible MAO drugs (Tipton, O'Carroll et al. 1983). Several reversible inhibitors that target specifically MAO A but not MAO B are described in the literature. The endogenous beta-carboline,

harmane, is one of those compounds and has been shown to bind specifically to MAO A along with harmine and harmaline (Anderson 2006, Fowler 1977) Most tetrahydro- β -carbolines are shown to be potent MAO A inhibitors (Sparks and Buckholtz 1985). Tetrindole (2,3,3a,4,5,6-hexahydro-8-cyclohexyl-1H[3,2,1-j,k] carbazole) and pirlindole (2,3,3a,4,5,6-Hexahydro-8-methyl-1H-pyrazino[3,2,1-j,k] carbazole) are among selective and competitive reversible MAO A specific inhibitors as well (Medvedev 1994; Medvedev 1998). The following compounds, on the other hand, are shown to inhibit MAO B with K_i values in the low micromolar range: isatin, 8-(3-chlorostyryl) caffeine, 1,4-diphenyl-2-butene, safinamide and trans,trans-farnesol (Figure 1.16). Interestingly, a study performed in 2006 using these inhibitors, showed the versatility of MAO B specific inhibition. The well-studied bovine MAO B contains a Phe in the position 199 instead of an Ile (Hubalek, Binda et al. 2005), therefore Ile199 of MAO B was mutated to Phe. The presence of Phe increases the bulkiness in the entrance cavity and prevents MAO B specific inhibitors from binding (Hubalek, Binda et al. 2005). This finding was a strong example on the elasticity of MAO B selectivity and also showed that each amino acid around the active site has the potential to play a crucial role on the substrate/inhibitor selectivity. Moreover, it presented that not all the inhibitors that inhibit human MAO B also inhibits bovine MAO B and delicate analyses is required prior the usage of different MAO sources for drug development studies.

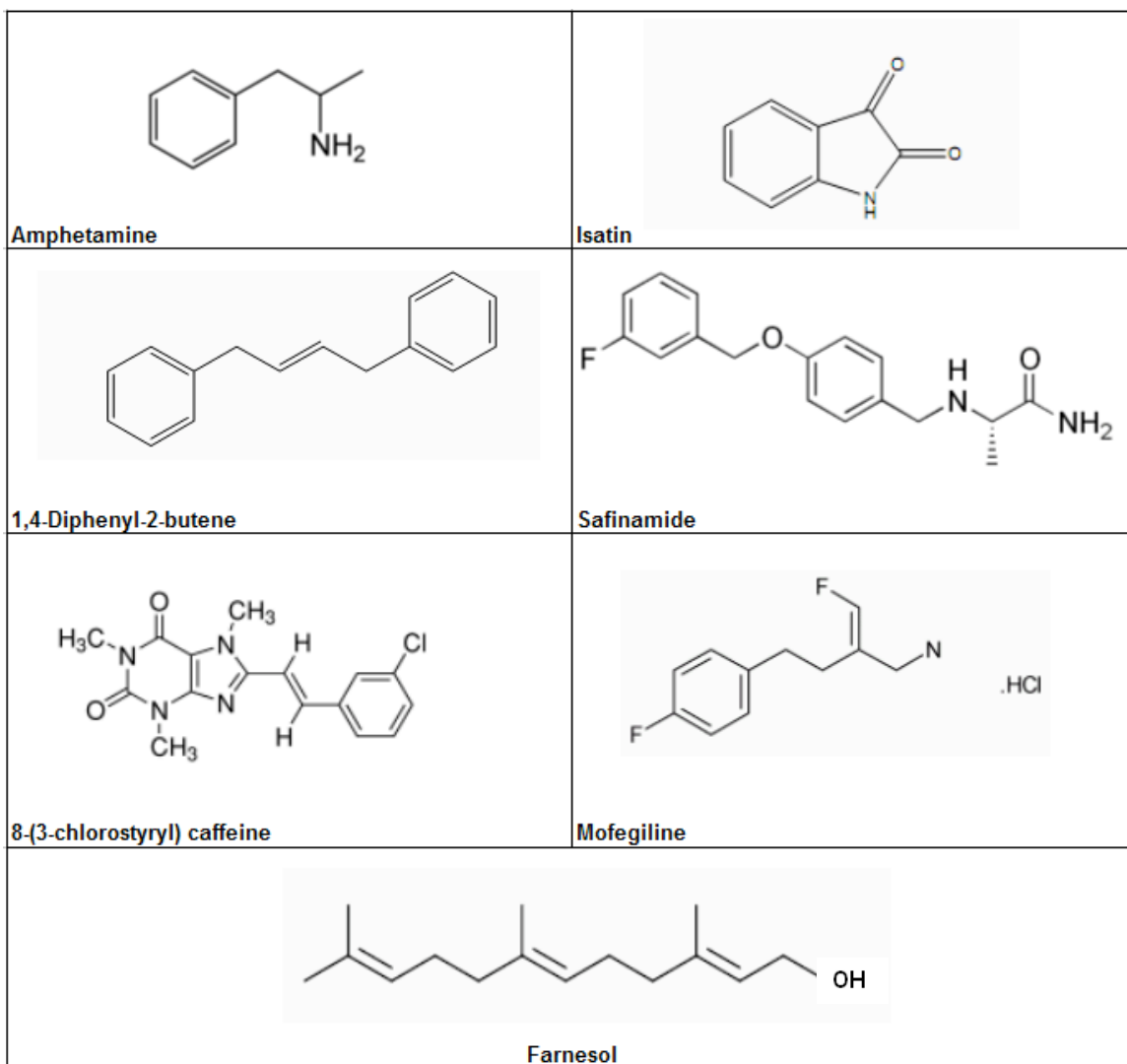


Figure 1.16: Structures of reversible MAO inhibitors used in this study

Amphetamine and isatin are non-selective, reversible MAO inhibitors. Mofegiline, Farnesol, CSC, Safinamide and 1,4-Diphenyl-2-butene target specifically MAO B.

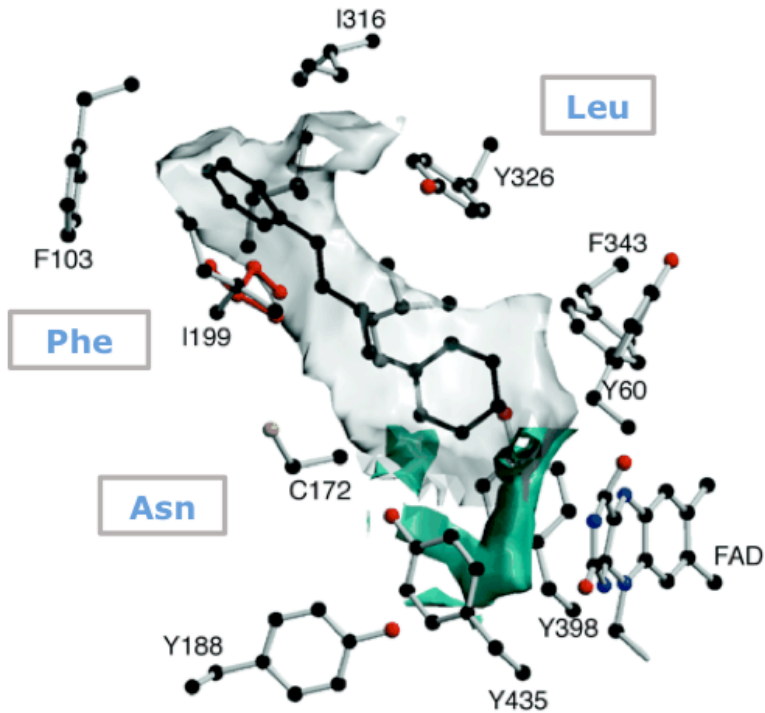


Figure 1.17: Structure of Human MAO B in complex with 1,4-diphenyl-2-butene.

The conformation of the Ile199 “the gate” (red) and the corresponding residues that differ in MAO A are (blue) are shown by GRID molecular interaction fields computed with an aromatic sp² carbon probe (gray) and with a NH₂ probe (cyan). The picture was generated by using the coordinates from the 1,4-diphenyl-2-butene complex with MAO B. Together with Ile199, Phe103 and Ile316 occupies the entrance cavity space
Figure adapted from (Binda, Li et al. 2003) , copyright permission pending.

		Inhibitor	Specificity	K_i (μM)	
Irreversible Inhibitors	N-propargyl-Aminoindans^a	<i>R</i> -PAI	MAO B	32	
		<i>S</i> -PAI	MAO A	160	
		<i>R</i> -HPAI	MAO B	17	
		<i>S</i> -HPAI	MAO A	50	
	Acetylenic	Clorgyline	MAO A	15	
		Pargyline	MAO B	21	
		Deprenyl	MAO B	14	
		Rasagiline	MAO B	0.7	
	Hydrazines	Phenylethylhydrazine	MAO B	15 ± 2	
		Phenylhydrazine	MAO A	205 ± 4	
		Benzylhydrazine	MAO B	26 ± 1	
	Reversible Inhibitors		Harmane	0.58 ± 0.20	MAO A
			Tetrindole Mesylate	5.27 ± 0.24	
		Pirlindole Mesylate	0.92 ± 0.04		
		Safinamide	0.45 ± 0.13	MAO B	
		Farnesol	2.3 ± 0.4		
		Chlorostyryl caffeine	0.27 ± 0.08		
		1,4-diphenyl-2-butene	34.5 ± 1.4		
		Amphetamine	3.7 ± 0.5 (A) 3.9 ± 0.2 (B)		
		Mofegiline ^b	1.1 (A) 28 nm (B)		

Table 1.2. Summary of MAO Inhibitors and their K_i values

^aN-propargyl-aminoindans are abbreviated as follows: N-propargyl-1(*S*)-aminoindan (*S*-PAI), N-propargyl-1(*R*)-aminoindan (*R*-PAI), 6-hydroxy-N-propargyl-1(*R*)-aminoindan (*R*-HPAI), 6-hydroxy-N-propargyl-1(*S*)-aminoindan (*S*-HPAI) and N-propargyl-1(*R*)-aminoindan (Rasagiline) (Hubalek, Binda et al. 2004).

^bMofegiline is only reversible for human MAO A but not human MAO B (Milczek 2008)

Part II: Zebrafish MAO

1.3 What makes Zebrafish MAO Important?

1.2.1 Molecular Properties

All mammals contain two forms of MAO, MAO A and MAO B, that are located in the mitochondrial outer membrane and are responsible for oxidative deamination of endogenous and exogenous amines including dopamine, serotonin, noradrenalin (Tipton 1972). The two forms are distinguished from each other by their affinity for inhibitors and substrates. For example, MAO A predominantly deaminates serotonin, whereas MAO B reacts with phenylethylamine (Edmondson 2007). Similarly, while MAO A is inhibited by clorgyline, MAO B is inhibited by deprenyl (Edmondson 2007). So, how do these proteins that have ~70% sequence identity have such distinct functional properties? What makes these enzymes highly specific? Why do mammals have two forms of MAO?

Understanding the origins of MAO A and B is necessary to answer these questions. Not all organisms have two forms of MAO. It is proposed that the present MAO genes have evolved from a single form of MAO (a so-called ancestor MAO gene) by a gene duplication event (Chen 1994). Jean Shih's group was first to clone and sequence a teleost (fish) MAO from trout (Chen 1994) and proposed that this teleost contains a single form of MAO. In 2005, the gene sequence of zebrafish (*Danio rerio*) MAO (zMAO) was determined which confirmed that teleosts are found to contain only a single form of MAO gene (Setini 2005) (Anichtchik 2006). To probe the differential functional and structural properties of human MAO enzymes to develop highly selective inhibitors, identifying the properties of this single MAO form is important. Such information would

be significant for drug development studies that use zebrafish as a model organism and hopefully understand the importance of the two isozymes present in mammals.

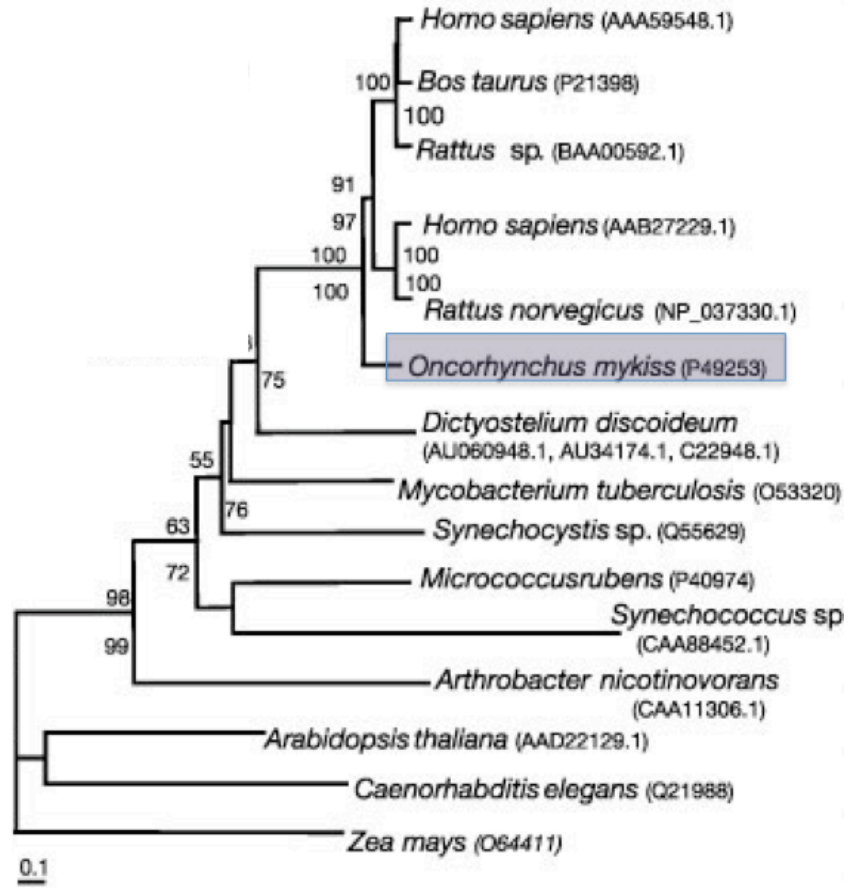


Figure 1.18: Phylogenetic tree showing evolutionary history of Monoamine Oxidases. Adapted by permission from Macmillan Publishers Ltd: [\[Nature\]](#) (Stanhope 2001), copyright 2001

Numbers at nodes indicate bootstrap support values for both neighbor joining and parsimony analysis. MAO is one of the unique proteins that do not follow horizontal gene transfer. The teleost organism (*Oncorhynchus mykiss*) is indicated in bold and is a co-ortholog of human MAOs (Stanhope 2001). Note that no-flavin containing monoamine oxidase is found in bacteria and the corresponding bacterial enzymes are predicted amine oxidases with an average of 20% sequence identity to human MAOs.

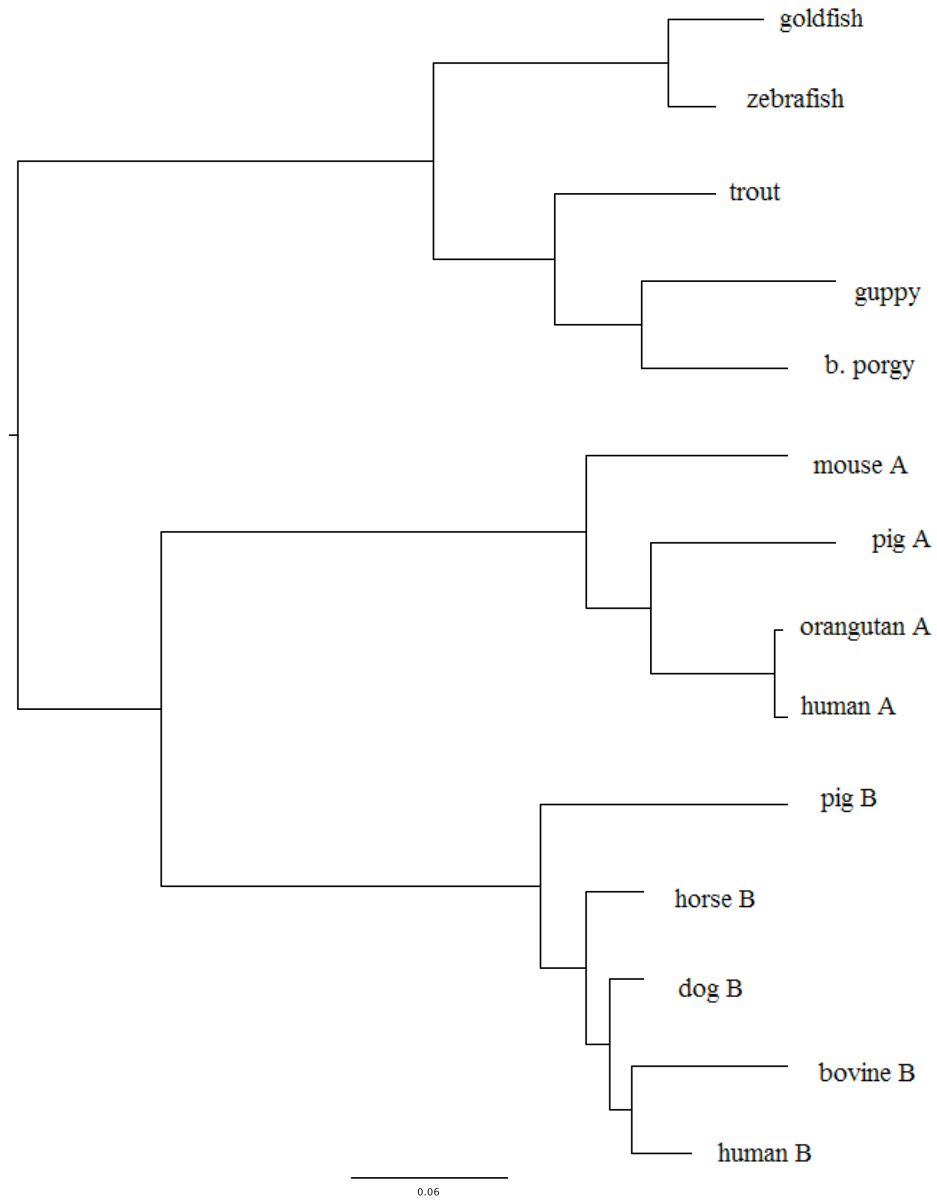


Figure 1.19: Phylogenetic tree of MAO showing the separation of mammals from teleosts.

As seen, humans and zebrafish share a common ancestor before separation. It is still not known why higher organisms like humans need two MAO genes. Trees are prepared via MrBayes (Huelsenbeck, J. P. and F. Ronquist. 2001. MRBAYES: Bayesian inference of phylogeny. *Bioinformatics* 17:754-755)

1.2.2 Comparison to Human MAO A and MAO B

The recently completed genome sequence of zebrafish demonstrates a single gene expressing MAO (Setini 2005) that exhibits ~70% identity to either human isozymes. The latest data in the literature implies that zMAO is inhibited by the acetylenic MAO A inhibitor clorgyline and by the acetylenic MAO B inhibitor deprenyl, suggesting that zMAO displays the properties of both human MAO isozymes. On the other hand, zMAO can catalyze the oxidation of serotonin, a MAO A selective substrate better than MAO B substrate phenylethylamine (Anichtchik 2006). It has to be noted here that none of these studies were done with either over-expressed or pure zMAO, but with whole neuron tissues obtained from zebrafish.

The overall genomic structure of the zMAO gene is highly analogous to human MAO A and B (Table 1.3-5, Figure 1.20). The number of exons and the length of each exon in zMAO gene are exactly the same as in human MAO genes (Anichtchik 2006). When it comes to corresponding active site sequence similarity analysis for substrate and flavin binding domains, zMAO has a higher sequence identity to human MAO A than human MAO B. In human MAO A, the active site residues are Tyr69, Phe177, Ile180, Asn181, Tyr197, Ile207, Phe208, Gln215, Ile335, Phe352, Tyr407 and Tyr444. In human MAO B, these residues are Tyr60, Phe168, Leu171, Cys172, Tyr188, Ile198, Ile199, Gln206, Tyr326, Phe343, Tyr398 and Tyr435, correspondingly. Therefore, zMAO resembles human MAO A more than human MAO B in this aspect; most of the residues of human MAO A are conserved in zMAO. The following are the only mismatches between MAO A and zMAO binding site: Leu171 to Val, Cys172 to Asn, Ile199 (“the gate”, Figure 1.6)

to Phe and Tyr326 to Leu. These four residues are unique in zebrafish, suggesting that zMAO might have different properties than either human isoform. Hence, the enzyme might have MAO A-like properties while also exhibiting completely unique properties to its own. Another interesting aspect is found in the membrane binding domain sequence alignment. Zebrafish MAO shows ~20% sequence identity to either human isoform's membrane binding domain (sequences 493 to 513) (Table 1.3). Human MAO A and B do not share high sequence identity between each other, either (approximately 30%). It was already proposed that the membrane anchoring domain has no role for targeting MAO A or MAO B to the outer mitochondrial membrane (Weyler 1994, Chen 1996). Therefore the low sequence identity does not prevent zMAO from being a membrane binding domain.

Function	<i>Catalyzes the oxidative deamination of biogenic and xenobiotic amines</i>
Isoelectric Point	9.3
Sequence Length	522 amino acids
Cofactor	<i>Flavin (Not specified)</i>
Sub-cellular Location	<i>Mitochondrial Outer Membrane (Not specified)</i>
Miscellaneous	<i>Single form exists in Zebrafish. In mammals two forms (as MAO A and MAO B) exist.</i>
Molecular Function	<i>Oxidoreductase</i>
Catalytic Activity	$RCH_2NHR' + H_2O + O_2 = RCHO + R'NH_2 + H_2O_2$
Total Mass	59.55 kDa

```

      10      20      30      40      50      60
MTANAYDVIV IGGGISGLSA AKLLVDSGLN PVVLEARSRV GGRTYTVQNK ETKWVDLGGG
      70      80      90     100     110     120
YIGPTQNRIL RIAKQYGVKT YKVNEEESLV HYVRGKSYPF KGPFPPMWNP FAYMDYNNLW
      130     140     150     160     170     180
RTMDKMGMEI PKEAPWRAPH AEEWDKMTMQ QLFDKICWTR SARRFATLFV NVNVTSEPEH
      190     200     210     220     230     240
VSALWFLWYV KQCGGTRIF STTNGGQERK FAGGANQISE GMARELGDRV KLSRAVCSID
      250     260     270     280     290     300
QTGDLVEVRT VNEEVYKAKY VILAIPPGLN LKIHFNPELP PLRNQLIHRV PMGSVIKCMV
      310     320     330     340     350     360
YYKENFWRKK GYCGSMVIEE EDAPIGLTLD DTKPDGSPVA IMGFILARKS RKLANLTRDE
      370     380     390     400     410     420
RKRRCICEIYA RVLGSEEALY PVHYEKNWC EEEYSGGCYT AYFPPGIMTQ FGRVLRPEVQ
      430     440     450     460     470     480
RLYFAGTETA TEWSGYMEGA VQAGERASRE VMCAMKGLHA SQIWQSEPEP HDVPARPFVT
      490     500     510     520
TFWERNLPSV GGFLKFMGVS SFLAAATAAG LVACKKGLLP RC

```

```

CHAIN          1-522      Amine oxidase [flavin-containing].
TOPO_DOM      1-492      Cytoplasmic (Potential).
TRANSMEM      493-513    Anchor for type IV membrane protein
TOPO_DOM      514-522    Mitochondrial intermembrane (Potential).

```

Table 1.3: An overview analysis zebrafish MAO (zMAO)

- A list of general properties at a glance (E.C. 1.4.3.4)
- Sequence of zMAO with potential domain analysis (retrieved from ExPASy, protein code: Q6NSN2)

```

WT-MA0A-pro.seq  MENQEKASIAGHMFDVVVIGGGISGLSAAKLLTEYGVSVLVLEARDRVGGRTYTIKMEHV 60
WT-MA0B-pro.seq  MSN-----KCDVVVVGGSISGMAAAKLLHDSGLNVVLEARDRVGGRTYTLRNQKV 51
z-MA0.pro        MTAN-----AYDVVIVIGGGISGLSAAKLLVDSGLNPPVLEARSRVGGRTYTVQNKET 52
*                **::*****:***** : *.: *****.*****::*:.

WT-MA0A-pro.seq  DYVDVGGAYVGPQTQRILRLSKELGIETYKVMVSERLVQYVKGYTPFRGAFPPVWNP 120
WT-MA0B-pro.seq  KYVDLGGSYVGPQTQRILRLAKELGLETYKVMNEVERLIHHVKGKSYFFRGPFPPVWNP 111
z-MA0.pro        KWVDLGGAYIGPQTQRILRLIAKQYGVKTYKVMEEESLVHYVKGKSYFFKGFPPPMW 112
.:**::**:*:*****::*.: ***** * *:::****:***:*.***:****:

WT-MA0A-pro.seq  YLDYNNLWRTIDNMGKEIPTDAPWEAQHADKWDKMTMKELDKICWTKTARRFAYLFVNI 180
WT-MA0B-pro.seq  YLDHNNFWRTMDDMGREIPSDAPWKAPLAEEDNMTMKELLDKLCWTESAKQLATLFVNL 171
z-MA0.pro        YMDYNNLWRTMDKMGMEIPKEAPWRAPHAEEWDKMTMQQLFDKICWTRARRFATLFVNV 172
*.:**::**:*:*. ** **:::***.* *:::***:***:*.***:***.:.***:***:

WT-MA0A-pro.seq  NVTSEPHVVSALWFLWYVKQCGGTRIFSVINGGQERKFGVGGSGQVSERIMDLLGDQVK 240
WT-MA0B-pro.seq  CVTAETHVVSALWFLWYVKQCGGTRIIISTINGGQERKFGVGGSGQVSERIMDLLGDRV 231
z-MA0.pro        NVTSEPHVVSALWFLWYVKQCGGTRIFSTINGGQERKFGAGGANQISEGMQKELGDRV 232
**:*.:***** **:*.:*****.***:*.*** : . ***:***

WT-MA0A-pro.seq  NHPWTHVDQSSDNIIETLNHEHYECKYVINAIPTLTAKIHFRELPALPEPQLIQRLPM 300
WT-MA0B-pro.seq  ERPVIYIDQTRENVLVETLNHEMYEAKYVISAIPPTLGMKIHFNPLPMMFNQMITRVPL 291
z-MA0.pro        SKAVCSIDQTGDLVEVRTVNEEVYKAKYVILAIPPGLNLKIHFNPELPLPQLIHRVPM 292
.:.* **::: : : :.*:*.* *.:**** ** ** * ** **:::***:***:

WT-MA0A-pro.seq  GAVIKCMMYYKEAFWKKKDYCGCMIEDEDAPISITLDDTKPDGSLPAIMGFILARKADR 360
WT-MA0B-pro.seq  GSVIKCIVYYKEPFWRKKDYCGTMIIDGEEAPVAYTLDDTKPEGNVAAIMGFILAHKARK 351
z-MA0.pro        GSVIKCMVYYKENFWRKKGYCGSMVIEEEDAPIGLTDDTKPDGSPVPAIMGFILARKSRK 352
*:*:*:*:**** **::**:*.* **:::*.***. *****:*. .*****:***:

WT-MA0A-pro.seq  LAKLHKEIRKKKICELYAKVLGSEALHPVHYEEKNWCEEQYSGGCYTAYFPPGIMTQYG 420
WT-MA0B-pro.seq  LARLTKEERLKKLCELYAKVLGSEALEPWHYEEKNWCEEQYSGGCYTAYFPPGILTQYG 411
z-MA0.pro        LANLTRDERKRRIICEIYARVLGSEALYPVHYEEKNWCEEEYSGGCYTAYFPPGIMTQFG 412
**.* : : * :*:**:*.* ** *****:*****:*****:***:

WT-MA0A-pro.seq  RVIRQPVGRIFFACTETATKWSGYMEGAVEAGERAAREVLNGLGKVTEDIWQEPESKD 480
WT-MA0B-pro.seq  RVLRQPVDRIYFACTETATHWSGYMEGAVEAGERAAREILHAMGKIPEDIWQSEPEPVD 471
z-MA0.pro        RVLRQPVGRLYFACTETATEWSGYMEGAVQAGERASFEVHCAMGKLHASQIWQSEPEPMD 472
**:*:**.*:*****.*****:*****:***: .:***: .:***.**** *

WT-MA0A-pro.seq  VPAVEIHTTFWERNLPSVSGLLKIIGFST---SVTALGFVLYKYKLLPRS 527
WT-MA0B-pro.seq  VPAQPITTTFLERHLPVSGLLRLIGLTTIF-SATALGFLAHKRGLLRV 520
z-MA0.pro        VPARPFVTTFWERNLPSVSGFLKFMGVSSFLAAATAAGLVACKKGLLPRC 522
*** .: ** **:*.* **:::***:***: .:***: .:***.**** *

```

Figure 1.20: Multiple sequence alignment of zMAO, human MAO A and B.

Zebrafish accession number AY185211. (*) signs indicate the conserved residues, (:) indicate conserved residues between two species, (.) refers to different residues among all three species. Alignment is prepared via Clustal 2.0.5 program available here: <http://www.ebi.ac.uk/Tools/clustalw2/>

Specific contacts							

Residue		Dist (A)	Surf (A)	HB	Arom	Phob	DC

19A	ILE*	3.5	19.4	-	-	+	+
20A	GLY*	3.3	13.6	-	-	-	-
21A	GLY	3.8	0.7	+	-	-	-
22A	GLY*	3.2	30.7	+	-	-	-
23A	ILE*	3.2	13.3	+	-	-	+
24A	SER*	2.6	35.3	+	-	-	-
25A	GLY	4.3	0.5	+	-	-	-
42A	LEU	3.1	26.6	+	-	-	-
43A	GLU*	2.6	42.9	+	-	-	+
44A	ALA*	3.0	31.9	+	-	+	+
45A	ARG*	2.8	29.2	+	-	-	+
49A	GLY	3.6	4.5	+	-	-	-
50A	GLY*	3.1	31.8	+	-	-	-
51A	ARG*	2.8	109.4	+	-	+	+
52A	THR*	3.5	17.0	-	-	-	+
65A	VAL (Leu)	3.8	7.4	-	-	-	+
66A	GLY	3.6	12.5	+	-	-	-
67A	GLY*	3.2	13.3	-	-	-	-
68A	ALA*	3.2	10.4	+	-	-	+
69A	TYR*	3.0	62.3	+	-	+	+
74A	GLN*	4.9	1.6	-	-	-	+
215A	GLN*	5.9	0.7	-	-	-	-
242A	HIS (Lys)	7.6	-	-	-	-	-
243A	PRO* (Ala)	3.6	4.5	-	-	+	+
244A	VAL*	2.9	42.6	+	-	+	+
272A	ALA	3.6	19.3	+	-	-	+
273A	ILE*	3.4	33.4	-	-	+	+
274A	PRO*	4.0	8.2	-	-	-	+
277A	LEU*	3.4	37.6	+	-	+	+
281A	ILE*	4.4	4.0	-	-	-	+
303A	VAL*	3.6	18.8	-	-	+	-
305A	LYS*	4.1	15.2	-	-	+	-
352A	PHE*	4.4	9.1	-	+	+	-
397A	TRP*	3.4	42.2	-	-	+	+
402A	TYR*	3.4	29.5	+	+	+	+
403A	SER*	4.6	0.5	+	-	-	-
406A	CYS*	1.7	52.3	-	-	+	-
407A	TYR*	3.3	40.1	+	+	+	+
434A	GLY*	3.2	10.6	-	-	-	-
435A	THR*	2.7	41.8	+	-	-	+
443A	GLY	3.1	28.8	+	-	-	-
444A	TYR*	3.3	44.3	+	+	-	+
445A	MET*	2.6	50.7	+	-	+	+
446A	GLU	4.3	0.9	+	-	-	-
448A	ALA*	3.5	6.3	-	-	-	+
700A	HRM	3.9	16.0	-	+	-	-

Table 1.4: MAO A residues in contact with ligand flavin (FAD 600A) in PDB entry 2Z5X.

Corresponding zMAO residues are shown in parenthesis. As seen in the table, sequence of zMAO highly similar to that of hMAO A with minor differences. Data is obtained by the PyMOL Molecular Graphics System (DeLano Scientific, Palo Alto, CA) For legend explanations see Table 1.5.

Specific contacts							

Residue		Dist	Surf	HB	Arom	Phob	DC

69A	TYR*	3.9	14.6	-	+	-	-
97A	LEU*	5.6	3.4	-	-	-	-
111A	ALA (Pro)	4.8	3.1	-	-	-	+
180A	ILE* (Val)	3.4	23.4	-	-	+	+
			(Leu) B				
181A	ASN*	3.6	19.2	+	-	-	+
			(Cys) B				
207A	ILE	4.5	3.7	+	-	-	+
208A	PHE*	3.2	59.6	-	+	-	+
			(Ile) B				
210A	VAL* (Thr)	5.0	7.0	-	-	+	+
215A	GLN*	3.4	33.1	+	-	+	+
323A	CYS* (Ser)	4.0	10.8	-	-	-	-
			(Thr) B				
325A	ILE* (Val)	4.4	7.9	-	-	-	-
335A	ILE* (Leu)	3.1	41.1	-	-	+	+
			(Tyr) B				
336A	THR	4.1	1.1	-	-	-	-
337A	LEU*	3.6	41.5	-	-	+	-
350A	MET*	4.1	6.3	-	-	+	-
352A	PHE*	3.1	39.5	-	+	-	-
407A	TYR*	3.3	38.8	+	+	+	-
444A	TYR*	3.5	29.0	-	-	+	+
600A	FAD	3.9	25.1	+	-	-	-

Table 1.5: Comparative sequence analysis of zMAO with human MAO isoforms

Shown are the MAO A residues in contact with inhibitor Harmin700A in PDB entry 2Z5X ; in parentheses are the corresponding residues in zMAO, bold ones are potentially important; in red are the corresponding residues in human MAO-B. The data is obtained by the PyMOL Molecular Graphics System (DeLano Scientific, Palo Alto, CA). Legends are as follows:

Dist - nearest distance (Å) between atoms of the ligand and the residue.

Surf - contact surface area (Å²) between the ligand and the residue

HB - hydrophilic-hydrophilic contact (hydrogen bond)

Arom - aromatic-aromatic contact

Phob - hydrophobic-hydrophobic contact

DC - hydrophobic-hydrophilic contact (destabilizing contact)

+/- - indicates presence/absence of a specific contacts

* - indicates residues contacting ligand by their side chain (including CA atoms)

1.2.3 Importance of Zebrafish in Drug Development

Zebrafish are vertebrate organisms originating from Southeast Asia that merit increasing attention for developmental biology & drug development studies. Their rapid growth rate, easy to maintain features, breeding in large quantities and inexpensive costs make them suitable for pharmacological practices. The fact that zebrafish embryos develop outside of the mother and are transparent creates a special condition for studying teratology (Lieschke and Currie 2007). The zebrafish genome has been sequenced recently and consequently increased the utility of this organism (Peitsaro 2007) (Jönsson 2007). Comparative studies show that zebrafish genes share high structural and functional similarities with their human homologs as well sharing extensive conserved fragments (Lieschke and Currie 2007). Thus, overall, studying the zebrafish would aid scientists in understanding various human diseases. Zebrafish are also shown to be an ideal organism in which to study Parkinson's disease (Salzmann 2006). As mentioned earlier, Parkinson's is one of the most common neurodegenerative diseases among the elderly and no drug that effectively treats the disease is available to date. Most animal models of Parkinson's are based on the use of the MPTP neurotoxin (1-methyl-4-phenyl-1,2,3,6-tetrahydropyridine) which is metabolized to MPP⁺ by MAO B. MPP⁺ leads to dopaminergic neuron apoptosis in the substantia nigra of mammals (Salzmann 2006). Zebrafish have the same MPTP metabolism as humans and their brain contains catecholaminergic and serotonergic neuron populations and is potentially a feasible model for Parkinson's disease studies (Salzmann 2006). MAO enzymes are known to have a role in Parkinson's, and, prior to utilizing zebrafish for Parkinson's studies, details of zebrafish MAO reaction mechanism are required.

1.3 Dissertation Objectives

There are two forms of Monoamine oxidases in mammals but there is only one form in teleost. Genome of zebrafish contains one single copy of MAO that has 70% sequence identity to human MAO isoforms. The selective differences between human isoforms have been puzzling since discovered; therefore analysis of a single form of the enzyme to understand the origins of MAO is significant. The main objective of this dissertation is to understand why humans have two forms of MAO genes. My approach is to identify the single MAO from zebrafish in comparison to human MAO isozymes as outlined accordingly:

(1) Developing a high-level expression and purification system for zebrafish MAO:

Our laboratory has already developed expression systems for rat MAO B and human MAO isoforms using yeast *Pichia pastoris* (Newton-Vinson 2000; Li 2002; Upadhyay 2008). The first objective of my dissertation is to utilize these systems for expression and purification of zebrafish MAO. Chapter 2 provides a detailed description for expression and purification of zebrafish MAO to obtain sufficient amounts of the enzyme for further analyses.

(2) Determination of the substrate and inhibitor properties of zebrafish MAO:

The second aim of my dissertation is to provide detailed understanding on the inhibitor and substrate selectivity of this enzyme and to compare the properties with human MAO A and human MAO B. Human MAO isoforms have specific substrate and inhibitor

properties despite their high sequence identity. The zebrafish, which contains a single MAO, is proposed to be the precursor for human MAO enzymes with properties of both A and B. In addition, selective advantages of the zebrafish in pharmacological applications make the analysis of zebrafish MAO crucial for using this organism as a model to develop better MAO inhibitors. To date, there is no detailed identification and characterization of the protein available in the literature.

(3) *Quantitative structure-activity relationship (QSAR) analysis of zebrafish MAO:*

The third objective of my dissertation is to utilize several benzylamine and phenylethylamine analogues to analyze the structure-activity relationship of zebrafish MAO. Previously *para*-substituted benzylamine and *meta*-substituted phenylethylamine analogues were analyzed comparatively with MAO A and MAO B (Walker 1994; Miller 1999). It was shown that the MAO A isoform exhibits a strong influence from electronic effects of the *para*- substituent; MAO B does not (Walker 1994; Miller 1999). As proposed, the main influence behind this effect is the orientation of the benzyl ring in the active site. Therefore, while the conformation of the substrate leads to an electronic effect on reaction rate in human MAO A, it does not show any electronic effect on substrate turnover in human B. Of interest is to determine which behavior zebrafish MAO exhibits. Thus, chapter 4 of this thesis outlines the comparative investigation of zebrafish MAO QSAR properties with a variety of *meta*- and *para*-substituted benzylamines as well as *meta*- and *para*- substituted phenylethylamines to understand the active site structure in depth. These are the main objectives of this dissertation.

1.4 References:

- Akopyan, Z. I., Veryovkina, I.V., Levyant, M.I., Moskvitina, T.A., Gorkin, V.Z., Orekhovich, V.N. (1971). "On the isolation and purification of structure-bound proteins. Monoamine oxidases of mitochondrial membranes." Int J Protein Res **3**(3): 121-9.
- Anderson, N. J. T., Robin J.; Husbands, Stephen, M.; Nutt, David, J.; Hudson, Alan, L.; Robinson, Emma, S. J. (2006). "In vitro and ex vivo distribution of [3H]harmaline, an endogenous beta-carboline, in rat brain." Neuropharmacology **50**(3): 269-76.
- Anichtchik, O., Sallinen, V., Peitsaro, N., Panula, P. (2006). "Distinct structure and activity of monoamine oxidase in the brain of zebrafish (*Danio rerio*)." Journal of Comparative Neurology **498**(5): 593-610.
- Bach, A. W., N. C. Lan, Johnson, D.L., Abell, C.W., Bembenek, M.E., Kwan, S.W., Seeburg, P.H., Shih, J.C. (1988). "cDNA cloning of human liver monoamine oxidase A and B: molecular basis of differences in enzymatic properties." Proc Natl Acad Sci U S A **85**(13): 4934-8.
- Bernheim, F. (1984). Guide to the Frederick Bernheim and Molly Bernheim Interview, 1984. The Duke University Medical Center. North Carolina, Archives and Memorabilia Department: 24.
- Bianchi, P., Kunduzova, O., Masini, E., Cambon, C., Bani, D., Raimondi, L., Seguelas, M. H., Nistri, S., Colucci, W., Leducq, N., Parini, A. (2005). "Oxidative stress by monoamine oxidase mediates receptor-independent cardiomyocyte apoptosis by serotonin and postischemic myocardial injury." Circulation **112**(3297-3305).
- Binda, C., Hubalek, F., Li, M., Edmondson, D. E., Mattevi, A. (2004). "Crystal structure of human monoamine oxidase B, a drug target enzyme monotonically inserted into the mitochondrial outer membrane." FEBS Lett **564**(3): 225-8.
- Binda, C., M. Li, Hubalek F., Restelli, N., Edmondson, D.E., Mattevi, A. (2003). "Insights into the mode of inhibition of human mitochondrial monoamine oxidase B from high-resolution crystal structures." Proc Natl Acad Sci U S A **100**(17): 9750-9755.

- Binda, C., Mattevi, A., Edmondson, D. E. (2002). "Structure-function relationships in flavoenzyme-dependent amine oxidations. A comparison of polyamine oxidase and monoamine oxidase." Journal of Biological Chemistry **277**(27): 23973-23976.
- Binda, C., Newton-Vinson, P., Hubalek, F., Edmondson, D. E., Mattevi, A. (2002). "Structure of human monoamine oxidase B, a drug target for the treatment of neurological disorders." Nat Struct Biol **9**(1): 22-6.
- Binda, C., Wang, J., Li, M., Hubálek, F., Mattevi, A., and Edmondson, D. E. (2008). "Structural and mechanistic studies of arylalkylhydrazine inhibition of human monoamine oxidases A and B." Biochemistry **47**: 5616-5625.
- Caspi A, M. J., Moffitt T, Mill J, Martin J, Craig I, Taylor A, Poulton R (2002). "Role of genotype in the cycle of violence in maltreated children." Science **297**(5582): 851-4.
- Checkoway, H., Franklin, GM., P. Costa-Mallen, T. Smith-Weller, J. Dilley, P. D. Swanson, L. G. Costa (1998). "A genetic polymorphism of MAO-B modifies the association of cigarette smoking and Parkinson's disease." Neurology **50**(5).
- Chen, J. J., Swope, D. M. (2007). "Pharmacotherapy for Parkinson's disease. ." Pharmacotherapy **27**(161-173).
- Chen, K., H. F. Wu, et al. (1996). "Influence of C terminus on monoamine oxidase A and B catalytic activity." J Neurochem **66**(2): 797-803.
- Chen, K., Wu, H. F. Grimsby, Shih, J. C. (1994). "Cloning of a novel monoamine oxidase cDNA from trout liver." Mol Pharmacol **46**(6): 1226-33.
- Coccini, T., Castoldi, A. F., Gandini, C., Randine, G., Vittadini, G., Baiardi, P., Manzo, L. (2002). "Platelet monoamine oxidase b activity as a state marker for Alcoholism: trend over time during withdrawal and influence of smoking and gender " Alcohol alcohol **37**: 566-572.
- De Colibus, L., Li, M., Binda, C., Lustig, A., Edmondson, D. E., Mattevi, A. (2005). "Three-dimensional structure of human monoamine oxidase A (MAO A): Relation to the structures of rat MAO A and human MAO B." Proc Natl Acad Sci U S A **102**(36): 12684-12689.

- Edmondson, D. E., Bhattacharyya, A. K., Walker, M. C. (1993). "Spectral and kinetic studies of imine product formation in the oxidation of p-(N,N-dimethylamino)benzylamine analogues by monoamine oxidase B." Biochemistry **32**(19): 5196-202.
- Edmondson, D. E., Binda, C., Mattevi, A. (2004). "The FAD binding sites of human monoamine oxidases A and B." Neurotoxicology **25**(1-2): 63-72.
- Edmondson, D. E., Binda, C., Wang, J., Upadhyay, A., Mattevi, A. (2009). "Molecular and Mechanistic Properties of the Membrane-Bound Mitochondrial Monoamine Oxidases." Biochemistry **48**(20): 4430-4230.
- Edmondson, D. E., DeColibus, L., Binda, C., Li, M., Mattevi, A. (2007). "New insights into the structures and functions of human monoamine oxidases A and B." Journal of Neural Transmission **114**(6): 703-705.
- Edmondson, D. E., Ghisla, S. (1999). "Flavoenzyme structure and function. Approaches using flavin analogues." Methods Mol. Biol. **131**(157-79).
- Edmondson, D. E., A. Mattevi, Binda, C., Li, M., Hubalek, F. (2004). "Structure and mechanism of monoamine oxidase." Curr Med Chem **11**(15): 1983-93.
- Fowler, C. J., B. A. Callingham, Houslay, M.D. (1977). "The effect of tris buffers on rat liver mitochondrial monoamine oxidase." J Pharm Pharmacol **29**(7): 411-5.
- Fowler, J., Volkow, ND., Wang, GJ., Pappas, N., Logan, J, MacGregor, R, Alexoff, D, Wolf, AP, Warner, D, Cilento, R, Zezulkova, I (1998). "Neuropharmacological actions of cigarette smoke: brain monoamine oxidase B (MAO B) inhibition." Journal of addictive diseases **17**(1): 23-34.
- Fowler, J., Wiberg., Orelund, L., Marcusson, J., Winblad, B. (1980). "The effect of age on the activity and molecular properties of human brain monoamine oxidase." J Neural Transm **49**: 1-20.
- Ghisla, S., Hemmeric., P. (1971). "New Flavocoenzymes." Angewandte Chemie-International Edition **10**(11): 833-&.
- Hare, M. (1928). "Tyramine oxidase. I. A new enzyme system in liver." Journal of Biochemistry **22**(): 968-979.

- Hiro, I., Tsugeno, Y., Hirashiki, I., Ogata, F., Ito, A. (1996). "Characterization of rat monoamine oxidase A with noncovalently-bound FAD expressed in yeast cells." Journal of Biochemistry **120**(4): 759-65.
- Hubalek, F., Binda, C., Li, M., Herzig Y., Sterling J., Youdim M., Mattevi A., Edmondson D.E. (2004). "Inactivation of purified human recombinant monoamine oxidases A and B by rasagiline and its analogues." J Med Chem **47**(7): 1760-6.
- Hubalek, F., Binda, C., Khalil, A., Li, M., Mattevi, A., Castagnoli, N., Edmondson, D. E. (2005). "Demonstration of isoleucine 199 as a structural determinant for the selective inhibition of human monoamine oxidase B by specific reversible inhibitors." Journal of Biological Chemistry **280**(16): 15761-15766.
- Husain, M., Edmondson, D.E. (1982). "Kinetic studies on the catalytic mechanism of liver monoamine oxidase." Biochemistry **21**(3): 595-600.
- Jönsson, M.E., Orrego, R., Woodin, B.R., Stegeman, J. J., Goldstone, J.V. (2007). "Basal and 3,3',4,4',5-pentachlorobiphenyl-induced expression of cytochrome P450 1A, 1B and 1C genes in zebrafish." Toxicol Appl Pharmacol. **221**(1):29-41"
- Kalir, A., A. Sabbagh, Youdim, M. (1981). "Selective acetylenic 'suicide' and reversible inhibitors of monoamine oxidase types A and B." Br J Pharmacol **73**(1): 55-64.
- Kline, N. S. (1958). "Clinical experience with iproniazid (marsilid)." J Clin Exp Psychopathol **19**(2, Suppl. 1): 72-8; discussion 78-9.
- Lan, N. C., C. H. Chen, et al. (1989). "Expression of functional human monoamine oxidase A and B cDNAs in mammalian cells." J Neurochem **52**(5): 1652-4.
- Lea, R., Chambers, G. (2007). "Monoamine oxidase, addiction, and the "warrior" gene hypothesis." N. Z. Med. J **120**: 1250.
- Li, M., Hubalek, F., Newton-Vinson, P., Edmondson, D. E. (2002). "High-level expression of human liver monoamine oxidase A in *Pichia pastoris*: comparison with the enzyme expressed in *Saccharomyces cerevisiae*." Protein Expr Purif **24**(1): 152-62.
- Lieschke, G. J. and P. D. Currie (2007). "Animal models of human disease: zebrafish swim into view." Nature Reviews Genetics **8**(5): 353-367.

- Lotufo-Neto F, T. M., Thase ME (1999). "Meta-analysis of the reversible inhibitors of monoamine oxidase type A moclobemide and brofaromine for the treatment of depression." Neuropsychopharmacology **20**(3): 226-47.
- Maurel, A., Hernandez, C., Kunduzova, O., Bompart, G., Cambon, C., Parini, A., Frances, B. (2003). "Age-dependent increase in hydrogen peroxide production by cardiac monoamine oxidase A in rats." Am. J. Physiol. **284**: 1460-1467.
- Mc Dermott, T. D., Cowden, J., Frazzetto G., Johnson D.P. (2009). "Monoamine oxidase A gene (MAOA) predicts behavioral aggression following provocation." Proc Natl Acad Sci U S A **106**(7): 2118-2123.
- Medvedev, A. D., A. V. Veselovsky, V. I. Shvedov, O. V. Tikhonova, T. A. Moskvitina, O. A. Fedotova, L. N. Axenova, N. S. Kamyshanskaya, A. Z. Kirkel, and A. S. Ivanov*† (1998). "Inhibition of Monoamine Oxidase by Pirlindole Analogues: 3D-QSAR and CoMFA Analysis Abstract." J. Chem. Inf. Comput. Sci. **38**(6): 1137-1144.
- Medvedev, A. E., Kirkel, A.A., Kamyshanskaya, N.S., Moskvitina, T.A., Axenova, L.N., Gorkin, V.Z., Andreeva, N.I., Golovina, S.M., Mashkovsky, M.D. (1994). "Monoamine oxidase inhibition by novel antidepressant tetrindole." Biochem Pharmacol. **47**(2): 303-8.
- Milczek, E. M., Bonivento, D., Binda, C., Mattevi, A., McDonald, I. A., Edmondson, D. E. (2008). "Structural and Mechanistic Studies of Mofegiline Inhibition of Recombinant Human Monoamine Oxidase B." Journal of Medicinal Chemistry **51**(24): 8019-8026.
- Miller, J. R. and D. E. Edmondson (1999). "Influence of flavin analogue structure on the catalytic activities and flavinylation reactions of recombinant human liver monoamine oxidases A and B." Journal of Biological Chemistry **274**(33): 23515-25.
- Miller, J. R. and D. E. Edmondson (1999). "Structure-activity relationships in the oxidation of para-substituted benzylamine analogues by recombinant human liver monoamine oxidase A." Biochemistry **38**(41): 13670-83.

- Nagy, J., W. C. Kenney, Singer, T. (1979). "The reaction of phenylhydrazine with trimethylamine dehydrogenase and with free flavins." Journal of Biological Chemistry **254**(8): 2684-8.
- Nandigama, R. K. and D. E. Edmondson (2000). "Influence of FAD structure on its binding and activity with the C406A mutant of recombinant human liver monoamine oxidase A." Journal of Biological Chemistry **275**(27): 20527-32.
- Newton-Vinson, P., Hubalek, F., Edmondson, D. E. (2000). "High-level expression of human liver monoamine oxidase B in *Pichia pastoris*." Protein Expr Purif **20**(2): 334-45.
- Patek, D. R. and L. Hellerman (1974). "Mitochondrial monoamine oxidase. Mechanism of inhibition by phenylhydrazine and by aralkylhydrazines. Role of enzymatic oxidation." Journal of Biological Chemistry **249**(8): 2373-80.
- Peitsaro, N., M. Sundvik, Anichtchik, O., Kaslin, J., Panula, P. (2007). "Identification of zebrafish histamine H-1, H-2 and H-3 receptors and effects of histaminergic ligands on behavior." Biochemical Pharmacology **73**(8): 1205-1214.
- Ramsay, R. R. (1997). "Mechanistic study of monoamine oxidase: significance for MAO A and MAO B in situ." Vopr Med Khim **43**(6): 457-70.
- Ramsay, R. R., A. K. Tan, Weyler, W. (1994). "Kinetic properties of cloned human liver monoamine oxidase A." J Neural Transm Suppl **41**: 17-26.
- Rebrin, I., R. M. Geha, Chen, K., Shih, J. (2001). "Effects of carboxyl-terminal truncations on the activity and solubility of human monoamine oxidase B." Journal of Biological Chemistry **276**(31): 29499-506.
- Sallinen, V., M. Sundvik, Reenilä, I., Peitsaro, N., Khrustalyov, D., Anichtchik, O., Toleikyte, G., Kaslin, J., Panula, P. (2009). "Hyperserotonergic phenotype after monoamine oxidase inhibition in larval zebrafish." Journal of Neurochemistry **109**(2): 403-415.
- Salzmann, J., Anichtchik, O., Best, J., Richards, F., Fleming, A., Roach, A., Goldsmith, P. (2006). "P1 Development of a MPTP model of Parkinson's disease in zebrafish." Behavioural Pharmacology **17**(5-6): 541-541.

- Sandler, M., Reveley, M.A., Glover, V. (1981). "Human platelet monoamine oxidase activity in health and disease: a review." Journal of Clinical Pathology **34**: 292-302.
- Setini, A., F. Pierucci, Senatori, O., Nicotra, A. (2005). "Molecular characterization of monoamine oxidase in zebrafish (*Danio rerio*)." Comparative Biochemistry and Physiology B-Biochemistry & Molecular Biology **140**(1): 153-161.
- Son, S.-Y., Ma, Jichun., Youhei, Kondou., Masato, Yoshimura., Eiki, Yamashita., Tomitake, Tsukihara. (2008). "Structure of human monoamine oxidase A at 2.2-Å resolution: The control of opening the entry for substrates/inhibitors." Proc Natl Acad Sci U S A **105**(15): 5739-5744.
- Sparks, D. L. and N. S. Buckholtz (1985). "Combined inhibition of serotonin uptake and oxidative deamination attenuates audiogenic seizures in DBA/2J mice." Pharmacol Biochem Behav **23**(5): 753-7.
- Stanhope, M. J., A. Lupas, M.J. Italia, K.K. Koretke, V.C. Volker, and J.R. Brown (2001). "Phylogenetic analyses do not support horizontal gene transfers from bacteria to vertebrates. ." Nature **411**: 940-944.
- Sterling, J., A. Veinberg, Lerner, D., Goldenberg, W., Levy, R., Youdim, M., Finberg, J. (1998). "(R)(+)-N-propargyl-1-aminoindan (rasagiline) and derivatives: highly selective and potent inhibitors of monoamine oxidase B." J Neural Transm Suppl **52**: 301-5.
- Tipton, K. F. (1972). "Some properties of monoamine oxidase." Adv Biochem Psychopharmacol **5**: 11-24.
- Tipton, K. F., A. M. O'Carroll, et al. (1983). "Factors involved in the selective inhibition of monoamine oxidase." Mod Probl Pharmacopsychiatry **19**: 15-30.
- Upadhyay, A. K., P. P. Borbat, et al. (2008). "Determination of the oligomeric states of human and rat monoamine oxidases in the outer mitochondrial membrane and octyl beta-D-glucopyranoside micelles using pulsed dipolar electron spin resonance spectroscopy." Biochemistry **47**(6): 1554-1566.
- Upadhyay, A. K., Edmondson, D. E. (2008). "Characterization of detergent purified recombinant rat liver monoamine oxidase B expressed in *Pichia pastoris*." Protein Expr Purif **59**(2): 349-356.

- Walker, M. C. and D. E. Edmondson (1994). "Structure-activity relationships in the oxidation of benzylamine analogues by bovine liver mitochondrial monoamine oxidase B." Biochemistry **33**(23): 7088-98.
- Weyler, W. (1989). "Monoamine oxidase A from human placenta and monoamine oxidase B from bovine liver both have one FAD per subunit." Biochem J **260**(3): 725-9.
- Weyler, W. (1994). "Functional expression of C-terminally truncated human monoamine oxidase type A in *Saccharomyces cerevisiae*." J Neural Transm Suppl **41**: 3-15.
- Wolf, P., Feldman, R.G., Saint-Hilaire, M. (1991). "Precursors and natural history of Parkinson's disease: the Framingham study." Neurology **41**: 341.
- Youdim, M. B., Riederer, P. F. (2004). "A review of the mechanisms and role of monoamine oxidase inhibitors in Parkinson's disease." Neurology **63**(7 Suppl 2): S32-5.
- Zeller, E. A. (1974). "On the physico-chemical characterization of monoamine oxidase (MAO) as a basis for the study of its role in physiological and pathological processes." J Psychiatr Res **11**: 329-32.
- Zhang, Z., Chen, K., Shih, J.C, Teng, C.T. (2006). "Estrogen-related receptors stimulated MAO-B promoter activity is down regulated by estrogen receptors." Molecular Endocrinology **20**(7): 1547-61.
- Zhou, B. P., Wu, B., Kwan, S. W., Abell, C. W. (1998). "Characterization of a highly conserved FAD-binding site in human monoamine oxidase B." Journal of Biological Chemistry **273**(24): 14862-8.

CHAPTER 2

High-level expression and purification of zebrafish monoamine oxidase in *Pichia pastoris*

2.1 Introduction

To understand the molecular basis of the differences between human MAO A (hMAO A) and human MAO B (hMAO B) and to discover the characteristics of a single MAO enzyme in zebrafish, we have developed an expression and purification system for zebrafish MAO (zMAO). Studies have shown that the sequence of the zMAO (E.C. 1.4.3.4) gene exhibits approximately 70% sequence identity with those genes encoding the hMAO A and hMAOB (GenBank accession no. [AAO16681](#)) (Anichtchik 2006) (Setini 2005). In addition, studies done with zebrafish tissue fractions show that zMAO displays several catalytic properties common to both human MAO enzymes when it comes to the substrate and inhibitor specificities (Sallinen 2009) (Setini 2005) (Salzmann 2006).

To investigate the catalytic properties of purified zMAO, we have developed efficient expression and large-scale purification procedure using *Pichia pastoris* as a host. Methylotrophic yeast *Pichia pastoris* was also used for expressing large quantities of human (Li, Hubalek et al. 2002) (Newton-Vinson, Hubalek et al. 2000) and rat MAO enzymes (Upadhyay 2008) previously in our laboratory. Currently, there are a small number of examples of yeast expression systems developed for zebrafish proteins in the literature (Chung, Sen et al. 2004) (Goldstone, Jonsson et al. 2009). Hence, the high-level

heterologous expression method described in this chapter is one of the few examples of using yeast system to express a zebrafish protein.

Approximately 600 mg of purified zMAO can be expressed from 2 L of *Pichia* fermentation culture and purified in ~30% yield. We characterized the protein in detail and identified the kinetic parameters using several MAO A and MAO B specific substrates and inhibitors. The data presented in this chapter shows that zMAO exhibits functional properties of both human isozymes. These studies provide the groundwork to determine the structural properties of zMAO in detail.

2.2 Materials and Methods

2.2.1 Materials

Molecular Biology

Monoamine Oxidase cDNA in zebrafish (*Danio Rerio*) was provided from Open Biosystems, (Clone ID: 6960301) and stored at -80 °C at all times. TOPO Cloning Kit, the plasmids (pCR2.1 and pPIC3.5K), the Platinum *Taq* polymerase, and yeast strain KM71 were purchased from Invitrogen Corp (Carlsbad, CA). Restriction enzymes and T4 DNA Ligase were provided from Promega (Madison, WI). MiniElute Gel Extraction Kit, QIAprep Spin Miniprep Kit, MinElute Gel Extraction Kit was provided from Qiagen (Valencia, CA). The antibiotic G418 was purchased from Mediatech (Herndon, VA).

Purification

β -Octylglucopyranoside was obtained from Anatrace Inc (Maumee, OH). Reduced Triton X-100 was obtained from Fluka (Sigma-Aldrich, St. Louis, MO). Ceramic Hydroxyapatite column medium was purchased from BioRad (Hercules, CA).

Analytical Procedures

Buffers used for preparation of the in-gel digest from gel electrophoresis separated zMAO were prepared as described by Pierce Co (Rockford, IL). Trypsin was purchased from Promega (Madison, WI) Chymotrypsin was purchased from Roche, Waters Corp (Germany). HPLC columns and sep-Pak short body cartridge were purchased from Phenomenex (Torrance, CA). All other chemicals were purchased from Sigma-Aldrich (St. Louis, MO) unless otherwise stated.

2.2.2 Cloning of zebrafish MAO

The open reading frame (ORF) cDNA was amplified by PCR with custom primers. The forward primer was 5'-CCCG^AGATCCATGACTGCGAACGCATACGAC-3' which includes a *Bam*HI site (underlined); in the frame start codon and 21-bp gene-specific sequence. The reverse primer was 5'-GGCG^AAATTCTTAACACCGTGGGAGGA GCCC-3' which incorporated the *Eco*RI site (underlined) and the translation stop codon.

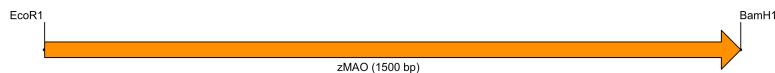


Figure 2.1 Representation of the zMAO gene before incorporation into the TOPO plasmid

The PCR conditions were 95 °C for 1 min, followed by 35 cycles of 95 °C /60 °C /72 °C for 50 sec/50 sec/2 min respectively. The gene was then A-tailed with Platinum *Taq* DNA Polymerase at 72 °C with a final extension of 15min. The template had a 20 ng final concentration. The size of amplified zMAO gene (1.5 kB) was determined by agarose gel electrophoresis, isolated and directly ligated into a pCR2.1-TOPO vector using TOPO Cloning Kit as per the manufacturer's protocol.

The ligate was then transferred into TOP10 cells and the cloned plasmid was obtained from the overnight culture using a QIAprep Spin Miniprep Kit. The gene was cut from the vector using *EcoRI* and *BamHI* restriction enzymes, products were separated on an agarose gel, and the linear DNA in a discrete band was extracted with MinElute Gel Extraction Kit followed by ligation into *Pichia* yeast vector pPIC3.5K using T4 DNA ligase. MAO gene and the T4 Ligase were incubated at room temperature for 1 hour, followed by incubation at 14 °C overnight. The ligation product was then transformed into electro-competent *E.coli* XL Blue cells via electrophoration. Selected colonies were grown in ampicillin-containing liquid media at 37 °C. DNA sequence analysis by Agencourt Corp (Beverly, MA) confirmed the correct insertion and orientation of the zMAO gene using an ABI Prism automated DNA sequencer.

2.2.3 Transformation of zebrafish MAO gene into *P. Pastoris*

The pPIC3.5K/zMAO construct was linearized with *SacI* enzyme to target integration into the AOX1 locus in the *Pichia* genome. The spheroplast transformation procedure used the KM71 strain and was performed as described in the Invitrogen *Pichia* expression kit manual.

2.2.4 Expression of zebrafish MAO

Screening of expression levels of zMAO transformants:

Colonies were then transferred to plates containing different concentrations of the antibiotic G418/ml (0.25 to 1.25 mg) to select for multiple gene insertion. Dose dependent appearances of colonies were detected after 4 days at 30 °C. Several G418

resistant colonies were chosen from each plate for small-scale expression in shake flasks as described previously (Newton-Vinson, Hubalek et al. 2000). Expression levels were monitored by activity assays using kynuramine as a substrate and the colony exhibiting the highest zMAO activity was selected. A stock culture was stored at -80 °C in 20% glycerol (v/v). Fermentation growth and over-expression was carried out as described previously for, human MAO A (Li, Hubalek et al. 2002).

Fermentation Procedure

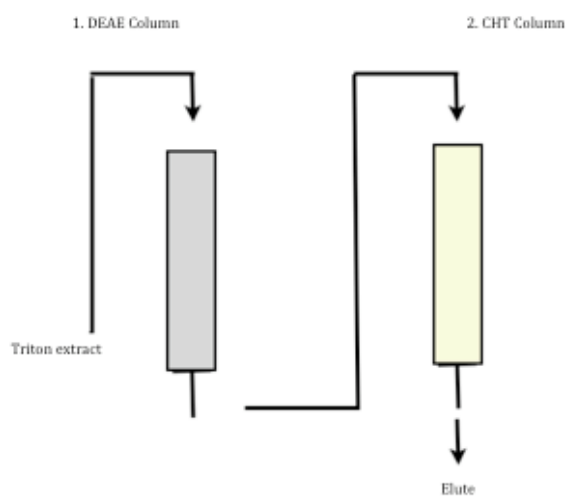
The transformant was subjected to fermentation-scale expression to obtain high levels of protein. The protocol used for zMAO high-level expression was adopted from high-level expression of human MAO A in *Pichia pastoris* (Li, Hubalek et al. 2002). After the fermentation, the cells were harvested by centrifugation at 4500 rpm for 10 minutes at 4 °C followed by washing with a breakage buffer (50 mM sodium phosphate, 5% glycerol, 1 mM EDTA, 1 mM PMSF pH =7.5) twice. The stock cells were stored at -80 °C.

2.2.5 Purification of zebrafish MAO

Zebrafish MAO was purified as using a protocol similar to that published for human MAO A (Li, Hubalek et al. 2002) with a number of modifications. The thawed cell paste was suspended in a 50 mM sodium phosphate buffer containing 1 mM EDTA, 1 mM PMSF and 5% glycerol and subjected to high-speed blending in a Biospec Bead-beater (Bartlesville, OK) with silica-zirconia beads (0.5 mm in diameter) in equal volume. Cell breakage occurred with 8 cycles, 2 min beating and 6 min cooling on a salt/ice bath. The cell lysate was separated from glass beads by filtration of the homogenate through a layer

of Micro-cloth (Calbiochem, EMD Chemicals Inc, Gibbstown, NJ). Unbroken cells and large cell debris were removed by centrifugation at 1000 g for 10 min at 4 °C.

The supernatant was collected and centrifuged at 100,000 g for 30 min. The pellet was resuspended in 0.1 M triethanolamine (TEA) buffer, pH 7.2 containing 25 mM CaCl₂. Membrane phospholipids were digested by incubation with 1 mg of phospholipase C (Type 1 from *C.perfringens*, Sigma) and 6700 units of phospholipase A₂ (partially purified from *Naja Naja* venom (Cremona and Kearney 1964) per 500 mg total protein. The digestion was carried with constant stirring at room temperature and pH maintained between 7.0 – 7.2 with 2 N NH₄OH in the dark. The suspension was centrifuged at 100,000g for 15 min at 4 °C and the pellet re-suspended into 10 mM potassium phosphate (pH= 7.5) to a final protein concentration of ~ 15 mg/mL. Triton X-100 was added to this suspension to a final concentration of 0.5% (w/v) and the mixture stirred at room temperature in the dark for 30 min followed by centrifugation at 100,000g for 15 min yielding bright yellow supernatant (Triton extract), containing zMAO activity.



Scheme 2.1 Representation of the system that is maintained during column purification of zMAO

Preliminary trials showed no zMAO activity bound to DEAE Sepharose or to Biorad High-Q resin unlike what is observed with hMAO A and hMAOB. Therefore, an alternate column purification procedure was developed. The DEAE Sepharose column provides some purification by removing contaminating protein from the Triton extract. Further experiments showed that zMAO binds to CHT (Ceramic Hydroxyapatite) column; therefore this resin was used for removal of contaminating proteins and the Triton detergent. Experimental details are as follows: the Triton extract was loaded onto a fast-flow DEAE-Sepharose ion-exchange column (25x600 mm) equilibrated with 20 mM potassium phosphate buffer with 0.5% (w/v) Triton X-100 and washed with one column volume of 20 mM potassium phosphate buffer (pH =7.2). The elute from the DEAE-column containing zMAO activity was combined and uploaded to a CHT (Ceramic Hydroxyapatite) column which was pre-equilibrated with 10 mM potassium phosphate buffer containing 20% glycerol and 0.5% (w/v) Triton X-100. The column was then washed with 10 mM potassium phosphate buffer containing 20% glycerol, 1 mM PMSF and 0.8% (w/v) OGP until the A_{280} of the flow-out dropped to negligible levels. zMAO was eluted from CHT column with a linear gradient of 10-300 mM potassium phosphate buffer containing 20% glycerol, 30 mM DTT, 0.8% (w/v) OGP and 1 mM PMSF (pH = 7.2). The procedure is represented in Scheme 2.1. Fractions with a $A_{280/450}$ ratio of less than 17 were combined and concentrated via Amicon Ultra 30K filter centrifugation and stored in 25 mM potassium phosphate buffer containing 20% glycerol and 0.8% (w/v) OGP (pH =7.2) in the dark at 4 °C.

2.2.6. Determination of the Protein Content

Biuret Method

The Biuret protein assay was used to determine the concentrations of more than 1mg/ml protein and was applied as described by Gornall, Bardwill and David. (Gornall 1949) The assay was standardized with bovine serum albumin (BSA) and fresh reagent was prepared prior to measurements.

Bearden Method

The Bearden protein assay was utilized for low concentrations of protein (< 1mg/ml) and was conducted as described by Bearden (Bearden 1978). BSA standard curve was used to determine the unknown protein concentration; each measurement was repeated with two different amounts (or more if necessary) of protein.

2.2.7 Steady-State Kinetics

All enzyme assays were carried out spectrophotometrically in 50 mM potassium phosphate buffer (pH= 7.4) with 0.5% (w/v) reduced Triton X-100 using a Perkin-Elmer Lambda-2 UV-Vis spectrophotometer at 25 °C. Kynuramine was used as a substrate during the purification procedure and thermal stability measurements. Activity assays were done via following the change in absorbance at 316 nm for the product 4-hydroxyquinone absorbance $\Delta\epsilon=12,000 \text{ M}^{-1}\text{cm}^{-1}$ (Wyler et al 1985). One unit activity of zMAO was defined as the amount of enzyme that is able to catalyze the formation of 1 μmole 4-hydroxyquinone per minute. An amplex red peroxidase-coupled spectrophotometric assay was used to assay the amine substrate phenylethylamine and

$[\alpha,\alpha,]^2\text{H}_2$]-phenylethylamine using method described previously (Holt et al.) The primary deuterium kinetic isotope effect of benzylamine oxidation was determined using $[\alpha,\alpha,]^2\text{H}_2$]-benzylamine as substrate. Formation of the oxidation product (benzaldehyde, $\Delta\epsilon_{250} = 12,800 \text{ M}^{-1} \text{ cm}^{-1}$) was followed when benzylamine was used as a substrate. For all the phenylethylamine measurements amplex-red peroxidase coupled assay was used. Anaerobic conditions were achieved by applying sufficient (about 10) argon – vacuum cycles to the enzyme solutions in a custom designed cuvette.

2.2.8 Mass Spectroscopy

MALDI-TOF mass spectral measurements for zMAO sequence analyses were performed on the in-gel tryptic digested zMAO. An in-gel digestion protocol designed for gel electrophoresis separated proteins (Pierce Co, Rockford, IL) was followed with some modifications. Prior to in-gel digestion the enzyme was reduced with DTT at 90 °C for 5 minutes to reduce all the disulfite bonds, and then cooled down to room temperature. Reduced and alkylated enzyme (5-10 ng) was first subjected to a 1-D gel electrophoresis separation and destained via a destaining solution at 37 °C for 30 minutes. Gel pieces containing the protein were shrunk by adding 50 μL of acetonitrile and incubated at room temperature for 15 minutes. Acetonitrile was removed and gel pieces were allowed to air-dry. Trypsin was then added to the tube (1:1 w/w ratio) and incubated at room temperature for 15 minutes. Digestion buffer was then added to the tube and sample was incubated at 37 °C for about 5 hours. The sample was dried in a speed vac and desalted via C18 ZipTip (Millipore). Approximately 1 μL of the peptide solution was spotted with an equal volume of α -cyano-4-hydroxycinnamic acid matrix in 70% (v/v) acetonitrile/water on the MALDI target.

2.2.9 HPLC Separation

Zebrafish MAO (~5 µg) was precipitated on ice with 100% (w/v) cold TCA to a final concentration of 20% (w/v) and then centrifuged for 10 min at 10,000x g. The pellet was washed twice with ice-cold water and re-suspended in 1 mL 0.1 M Tris.HCl, pH=8.0. Aliquots of trypsin and chymotrypsin were added to zMAO solution at a final ratio of approximately 1:20 (w/w) and the mixture was incubated at 37 °C for 20 hours under dark with constant stirring. Proteolytic enzymes were removed from the mixture by another TCA precipitation. The sample was then applied to a short body C18 separation column (Sep-Pak cartridge) for removal of undigested protein, salts and any non-binding peptides. Washing with two volumes of water followed by two volumes of ethanol and another two volumes of water equilibrated the small column. The peptide sample was applied to the column and washed with water while following the absorbance of 280 nm to monitor the washout. Once the absorbance at 280 nm decreased, flavinylated peptide was eluted via methanol and also detected under UV light. The sample then was subjected to roto-vap to remove excess solvent. The solution was then subjected to RP-HPLC separation on a Jupiter 5U C18 Column (300Å pore size, 250 x 4.6 mm) (Phenomenex). Elution of peptides was accomplished with a 70 min linear gradient of 3 to 40% (v/v) acetonitrile in 0.1% (v/v) TFA. Peptides absorbing at 350 nm were collected and subjected to MALDI-TOF.

2.2.10 Fluorescence Studies

The purified peptide was oxidized with performic acid to determine the nature of flavin attachment as described by Walker (Walker W. H. 1974) . The protein that was digested with trypsin and chymotrypsin and purified via small body column was oxidized with performic acid (Walker W. H. 1974). To accomplish performic acid oxidation, 1 nmole of flavin peptide was dissolved in 0.1 mL performic acid and incubated on ice for 2 hours followed by drying under vacuum. Peptides were subjected to a fluorometric analysis before and after oxidation. After measurement, the oxidized peptide was reduced by anaerobic dithionite titration to cleave the bond between flavin cofactor and the peptide (Edmondson and Singer 1976). The fluorescence measurement was repeated and the sample was left in dark for reoxidation.

2.2.11 Thermal Stability

To detect the thermal stability of the enzyme, zMAO was incubated at three different temperatures: 0 °C, 30 °C and 40 °C. The decrease and ultimate loss of the enzyme activity was determined in a 150 min time period. Each 10 min, 10 µL aliquots were removed for the determination of catalytic activity. The rate of 1 mM Kynuramine oxidation in 50 mM potassium phosphate buffer with 0.5% (w/v) reduced Triton X-100 (pH =7.5) was monitored at 316 nm.

2.2.12 Oxygen Affinity

$K_m(O_2)$ of zMAO was determined from steady-state assays. Using the Clarke-type oxygen electrode, the rate of oxygen consumption was measured using benzylamine / [α,α ,] 2H_2]-benzylamine and phenylethylamine / [α,α ,] 2H_2]-phenylethylamine as substrates. The dissolved oxygen concentrations in the reaction buffers were adjusted by mixing buffers purged with pure oxygen (960 μM in oxygen), pure nitrogen (60 μM oxygen), and at air saturation (240 μM oxygen) in required proportions. The concentrations of the dissolved oxygen in the reaction buffers were measured polarographically.

2.2.13 Data Analysis

Kinetic analyses were performed using software developed by either Origin (OriginLab Corporation, Northampton, MA) or Prism 5.0 (GraphPad Software). K_d values for benzylamine binding was calculated from steady-state deuterium kinetic isotope effect data as previously described by Klinman and Matthews (Klinman and Matthews 1985).

2.3 Results

2.3.1 Enzyme expression and purification

Previously our laboratory was able to express human MAO A (Li, Hubalek et al. 2002) and MAO B (Newton-Vinson, Hubalek et al. 2000) using the *Pichia* expression system. Since zMAO shares ~70% sequence identity with human MAO A and B enzymes, and has a similar codon bias, we employed the expression and purification procedures used successfully with the expressed recombinant zMAO.

We were able to express and purify >200 mg of zMAO with a 30% yield and a specific activity of 1.5 U/mg and a total activity of 310 U/mg from 125 g wet cells (Table 2.1). Similar to human MAO A and MAO B (Edmondson, Mattevi et al. 2004) recombinant zMAO, over-expressed in *Pichia*, is found to be a membrane-bound enzyme that requires phospholipase treatment and detergent extraction to liberate it from the mitochondrial membrane. All catalytic activity is found in the mitochondrial fraction of the cells as prepared according to the method (Daum, Bohni et al. 1982), demonstrating that expressed zMAO is localized in the mitochondria (presumably the outer membrane) as are the human enzymes.

One of the biggest differences in the purification procedure of zMAO, compared with the recombinant human enzymes is the column fractionation method for further purification of the TritonX-100-solubilized enzyme. Attempts to use anion exchange columns that are successfully used for human MAO A and human MAO B (DEAE Sepharose and High Q resin, respectively) to purify solubilized zMAO were unsuccessful. Eventually we found that the enzyme solution is able to bind to a different resin, Ceramic Hydroxyapatite (CHT). Additionally, we observed that using DEAE Sepharose resin prior to CHT removes some protein impurities; therefore, we coupled the DEAE Sepharose column, with the CHT column step and equilibrated both columns at pH 7.2 to obtain improved purification.

Purification Step	Total Protein (mg)	Total Activity (U ^a)	Specific Activity (U/mg)	% Yield
Cell Lysate	13619	1275	0.09	100
Membrane Fraction	7496	1043	0.14	82
Phospholipase Digestion	7268	958	0.13	75
Triton X-100 Extract	2440	912	0.37	72
DEAE-Sepharose	1450	758	0.52	60
Pooled CHT column fractions	205	310	1.52	25

Table 2.1. Purification Scheme for zebrafish MAO expressed in *Pichia pastoris*

^a 1U = 1 μmol kynuramine oxidation product per minute at 25 °C in air saturated 50 mM KPi, pH=7.4 buffer

2.3.2 Characterization of Zebrafish MAO

The purified recombinant zMAO preparation obtained on purification displays a single band on SDS-PAGE with a mobility similar to that of human MAO A (or MAO B) (Figure 2.2A) with an M_r value of approximately 60,000 Da. The recombinant protein is yellow in colour; a characteristic of flavoenzymes (Edmondson and Newton-Vinson 2001). Western blot analysis using antisera specific for covalent flavin (Barber, Eichler et al. 1987) and the failure to observe any release of flavin on trichloroacetic acid treatment show that zMAO contains a covalently bound flavin cofactor as does human MAO A and B (Figure 2.2B). Despite exhibiting an ~70% sequence identity with human MAO A, the enzyme does not cross-react immunochemically to anti-sera raised against human MAO A on Western blot analysis.

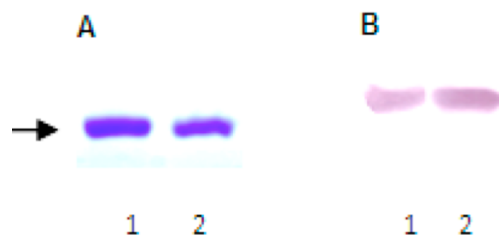


Figure 2.2: SDS-polyacrylamide gel electrophoresis of purified zMAO (lane 1) and human MAO A (lane 2)

(A) Coomassie-stained protein bands. (B) Western blot using antisera specific for covalent flavin coenzymes. Arrow signifies the 60 kD molecular weight. The enzyme does not exhibit a positive immunochemical response to antisera raised against human MAO A. Here, purified zMAO is shown to contain a covalently attached flavin and a molecular mass of (~60kD). These properties show a similarity to MAO A and to MAO B.

2.3.3 Spectral Properties

The UV-Vis absorption spectral properties of zMAO were monitored during inhibition with two inhibitors: clorgyline and deprenyl. Both clorgyline and deprenyl are selective (clorgyline: MAO A deprenyl: MAO B, respectively) and irreversible inhibitors. Likewise, zMAO is also inhibited by either inhibitor irreversibly through the formation of an N5 flavocyanine adduct. As the data in Figure 2.3 and 2.4 shows, a characteristic absorption band near 410 nm for deprenyl and for clorgyline inhibitors with relative extinction coefficients of ($\epsilon_{410} \sim 24 \text{ mM}^{-1}\text{cm}^{-1}$) is observed for zMAO. The stoichiometric conversion of zMAO flavin to its N(5) flavocyanine adduct suggests that the purified enzyme is fully functional.

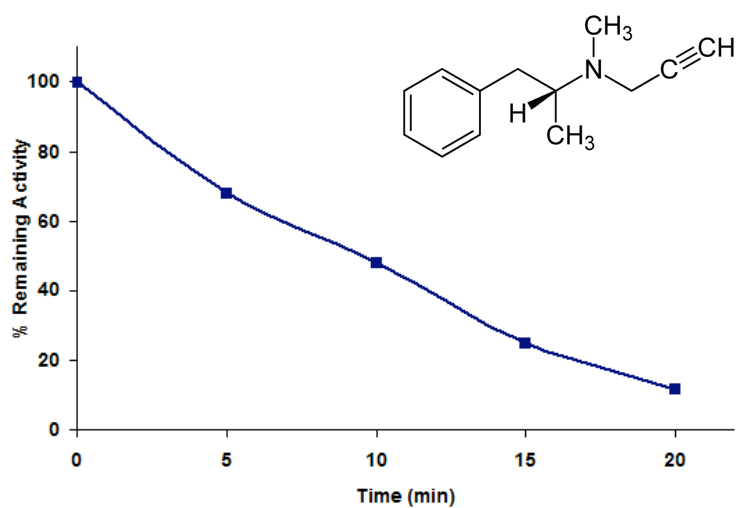
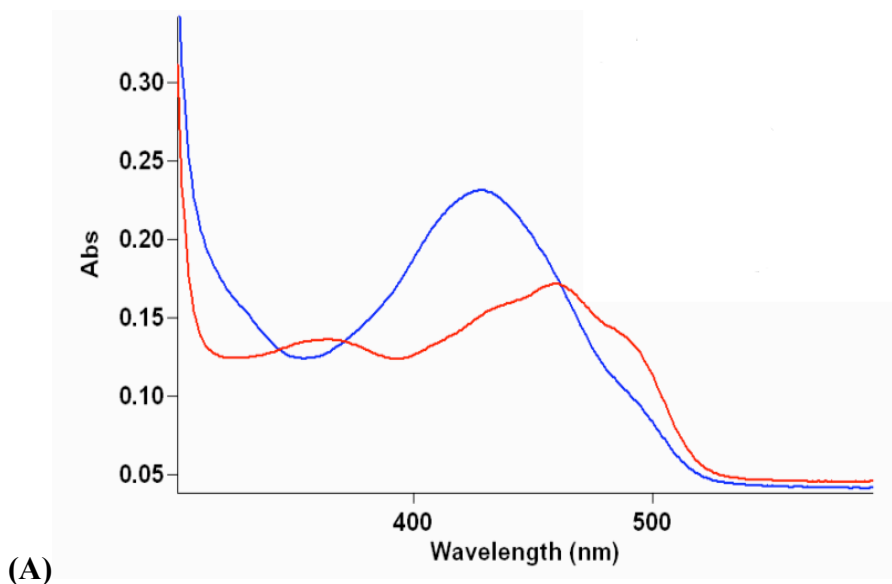


Figure 2.3: (A) UV-Vis spectra of purified zMAO before (red) and after (blue) the addition of 10-fold molar excess of MAO B specific deprenyl. (B) Time course inhibition of zMAO with deprenyl.

Shown inset, is the chemical structure of deprenyl. The reaction was performed in 50 mM potassium phosphate buffer (pH 7.2) containing 20% glycerol and 0.8% (w/v) β -octylglucopyranoside

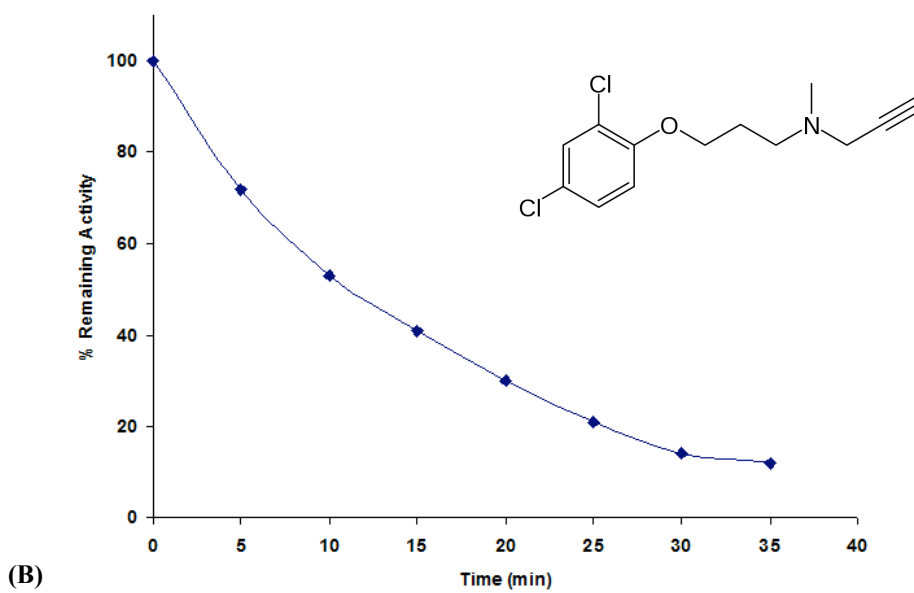
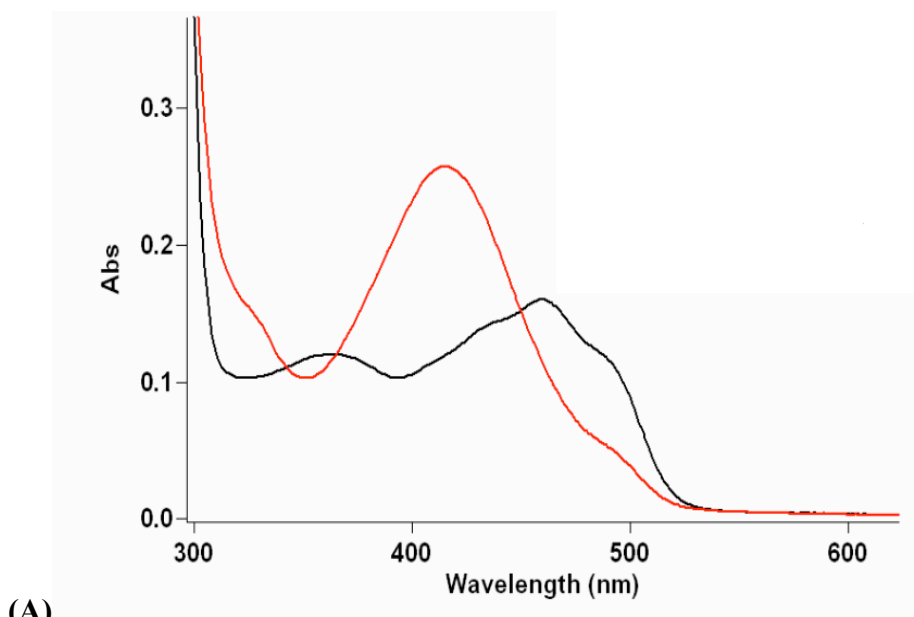


Figure 2.4: UV-Vis spectra of purified zMAO before (black) and after (red) the addition of 10-fold molar excess of clorgyline (A). (B) Time course inhibition of zMAO by MAO A specific clorgyline.

Shown inset, is the chemical structure of clorgyline. The reaction was performed in 50 mM potassium phosphate buffer (pH 7.2) containing 20% glycerol and 0.8% (w/v) β -octylglucopyranoside

2.3.4 Determination of the nature of the covalent flavin linkage

Sequence alignment studies show that the proposed zMAO flavin binding domain is identical with that of hMAO A and has an 80% identity with that of hMAO B. To identify the flavin linkage, our initial approach was to test whether FAD is attached to the enzyme via an 8 α -S-cysteinyl linkage as seen in human isoforms (Walker, Kearney et al. 1971). The first step was to determine the flavin-binding site. Using published protocols for liberation of the flavin peptide from human MAO A and bovine MAO B (Edmondson and Singer 1973), a combined trypsin and chymotrypsin digestion was performed as described above. After digestion, the liberated peptides were desalted using a Sep-Pak C18 small cartridge and the flavin-containing peptide eluted with methanol. The flavin peptide fraction was dried and subjected to RP-HPLC separation. HPLC fractions exhibiting an absorbance at 350 nm (Figure 2.5) were eluted and were characterized as following:

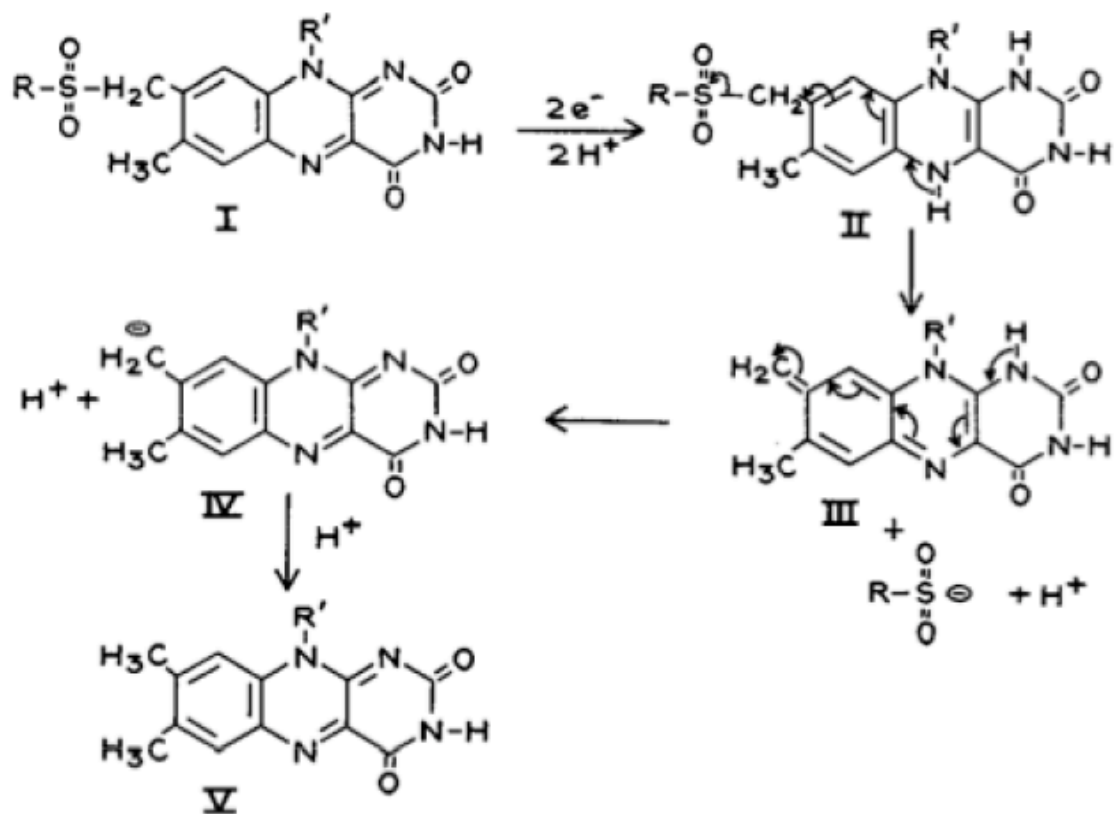
1) Mass Spectral Analyses

The purified peptide was subjected to MALDI-TOF mass spectra. Out of the peptides that were obtained, none of them yielded a flavin-containing one. As an alternate method, peptides were subjected to HPLC separation monitored at 280 nm and all fractions were collected. The fractions were then dried via speed-vac and subjected to MALDI-TOF/TOF. Each collected fraction was fragmented and then subjected to a global network analysis. The obtained sequences did not yield a flavin-containing peptide but corresponded to other hydrophobic peptides of zMAO. Recovered sequences are combined and in sum reported in Table 2.3. The next approach was first to in-gel digest

the enzyme with trypsin, chymotrypsin and endoproteinase GluC. The protein samples were resolved on a SDS gel and stained by Coomassie blue. The corresponding zMAO band was excised and subjected to in-gel tryptic digestion. The resulting peptides were analyzed by reverse-phase chromatography coupled by tandem mass spectroscopy using an LTQ-Orbitrap mass spectrometer (Thermo Finnigan, San Jose, CA). The identified peptides were then subjected to a database search.

2) *Fluorometer Studies*

The liberated flavinylated peptide exhibits a very weak fluorescence intensity, which suggested, from knowledge of other covalent flavins, that the flavin cofactor is possibly attached to the peptide via an 8 α -S-cysteinyl linkage. To further characterize this property, performic acid oxidation using previously established methodology was performed on the liberated flavin peptide (Scheme 2.2) (Walker, Kearney et al. 1971). This oxidative treatment results in an ~60% increase in fluorescence intensity (Figure 2.7). These spectral properties suggest the presence of an 8 α -cysteinyl flavin in zMAO; as is also seen in human MAO A and B (Walker W. H. 1974) (Edmondson, Binda et al. 2004).



Scheme 2.2 Proposed mechanism for elimination of the 8 α -cysteinylsulfone to form unsubstituted flavin (Edmondson and Singer 1973). The proposed mechanism is as follows: (I) The oxidized flavin is reduced to its hydroquinone form. (II) Electron rearrangement to the e- deficient sulfur of the sulfone triggers the elimination of the cysteine sulfinate (III) Flavin-quinhydrone tautomerizes to form the unsubstituted flavin.

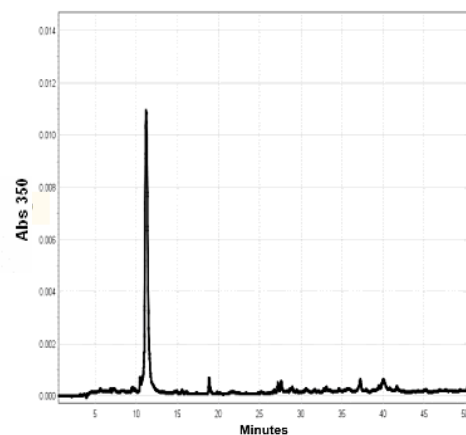
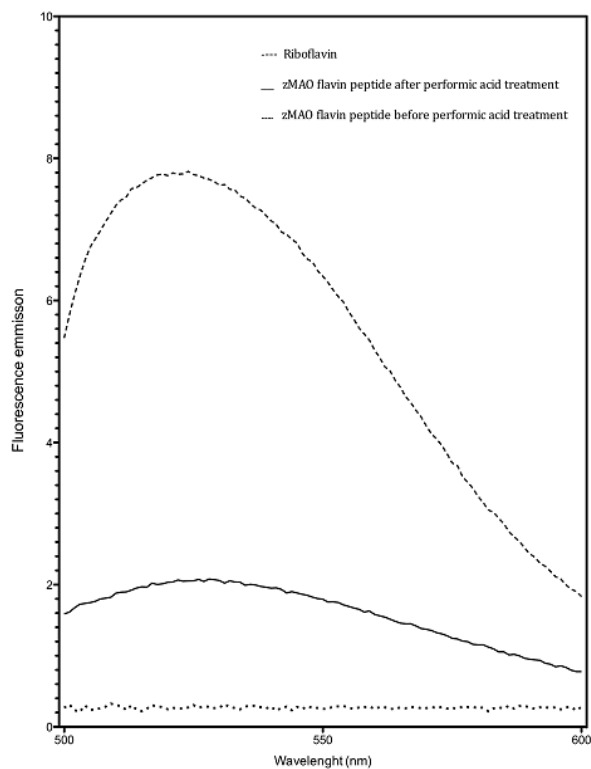


Figure 2.5: Fluorescence emission spectrum of liberated zMAO flavin peptide (left). The excitation wavelength was 345 nm. Oxidation of the ~ 1nmole flavin peptide with performic acid at 0 °C increases the quantum yield of fluorescence to 60% over that the untreated flavin peptide and approximately 15% of that given by equal amounts of riboflavin. Reduction of the peptide with dithionite resulted as the elimination of the flavin cofactor. **(right) HPLC elution profile of the flavinylated peptide at 350nm.**

2.3.5 Identification of the Flavin

To detect the coenzyme type of the flavin molecule, we used an apo-glucose oxidase reconstitution assay (Miller and Edmondson 1999). It has been shown the activity of the apo-glucose oxidase can be reconstituted upon incubation with FAD (Scheme 2.1) (Edmondson and Singer 1973). Therefore we measured the activity of glucose oxidase obtained by recombination of the apo-enzyme with zMAO flavinylated peptide. Flavin peptide was reduced beforehand, to eliminate the peptide bond between the -S of cysteine and the 8 α carbon of the flavin (Scheme 2.2) (Edmondson and Singer 1976).



Scheme 2.3: Incubation of FAD with inactive apo-Glucose Oxidase (apoGO) results as the active holo-Glucose Oxidase

To understand whether zMAO contains a flavin cofactor in the FAD form or FMN form, following experiments were performed:

- (1) zMAO was treated with trypsin and chymotrypsin
- (2) Peptides were purified via Sep-Pak C18 cartridge
- (3) Sufficient amount of purified zMAO peptides were treated with performic oxidase. Performic acid oxidation treatment oxidizes the thioether to a sulfone. Reduction eliminates the 8 α sulfinate to form an unsubstituted flavin (Scheme 2.2) (Walker, Kearney et al. 1971). Therefore if FAD is present in zMAO, by incubating this solution with apo-glucose oxidase, the activity of apo-glucose oxidase should be recovered. If FMN is the eliminated form of flavin from zMAO peptide, no activity should be observable (Scheme 2.3).

Hence, several dilutions of the eliminated cofactor was incubated with apo-glucose oxidase in 0.2 M sodium phosphate buffer (pH=6.4) at room temperature over night. Untreated flavinylated peptide, pure FAD and FMN were also incubated with apo-glucose oxidase as controls. After the overnight incubation, samples were assayed using amplex-red peroxidase-coupled assay. Results are summarized in Table 2.2 and show that the activity of glucose oxidase was recovered on incubation with the eliminated zMAO flavin cofactor, which identifies the flavin molecule in zMAO as “FAD”.

Apo-glucose oxidase incubated with ^a :	Apo-glucose oxidase activity (% FAD)
[FAD]	100
[FMN]	Not detectable
zMAO flavin peptide after performic acid oxidation and reductive elimination	35
zMAO flavin peptide before performic acid oxidation	<1

Table 2.2: Reconstitution of the apo-glucose oxidase activity.

All activity assays are done at air saturation at 30 °C using the amplex-red peroxidase assay to monitor H₂O₂ produced in the glucose oxidase catalyzed reaction. The apo-enzyme exhibited less than 1% of the activity of the FAD-reconstituted enzyme. ^aAll values are normalized to ~200 picomoles

2.3.6 Protein Sequence Analysis

We performed in-gel tryptic digestion and MALDI-TOF-MS on to purified zMAO to determine a partial amino acid sequence. The recovered sequences were combined with detailed mass spectral analyses for flavin binding domain described above, overall 62% of the protein residues was sequenced and are shown in Table 2.3.

Monoisotopic Masses		Error (Da)	Residues		Missed Cut	Peptide Sequence
Observed	Computed		Start	End		
805.009	804.377	0.632	126	132	0	MGMEIPKI
852.925	852.423	0.502	44	50	0	TYTVQNK
1031.639	1031.581	0.058	486	495	0	NLPSVGGFLK
1037.735	1037.624	0.111	414	421	0	VLREPVGR
1082.55	1081.482	1.068	138	146	0	APHAEEWDK
1122.407	1122.337	0.07	364	371	0	RICEIYARV
1141.597	1141.378	0.219	147	155	0	MTMQQLFDK
1209.627	1208.578	1.049	199	209	0	IFSTTNGGQER
1332.789	1332.568	0.221	273	283	0	KIHFNPPLR
1536.758	1536.802	0.44	211	224	1	KFAGGANQISEGMAR
1410.763	1409.864	0.899	260	272	0	YVILAIPPGLNLK
1445.726	1444.592	1.134	83	94	0	VNEEESLVHYVK
1589.8	1588.79	1.01	464	479	0	LLVDSGLNPVVLEAR
1594.958	1594.872	0.086	23	37	0	LLVDSGLNPVVLEAR
1646.873	1646.823	0.05	54	68	0	WVDLGAYIGPTQNR
1862.959	1863.054	0.095	372	387	0	VLGSEEALYPVHYEEK
1915.455	1915.284	0.171	496	515	0	FMGVSSFLAAATAAGLVACK
2181.068	2180.444	0.624	1	22	0	MTANAYDVIVIGGGISGLSAAK
2567.833	2567.06	0.773	235	249	0	AVCSIDQTGDLVEVRTVNEEVYK
2645.035	2643.208	1.827	102	121	1	GPFPPMWNPFAYMDYNNLWRT
2724.321	2724.217	0.104	422	446	0	LYFAGTETATEWSGYMEGAVQAGER
3345.850	3345.716	0.134	458	485	0	LHASQIWQSEPEMSDVPARPFVTTFWER

Table 2.3: Mass profile of the recovered peptide for tryptic-digested zMAO

Using Profound software (<http://www.prowl.rockefeller.edu>) with the obtained mono-isotopic masses ~30% recovery of the zMAO protein sequence is demonstrated. The missing peptides are most likely due to the incomplete trypsin digestion, missed cleavages site, or to insolubility and loss of hydrophobic peptides.

1	mtanaydviv	igggisglsa	<u>akllvdsgln</u>	pvvlearsr	ggrtytvqnk	etkwvdlgga
61	yigptqnril	riakqygvkt	ykvneeeslv	hyvkgksypf	kgpfpmpnp	faymdynnllw
121	rtmdkmgmei	pkeapwraph	aeewdkmtmq	qlfdkicwtr	sarrfatlfv	nvnvtsephe
181	vsalwflwyv	kqcggtmrif	sttnggqerk	fagganqise	gmarelgdrv	klsravcsid
241	qtgdlvevrt	vneevykaky	vilaippgln	lkihfnpelp	plrnqlihrv	pmgsvikcmv
301	yykenfwrkk	gycgsmviee	edapigltd	dtkpdgsvpa	imgfilarks	rklanltrde
361	rkrriceiya	rvgseealy	pvhyeeknwc	eeey sggcy t	ayfppgimtq	fgrvlrepvg
421	rlyfagteta	tewsgymega	vqagerasre	vmcamgklla	sqiwwqsepes	mdvparpfvt
481	tfwernlpsv	ggflkfmgvs	sflaaataag	lvackkgllp	rc	

Table 2.4: Representation of the identified peptides of zMAO

About 60% of the sequence is identified. Highlighted in grey and shown in bold letters are the corresponding recovered zMAO peptides. Highlighted in yellow is the sequence for the predicted flavin binding site, which could not be identified and still under investigation.

2.3.7 Thermal Stability

The thermal stabilities of hMAO A and hMAO B have been previously determined and are shown in Figure 2.6. The data showed that the activity of hMAO A decreases by 60% and that of hMAO B decreases 40% after 60 min incubation at 30 °C. Therefore, the human isoforms differ in their thermostabilities. Our aim was to determine and compare the temperature stability of zMAO in comparison to those human forms under identical conditions. To test the stability of purified zMAO we incubated the enzyme at various temperatures. The data in Figure 2.6 show that the pure enzyme is relatively stable at 30 °C for 60 min and loses only 20% of its initial activity. At 40 °C the enzyme rapidly loses activity at incubation. Overall, these data shows that zMAO is more thermostable than either of the human isoforms.

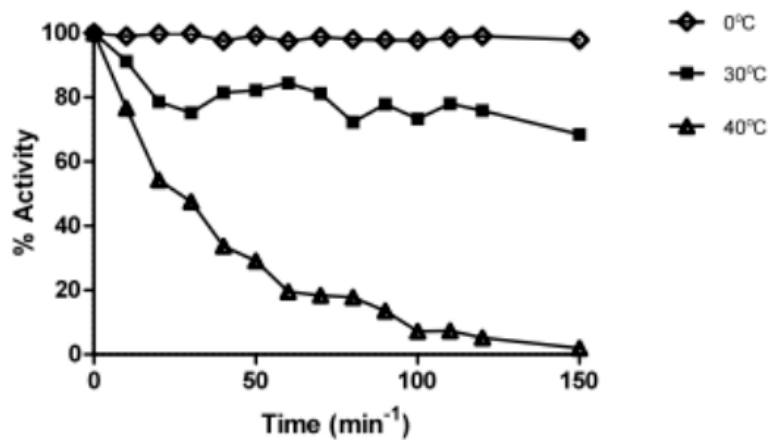
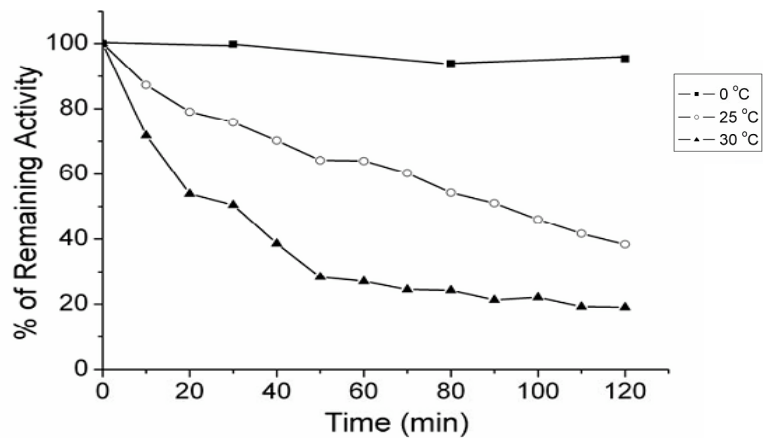


Figure 2.6: Comparison of thermal stabilities of human MAO A and zebrafish MAO

Profiles of percentage of original enzyme activity versus incubation time are shown for zMAO (bottom) and for human MAO A (upper panel).

2.3.8 Catalytic Properties

A number of MAO A and MAO B specific substrates are tested with zMAO. Detailed steady-state kinetics information is available in Chapter 3. In this chapter, the relative binding constants and kinetic isotope effects of zMAO with two commonly used MAO substrates were also determined. Benzylamine and phenylethylamine were used in this study and peroxidase-coupled assay was used to measure the steady-state kinetic properties of these substrates. The results are in agreement with published data on human MAO A (Newton-Vinson, Hubalek et al. 2000), and MAO B (Li, Hubalek et al. 2002), and demonstrate that zMAO exhibits a deuterium kinetic isotope effect on benzylamine and phenylethylamine oxidation. The results are summarized in Table 2.5.

A distinguishing property on comparison of the functional behaviors of MAO A and MAO B are their different $K_m(O_2)$ values (12 μM (Ramsay, Tan et al. 1994) and 240 μM (Walker and Edmondson 1994), respectively) towards benzylamine. Therefore, the turnover number of MAO A is maximal at air saturation ($\sim 240 \mu\text{M}$) while MAO B functions at approximately one-half of its maximal turnover. As summarized in Table 2.5, $K_m(O_2)$ value of zMAO is found to be 108 μM ; which is approximately one-half that of MAO B and ~ 10 fold higher than the measured value for MAO A (Figure 2.7).

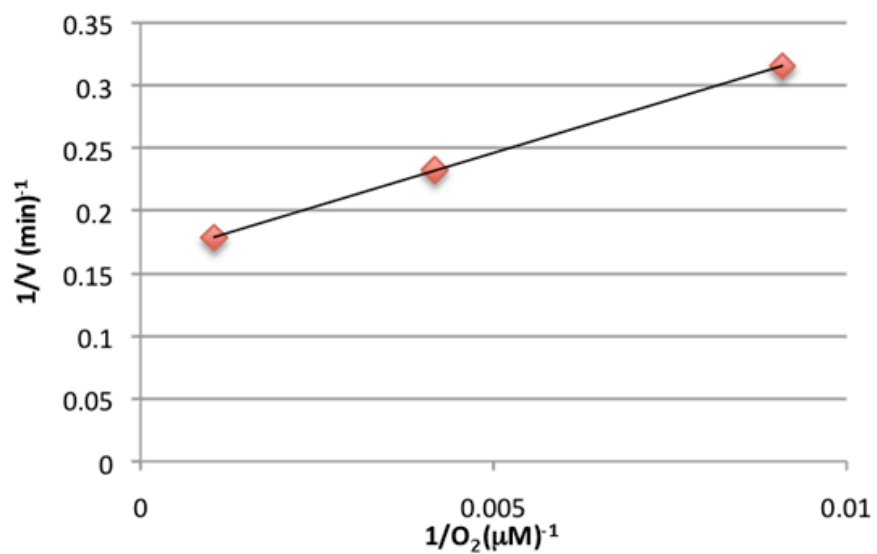


Figure 2.7: Lineweaver-Burk plot of the effect of $[O_2]$ on rate of zMAO oxidation of benzylamine

$K_m(O_2)$ value for zMAO is $108 \mu\text{M}$ which is half that of MAO B and ~ 10 -fold higher than that of MAO A. Measurements are done using peroxidase-coupled assay for an increased sensitivity.

Kinetic Parameter	Benzylamine	Phenylethylamine
K_m (μM)	82.2 ± 9.0	86 ± 13
k_{cat} (min^{-1})	4.71 ± 0.14	203.8 ± 8.7
k_{cat}/k_m ($\text{min}^{-1} \mu\text{M}^{-1}$)	0.057 ± 0.005	2.37 ± 0.19
$K_m(\text{O}_2)$ (μM)	108.5 ± 4.6	140 ± 21
K_m (μM) (Saturated Oxygen)	310 ± 86	22 ± 4
k_{cat} (min^{-1}) (Saturated Oxygen)	5.59 ± 0.67	324 ± 14
	$[\alpha, \alpha\text{-}^1\text{H}_2\text{-}]$ Benzylamine	$[\alpha, \alpha\text{-}^1\text{H}_2\text{-}]$ Phenylethylamine
K_m (μM)	163 ± 32	80 ± 11
k_{cat} (min^{-1})	2.34 ± 0.20	16.8 ± 0.6
Deuterium Isotope Effect		
$^{\text{D}}k_{cat}$ (min^{-1})	2.1 ± 0.2	12.1 ± 1.2
$^{\text{D}}(V/K)$	4.1 ± 0.5	11.4 ± 1.1
Apparent K_d (μM)	209.5 ± 15.0	80.5 ± 5.8

Table 2.5: Steady state kinetic parameters of zebrafish MAO measured under air saturation and saturated oxygen All measurements were performed in 50mM potassium phosphate with 20% glycerol and 0.5 % (w/v) Triton X-100, pH =7.2, at 25 °C

Studies with human MAO A and MAO B have shown that both isozymes have kinetic isotope effect on the steady state turnover rate for the α -protons of benzylamine ($^{\text{D}}k_{cat}$ (min^{-1}) = 11.0) and ($^{\text{D}}k_{cat}$ (min^{-1}) = 4.7) respectively. On the other hand, while deuterium isotope substitution of the α -protons of phenylethylamine results in large kinetic isotope effect on the steady state turnover rate ($^{\text{D}}k_{cat}$ (min^{-1}) = 7.0) for MAO A; a small kinetic isotope effect has observed for human MAO B with phenylethylamine ($^{\text{D}}k_{cat}$ (min^{-1}) =

1.7) Steady state kinetic isotope effects with α,α -[D₂]benzylamine and α,α -[D₂]phenylethylamine demonstrate that the α -C-H bond cleavage kinetic step is rate limiting in catalysis in zMAO. Therefore, zMAO exhibits properties closer to MAO A when on comparison of steady-state kinetic isotope effects measured for α,α -[D₂]benzylamine and α,α -[D₂]phenylethylamine turnover (Table 2.5).

2.4 Discussion

The recently completed zebrafish (*Danio rerio*) genome shows the existence of a single MAO gene in this teleost (Anichtchik 2006). In addition to the high sequence identity (~70%) of this single MAO gene with those of the human isoforms, zebrafish has many selective advantages in pharmacological applications and drug-development studies. Moreover, phylogeny studies suggest that this single MAO form might be the last common ancestor between mammals and other organisms. Currently there is no detailed characterization of this interesting enzyme in the literature. Thus, as a first approach, we developed the first high-level expression and characterization procedure of an evolutionary precursor of mammalian MAO enzyme, zebrafish MAO.

Due to our successful experience with rat and human MAO expression systems, we selected *Pichia pastoris* as the host organism to express zMAO. The results described here demonstrate that *Pichia pastoris* serves as an efficient expression system for the zMAO as well. While the expression system that is used for human MAO enzymes are readily applicable to zMAO, several changes were required for the purification procedure. The most striking difference that distinguished zMAO from human isoforms was at the column purification step. The inability of zMAO to bind to ion-exchange

resins is most likely as a result of differences in *pI* value of zMAO. The amino acid sequence of zMAO predicts a *pI* of 8.9 whereas the sequences of human MAO A and B predicted a *pI* of 7.9 and 7.2 respectively. Thus, the zMAO surface charge is more basic than either of the human enzymes, and required the use of an absorption matrix rather than an ion exchange matrix used for human MAO A and B.

The described expression and purification methodology reveals that zMAO contains a covalently attached flavin cofactor. It was of interest to determine the nature of the flavin cofactor and its attachment site and properties. For our initial goal, we followed a procedure that was developed earlier by Walker et al (Walker, Kearney et al. 1971). The observed increase at the fluorescence intensity of the liberated flavin peptide after performic acid oxidation and the cleavage of the peptide flavin link via dithionite reduction provide strong evidence that the flavin cofactor is linked to zMAO via an 8 α -cysteinyl thioether bond as in human MAO A and B. When we incubated the eliminated flavin cofactor with apo-glucose oxidase, we observed reconstitution of glucose oxidase activity, demonstrating the flavin cofactor of zMAO contains is an FAD molecule. Investigation of the functional characteristics of zMAO was another important task. Alignment studies show that the substrate domain of zMAO is completely identical to hMAO A and has 70% sequence identity to hMAO B. The flavin-binding domain of zMAO is 80% identical to either enzyme, while membrane anchoring domain has 30% sequence identity to hMAO A and 20% sequence identity to hMAO B (Anichtchik 2006) (Chapter 1.2.2). Taken together, zMAO sequence is similar to both MAO isoforms with a slightly higher similarity to hMAO A.

The data in the literature shows that zMAO in whole zebrafish brain tissue samples is inhibited by the MAO A-specific inhibitor clorgyline and by the MAO B-specific inhibitor deprenyl and can metabolize serotonin; a highly hMAO A specific substrate (Sallinen 2009). Overall these properties suggest that zMAO exhibits properties of both hMAO A and B with more similarities to hMAO A (Anichtchik 2006) (Sallinen 2009) (Setini 2005).

To investigate the validity of these statements and to provide further improved comparative data with purified zMAO, we tested a number of human MAO A and MAO B specific substrates and inhibitors. Our kinetics data show that the MAO B specific substrate phenylethylamine is oxidized by zMAO at a rate approximately equivalent to that exhibited by MAO B but three-fold higher than MAO A. Benzylamine, a MAO B specific substrate is oxidized by zMAO at rates approximately two-fold higher than MAO A as well. Overall, based on the substrate data, we confirmed that zMAO can oxidize the substrates of both human isoforms. Our detailed steady-state kinetic analyses that are further presented in next chapter supports this statement as well. Another striking difference of human MAO A and B is their $K_m(O_2)$ (oxygen binding) values. We comparatively analyzed $K_m(O_2)$ values of zMAO and showed that zMAO exhibits a $K_m(O_2)$ of 108 μ M for benzylamine oxidation which is approximately one-half that of MAO B and ~10 fold higher than the measured value for MAO A. The inhibition study is based on the MAO present in whole zebrafish tissue preparations and suggests that zMAO is inhibited by the MAO A specific inhibitor clorgyline and by the MAO B specific inhibitor deprenyl (Setini 2005) (Anichtchik 2006). We were able to confirm these data with purified zMAO; additionally based on the spectral data, we show the

irreversible inhibition of zMAO by these two inhibitors is through the formation of N5 flavocyanyne adducts, as is observed with the human MAO isoforms. Moreover, zMAO exhibits kinetic isotope behaviors to hMAO A, with α - α - [D₂]-benzylamine and α - α - [D₂]-phenylethylamine indicating that C_α-H bond is the rate-limiting step in catalysis.

Altogether these data demonstrates that zMAO exhibits substrate and inhibitor specificity that broadly spans both of those known for MAO A and for MAO B. Kinetic isotope effect properties closer to human MAO A. Therefore we conclude that zMAO has the properties similar to both human MAO enzymes with properties to some extent closer to human MAO A. The described expression and purification methodology will serve as an essential tool to study the structural and mechanistic properties of zMAO in the future, which can be used as a model system for drug development to study MAO-related human diseases.

References:

- Anichtchik, O., Sallinen, V., Peitsaro, N., Panula, P. (2006). "Distinct structure and activity of monoamine oxidase in the brain of zebrafish (*Danio rerio*)."
Journal of Comparative Neurology **498**(5): 593-610.
- Barber, M. J., D. C. Eichler (1987). "Anti-flavin antibodies." Biochem J **242**(1): 89-95.
- Binda, C., Hubalek, F., Li, M., Edmondson, D. E., Mattevi, A. (2004). "Crystal structure of human monoamine oxidase B, a drug target enzyme monotonically inserted into the mitochondrial outer membrane." FEBS Lett **564**(3): 225-8.
- Binda, C., J. Wang, Leonardo, P., Carla, C., Angelo, C., Patricia, S., Edmondson, D.E., Mattevi, A. (2007). "Structures of human monoamine oxidase B complexes with selective noncovalent inhibitors: Safinamide and coumarin analogs." Journal of Medicinal Chemistry **50**(23): 5848-5852.
- Chen K., W. H., Grimsby, J., Shih J.C. (1994). "Cloning of a novel monoamine oxidase cDNA from trout liver." Mol. Pharmacol. **46**(6): 1226-33.
- Chung, W. G., Sen, A., Wang-Buhler, J.H., Yang, Y.H., Lopez, H., Merrill, F., Miranda, C., Hu, C., Buhler, D.H. (2004). "cDNA-directed expression of a functional zebrafish CYP1A in yeast." Aquatic Toxicology **70**(2): 111-121.
- Cremona, T. and E. B. Kearney (1964). "Studies on Respiratory Chain-Linked Reduced Nicotinamide Adenine Dinucleotide Dehydrogenase .6. Further Purification + Properties of Enzyme from Beef Heart." J Biol Chem **239**(7): 2328-&.
- Daum, G., Bohni. P.C. (1982). "Import of Proteins into Mitochondria - Cytochrome-B2 and Cytochrome-C Peroxidase Are Located in the Intermembrane Space of Yeast Mitochondria." J Biol Chem **257**(21): 3028-3033.
- De Colibus, L., Li, M., Binda, C., Lustig, A., Edmondson, D. E., Mattevi, A. (2005). "Three-dimensional structure of human monoamine oxidase A (MAO A): Relation to the structures of rat MAO A and human MAO B." Proceedings of the National Academy of Sciences of the United States of America **102**(36): 12684-12689.
- E Edmondson, D. E., Binda, C., Mattevi, A. (2004). "The FAD binding sites of human monoamine oxidases A and B." Neurotoxicology **25**(1-2): 63-72.

- Edmondson, D. E., A. Mattevi, Binda, C., Li, M., Hubalek, F. (2004). "Structure and mechanism of monoamine oxidase." Curr Med Chem **11**(15): 1983-93.
- Edmondson, D. E. and P. Newton-Vinson (2001). "The covalent FAD of monoamine oxidase: structural and functional role and mechanism of the flavinylation reaction." Antioxid Redox Signal **3**(5): 789-806.
- Edmondson, D. E. and T. P. Singer (1973). "Oxidation-reduction properties of the 8 alpha-substituted flavins." J Biol Chem **248**(23): 8144-9.
- Edmondson, D. E. and T. P. Singer (1976). "8alpha-substituted flavins of biological importance: an updating." FEBS Lett **64**(2): 255-65.
- Goldstone, J. V., M. E. Jonsson (2009). "Cytochrome P450 1D1: A novel CYP1A-related gene that is not transcriptionally activated by PCB126 or TCDD." Archives of Biochemistry and Biophysics **482**(1-2): 7-16.
- Hall TR, Y. P., Figueroa HR, Urueña G, Olcese JM, Newton DK, Vorwald SR. (1982). "Monoamine oxidase types A and B in the vertebrate brain." Comp. Biochem. Physiol. C. **71C**(1): 107-10.
- Klinman, J. and R. G. Matthews (1985). "Calculation of substrate dissociation constants from steady-state isotope effects in enzyme-catalyzed reactions." J Am Chem Soc **107**: 1058-1060.
- Kumazawa T, S. H., Ishi A, Suzuki O, Sato K. (1998). "Monoamine oxidase activities in catfish (*Parasilurus asotus*) tissues." J Enzyme Inhib **13**: 377-384.
- Li, M., Hubalek, F., Newton-Vinson, P., Edmondson, D. E. (2002). "High-level expression of human liver monoamine oxidase A in *Pichia pastoris*: comparison with the enzyme expressed in *Saccharomyces cerevisiae*." Protein Expr Purif **24**(1): 152-62.
- Lieschke, G. J. and P. D. Currie (2007). "Animal models of human disease: zebrafish swim into view." Nature Reviews Genetics **8**(5): 353-367.
- Mc Dermott Rose, T. D., Cowden, J., Frazzetto G., Johnson D.P. (2009). "Monoamine oxidase A gene (MAOA) predicts behavioral aggression following provocation." Proc Natl Acad Sci U S A **106**(7): 2118-2123.

- Michael J. Stanhope, A. L., Michael J. Italia, Kristin K. Koretke, and J. R. B. Craig Volker (2001). "Phylogenetic analyses do not support horizontal gene transfers from bacteria to vertebrates." Science **2001**: 940-944.
- Miller, J. R. and D. E. Edmondson (1999). "Influence of flavin analogue structure on the catalytic activities and flavinylation reactions of recombinant human liver monoamine oxidases A and B." J Biol Chem **274**(33): 23515-25.
- Natalie Weder, B. Z. Y., Heather Douglas-Palumberi, Johari Massey, John H Krystal, Joel Gelernter, Joan Kaufman (2009). "MAOA Genotype, Maltreatment, and Aggressive Behavior: The Changing Impact of Genotype at Varying Levels of Trauma." Biol Psychiat **65**(5): 417-42.
- Newton-Vinson, P., Hubalek, F., Edmondson, D. E. (2000). "High-level expression of human liver monoamine oxidase B in *Pichia pastoris*." Protein Expr Purif **20**(2): 334-45.
- Ramsay, R. R., A. K. Tan, Weyler, W. (1994). "Kinetic properties of cloned human liver monoamine oxidase A." J Neural Transm Suppl **41**: 17-26.
- Sallinen, V., Sundvik, M., Reenilä, I., Peitsaro, N., Khrustalyov, D., Anichtchik, O., Toleikyte, G., Kaslin, J., Panula, P. (2009). "Hyperserotonergic phenotype after monoamine oxidase inhibition in larval zebrafish." Journal of Neurochemistry **109**(2): 403-415.
- Sallinen, V., V. Torkko, Sundvik, M., Kolehmainen, J., Torkko, V., Tiittula, A., Moshnyakov, M., Podlasz, P. (2009). "MPTP and MPP plus target specific aminergic cell populations in larval zebrafish." Journal of Neurochemistry **108**(3): 719-731.
- Salzmann, J., Anichtchik, O., Best, J., Richards, F., Fleming, A., Roach, A., Goldsmith, P. (2006). "P1 Development of a MPTP model of Parkinson's disease in zebrafish." Behavioural Pharmacology **17**(5-6): 541-541.
- Setini, A., F. Pierucci, Senatori, O., Nicotra, A. (2005). "Molecular characterization of monoamine oxidase in zebrafish (*Danio rerio*)." Comparative Biochemistry and Physiology B-Biochemistry & Molecular Biology **140**(1): 153-161.
- Shih, J. C., K. Chen, Ridd, M.J. (1999). "Monoamine oxidase: from genes to behavior." Annu Rev Neurosci **22**: 197-217.

- Son, S.-Y., Ma, Jichun., Youhei, Kondou., Masato, Yoshimura., Eiki, Yamashita., Tomitake, Tsukihara. (2008). "Structure of human monoamine oxidase A at 2.2-Å resolution: The control of opening the entry for substrates/inhibitors." Proc Natl Acad Sci U S A **105**(15): 5739-5744.
- Streisinger, G., C. Walker, Dower, N., Knauber, D., Singer, F. (1981). "Production of Clones of Homozygous Diploid Zebra Fish (*Brachydanio-Rerio*)." Nature **291**(5813): 293-296.
- Upadhyay, A. K., Edmondson, D. E. (2008). "Characterization of detergent purified recombinant rat liver monoamine oxidase B expressed in *Pichia pastoris*." Protein Expr Purif **59**(2): 349-356.
- Walker, M. C. and D. E. Edmondson (1994). "Structure-activity relationships in the oxidation of benzylamine analogues by bovine liver mitochondrial monoamine oxidase B." Biochemistry **33**(23): 7088-98.
- Walker W. H., K. C., W., Edmondson D.E., Singer, T.P. (1974). "The Covalently Bound Flavin of Chromatium Cytochrome c552 ." Eur. J. Biochem **48**: 439-448.
- Walker, W. H., E. B. Kearney, Seng, R., Singer, T.P. (1971). "Sequence and Structure of a Cysteinylyl Flavin Peptide from Monoamine Oxidase." Biochemical and Biophysical Research Communications **44**(2): 287-292.
- Walker, W. H., E. B. Kearney, Seng, R., Singer, T.P. (1971). "Covalently-Bound Flavin of Hepatic Monoamine Oxidase .2. Identification and Properties of Cysteinylyl Riboflavin." European Journal of Biochemistry **24**(2): 328-331.
- Youdim, M. B. H., D. Edmondson, Tipton, K. (2006). "The therapeutic potential of monoamine oxidase inhibitors." Nature Reviews Neuroscience **7**(4): 295-309.

CHAPTER 3

Functional Analysis of Zebrafish MAO

3.1 Introduction

The study presented in this chapter aims to define the functional properties of zebrafish MAO (zMAO) and to compare them with human MAO A and MAO B. The goal is to investigate if zebrafish MAO demonstrate unique characteristics or does it exhibit properties closer to human MAO A or MAO B.

Using zebrafish as a model organism offers a number of advantages for drug development studies and is complimentary to the rat or mouse models used to study human diseases (Lieschke and Currie 2007). To determine the functional properties of zMAO, we expressed and purified the enzyme using the procedure described in the previous chapter. The catalytic properties and inhibitor specificities and comparison with previously established properties of human MAO A and MAO B are reported.

3.2 Materials and Methods

3.2.1 Materials

Zebrafish (*Danio rerio*) Monoamine Oxidase cDNA was purchased from Open Biosystems, (Clone ID: 6960301) and stored at -80 °C at all times. The plasmid (pPIC3.5K) and strain (KM71) were obtained from Invitrogen Corp. Reduced Triton X-100 was from Fluka (Sigma-Aldrich, St. Louis, MO). Glycerol, HEPES ((4-(2-hydroxyethyl)-1-piperazineethanesulfonic acid), isatin, benzylamine, kynuramine, phenylethylamine, serotonin, d-amphetamine, deprenyl, farnesol, 1,4-diphenyl-1,3-

butadiene, 1,4-diphenyl-2-butene and hydrazines (phenylethylhydrazine, benzylhydrazine and phenylhydrazine) were purchased from Sigma-Aldrich (St. Louis, MO). Rasagiline was a gift from Teva Pharmaceuticals (Jerusalem, Israel). Safinamide was a gift from Newron Pharma (Milan, Italy) and 8-(3-Chlorostyryl)-caffeine was a gift from Dr. N. Castagnoli of the Department of Chemistry, Virginia Technical University. Harmane, pirlindole mesylate and tetrindole mesylate were purchased from TOCRIS Bioscience (Ellisville, MO). All other commercially available reagents, solutions and inhibitors were of highest purity.

3.2.2 Preparation of Enzyme

Recombinant zMAO was expressed in *Pichia pastoris* KM71 strain as described in Chapter 2 using a 6 L fermentation tank for cell growth and induction. Purification of the zebrafish MAO also followed the procedure that was described in Chapter 2. Prior to use, the enzyme was concentrated using Amicon Ultra 30 centrifugal filtration device (Millipore Corporation, Bedford, MA) and immediately after the salt concentration was adjusted to 20 mM KPi by dilution with water and with the additions of 20% (v/v) glycerol and 0.8% (w/v) octyl β -D-glucoside to maintain the critical micelle concentration. Some zMAO preparations contained d-amphetamine for improvement in stability similar to earlier procedures described for human MAO A (De Colibus 2005). In that case, d-amphetamine was removed from the enzyme by passing through a G-25 Sephadex column (1 x 20 cm, Sigma-Aldrich, St. Louis, MO) prior to kinetic studies in 20 mM KPi buffer containing 0.8% (w/v) octyl β -D-glucoside and 20% glycerol, pH=7.2.

3.2.3 Steady-state Kinetics Experiments

Standard enzymatic assays were conducted for zMAO using a Perkin-Elmer Lambda 2 UV-Vis spectrophotometer or a Cary 50 UV-Vis spectrophotometer (Varian Associates, Sunnyvale, CA). Assays were conducted at 25 °C unless otherwise stated and were performed in 50 mM potassium phosphate, pH=7.4 buffer containing 0.5% reduced Triton X-100 (a catalytically hydrogenated form of the non-ionic detergent Triton X-100). All buffers were equilibrated for 30 min at 25 °C before usage.

Substrate	Wavelength nm	ΔExtinction Coefficient (ε) of product M⁻¹cm⁻¹
Kynuramine	316	12,300
Benzylamine	250	12,000
Phenylethylamine*	560*	54,000*

Table 3.1 Wavelength and the extinction coefficient values of the substrates

(*) An amplex red peroxidase coupled assay was conducted for phenylethylamine.

An amplex red-coupled horseradish peroxidase (HRP) assay was utilized for assays with phenylethylamine and its analogues since direct spectrophotometric measurements at the ultraviolet regions were not possible given that the products are not detectable in the UV-Vis range. The HRP assay is based on the detection of the hydrogen peroxide, the product of MAO catalysis and has a high sensitivity (Holt 1997) Amplex red is a stable and non-fluorescent derivative of resorufin and is recognized by HRP as a substrate in the presence of H₂O₂. Horseradish peroxidase was prepared at 1U/mL in 50 mM potassium

phosphate buffer (pH=7.5). Amplex red reagent (Molecular Probes, Inc. Carlsbad, CA) was prepared as 5 mM solution in DMSO. The overall enzyme assay was prepared by incubating amplex red, horseradish peroxidase, the desired MAO substrate in the assay buffer (50 mM potassium phosphate buffer with 0.5% reduced Triton X-100, pH=7.5), in a total volume of 1 mL at 25 °C. For assays, 5 or 10 µL of enzyme (depending on the enzyme's activity) was added to the reaction mixture and the absorbance reading at 560 nm was followed continuously. The absorption extinct coefficient (ϵ) of the product is 56,000 M⁻¹ cm⁻¹ (Zhou, Diwu et al. 1997).

Several MAO substrates containing ring hydroxyl groups such as serotonin, dopamine and tyramine are unsuitable for the amplex-red peroxidase coupled assay since they are substrates for horseradish peroxidase in competition with amplex red reagent subsequently reducing the color formation (Holt 2006). Therefore the catalytic activities for these substrates were assayed polarographically by following the rate of oxygen consumption using a Model 782 Oxygen Meter (Strathkelvin Instruments Ltd. North Lanarkshire, Scotland) interfaced to a PC. For assays that required conditions exhibiting a dissolved oxygen concentration different than the air saturation, pure oxygen, pure nitrogen or different amounts of mixed oxygen/nitrogen was bubbled directly into the solution via an air sparger. Starting approximately half hour prior to the experiment, the buffers were incubated at 25 °C. The gas mixtures were continuously passed over the surface of the solution during the experiment as well. The final oxygen concentrations were directly measured via an oxygraph cell prior to usage. One unit of enzyme activity is defined as the amount of enzyme required to oxidize 1 µmol of substrate in one minute.

3.2.4 Competitive Inhibition

Competitive inhibition assays for zMAO and MAO A were performed with kynuramine as the competing substrate while the competitive inhibition of MAO B was performed with benzylamine as the competing substrate. Assay buffers for hydrazine derivatives contained 1 mM EDTA to complex any trace levels of Cu^{2+} for increased stability of the hydrazine in solution (Cu^{2+} functions as a catalyst for hydrazine auto-oxidation). All assays were held at 25 °C unless otherwise is stated.

3.2.5 Data Analysis

Steady state kinetic data were fit to the Michaelis-Menten equation or to the Lineweaver-Burk plot using nonlinear least-squares fitting routine incorporated into the Origin (OriginLab Corporation, Northampton, MA) to calculate the turnover number (k_{cat}) and Michaelis constant (K_m). Inhibition constant (K_i) was measured by calculating the apparent K_m of the substrates at various concentrations of inhibitor.

3.2.6 Enzyme Functionality

To estimate the functionality of zMAO after purification from *Pichia pastoris*, the level of anaerobic reduction of the flavin cofactor by the substrate kynuramine was determined by the spectral changes of flavin absorbance. In average, the functionality of the enzyme was determined as ~70%. The enzyme lost an overall 60% of the activity within two weeks of purification under the conditions discussed above.

3.3 Results

3.3.1 Steady-State Kinetic Properties for the zMAO

To determine the substrate specificities and kinetic properties of purified zMAO, a number of commonly used human MAO A and B specific substrates were tested. As shown in Table 3.2, zMAO oxidizes serotonin (a MAO A-specific substrate) with a k_{cat} value 100 min^{-1} , which is approximately one-half the value exhibited by purified human MAO A and three times higher than that exhibited by human MAO B; zMAO oxidizes dopamine and kynuramine with k_{cat} values of $\sim 235 \text{ min}^{-1}$ and 243 min^{-1} , respectively, which are higher than either human enzyme.

Steady-state kinetic properties of zMAO with tyramine are deaminated by zMAO with a k_{cat} value intermediate between those exhibited by human MAO A and B. Phenylethylamine and benzylamine are also substrates of zMAO which were presented previously in Chapter 2 of this thesis. Overall kinetic data for zMAO are summarized in Table 3.2. These kinetic properties initially demonstrate that zMAO exhibits a substrate specificity that broadly spans both of those exhibited by MAO A and by MAO B.

Among all the substrates we tested, one interesting result was obtained with 4-phenylbutylamine. This arylalkylamine functions as a competitive inhibitor for human MAO A, but is found to be a substrate for human MAO B and for zMAO (Table 3.2). Another differential behavior is also observed using *p*-carboxybenzylamine, which is a substrate for zMAO and for human MAO A, but neither a substrate nor a competitive inhibitor for human MAO B (details are discussed in Chapter 4 extensively). These observations provide additional support for the promiscuous behavior of zMAO.

	zMAO		hMAO A		hMAO B	
Substrate	K_m (μM)	k_{cat} (min^{-1})	K_m (μM)	k_{cat} (min^{-1})	K_m (μM)	k_{cat} (min^{-1})
Kynuramine	49 ± 4	243 ± 4.6	130 $\pm 10^a$	125.4 $\pm 8.5^a$	27.1 $\pm 2.0^b$	95.5 $\pm 1.2^b$
Serotonin	450 \pm 30	100.75 ± 1.59	295 $\pm 46^a$	182.1 $\pm 8.2^a$	2270 $\pm 310^b$	32.6 $\pm 1.5^b$
Dopamine	61 ± 4	233.6 ± 1.0	240 $\pm 42^a$	71.4 $\pm 3.6^a$	128 $\pm 15^b$	65.0 $\pm 1.7^b$
Tyramine	37 ± 3	206.6 ± 16.0	427 $\pm 18^c$	182 $\pm 26^c$	107 $\pm 21^c$	343 $\pm 48^c$
Phenylbutylamine	256 ± 10	210.02 ± 25.6	Inhibitor $K_i = 31 \pm 5 \mu\text{M}$		19 ± 3	110 ± 5

Table 3.2 Comparison of steady-state kinetics values for zMAO, human MAO A, and human MAO B.

All assays were performed at air saturation and at 25 °C in 50mM KPi buffer, 0.5 % (w/v) reduced Triton X-100 (pH=7.4). Peroxidase coupled assay was used for phenylethylamine and benzylamine (only for zMAO) measurements. Serotonin, histamine and tyramine turnover rates were monitored by following the oxygen consumption. All other measurements were detected by monitoring the product formation directly via UV-Vis spectra.

^a Values taken from (Li, Hubalek et al. 2002)

^b from (Nandigama and Edmondson 2000)

^c from (O'Carroll et al.)

3.3.2 Competitive Inhibition

MAO A Specific Inhibitors

Tetrindole mesylate and pirlindole mesylate are tetracyclic anti-depressants that selectively target and reversibly inhibit the catalytic activity of MAO A (Andreeva 1992). Zebrafish MAO is inhibited by these indole inhibitors with 6-7 fold weaker affinities than observed with human MAO A under identical conditions. Another tricyclic MAO A specific inhibitor, Harmane, exhibits similar K_i values with zMAO and with human MAO A.

	zMAO	Human A	Ratio K_i values
	K_i (μM)		zMAO/hMAOA
Harmane	0.48 ± 0.03	$0.58 \pm 0.20^*$	0.83
Tetrindole Mesylate	34.1 ± 2.0	$5.27 \pm 0.24^*$	6.47
Pirlindole Mesylate	6.8 ± 0.3	$0.92 \pm 0.04^*$	7.39

Table 3.3. Comparison of zMAO with human MAO A specific inhibitors

* Data obtained from Dr. Jin Wang's Ph.D. thesis. Human MAO B is not inhibited by up to 100 μM inhibitor concentrations of either indole inhibitors

MAO B Specific Inhibitors

A variety of MAO B specific inhibitors were also tested with zMAO. (Table 3.4) The binding of farnesol, 8-(3-chlorostyryl)-caffeine, 1,4-diphenyl-2-butene, and 1,4-diphenyl-1,3-butadiene to zMAO with reasonable affinities is surprising considering the similarities of zMAO to MAO A in functional behavior and in amino acid residues in the active site (Chapter 1.1.2). The significance of this finding is discussed in Summary section of this chapter and potentially opens up a new area of investigation on the factors involved in defining the selectivity of MAO A and MAO B inhibitors.

	zMAO	Human B	Human A
	<i>K_i</i> (μ M)		
8-(3-Chlorostyryl)-caffeine	3.6 \pm 0.5	0.27 \pm 0.08 ^a	No inhibition
1,4-Diphenyl-1,3-Butadiene	1.0 \pm 0.1	7.0 \pm 0.2 ^a	No inhibition
1,4-Diphenyl-2-Butene	1.5 \pm 0.2	34.5 \pm 1.4 ^a	No inhibition
Farnesol	1.1 \pm 0.1	2.3 \pm 0.4 ^a	No inhibition
Safinamide	480 \pm 29	0.45 \pm 0.13 ^b	365.0 \pm 18.7 ^b
Mofegiline	3.5 \pm 0.2	28 nm ^c	2.1 ^c

Table 3.4: Comparison of zMAO with MAO B inhibitors

Kynuramine was used as a substrate during competitive inhibition of zMAO. Enzyme buffer was consist of 50mM KPi with 0.5% (w/v) reduced Triton-X-100, pH=7.4 Values from: ^a (Hubalek 2005) ^b (Binda, Wang et al. 2007) ^c (Milczek 2008) (Structures of these inhibitors are shown in Chapter 1)

Mofegiline is a highly selective, stoichiometric inhibitor of MAO B that forms an N(5) adduct flavocyanine adduct and irreversibly inhibits MAO B in nanomolar values (Milczek 2008). Unlike MAO B, MAO A is inhibited by mofegiline reversibly and without formation of the covalent flavin adduct (Milczek 2008). Inhibition profile of zMAO shows that the enzyme is inhibited by mofegiline in a range similar to MAO A rather than MAO B (Table 3.4). Mofegiline forms a covalent adduct with the flavin of MAO B but is a reversible inhibitor of MAO A. This differential aspect has not been tested with zMAO.

Aminoindans

We analyzed the inhibition profile of zMAO with *S* and *R* enantiomers of aminoindan (*R*-AI and *S*-AI) as well as their corresponding *N*-methylated derivatives (*R*-MAI and *S*-MAI). *R*-AI is the major metabolic product of a novel anti-Parkinson's drug rasagiline (Hubalek 2004). It is known that all the these aminoindan analogues reversibly inhibit human MAO A and MAO B, except for *S*-AI, which does not inhibit MAO B (Hubalek 2004; Binda 2005). Our studies show that *S*-AI inhibits zMAO with a K_i value almost 5-fold tighter than it does MAO A; zMAO is inhibited by *R*-AI with a similar value to MAO B but 2-fold tighter than MAO A. These data demonstrate that zMAO has a higher sensitivity towards inhibition by *R*-MAI and *S*-MAI (8 μ M for *R*-MAI, 6 μ M for *S*-MAI) than exhibited by human isoforms. Table 3.5 summarizes the inhibition data of aminoindan analogues.

	zMAO	hMAO A*	hMAO B*
	K_i (μM)		
<i>R</i> -AI	30 ±2.1	67	32
<i>S</i> -AI	32 ±1.7	160	1080
<i>R</i> -MAI	8.2 ±0.8	56	17
<i>S</i> -MAI	6.1 ±0.9	50	270

Table 3.5: K_i values and the structures of the aminoindan (AI) analogues tested with zMAO, in comparison to human isoforms

R-AI and *S*-AI are *R* and *S* enantiomers of aminoindan, while *R*-MAI and *S*-MAI correspond to *R* and *S* enantiomers of *N*-methylated aminoindan derivatives. * Values from (Binda 2005)

Rasagiline belongs to another set of inhibitors that are well characterized with human MAO isoforms: *N*-propargyl-aminoindans. Rasagiline irreversibly inhibits MAO B (Hubalek 2004) Studies with zMAO show that the enzyme is inhibited by this inhibitor with a similar K_i value to human MAO B ($0.79 \mu\text{M}$) with similar spectral properties (Figure 3.1) thus it behaves more like MAO B.

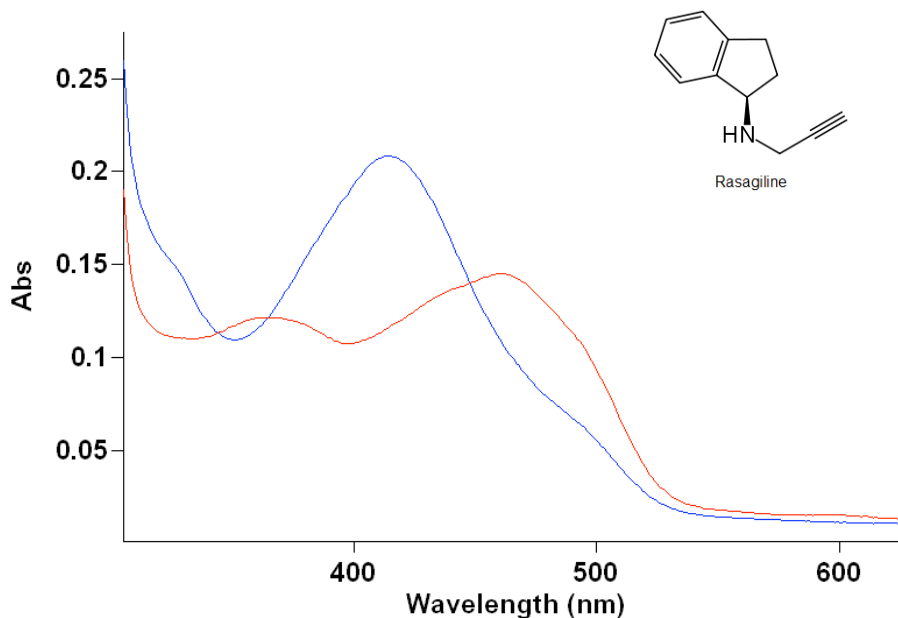


Figure 3.1: Ultraviolet-visible absorption spectra of zMAO before and after the addition of rasagiline. (Red line is before the addition of rasagiline, blue line is after the addition of 10-fold rasagiline)

	zMAO	hMAO A	hMAO B
	K_i (μM)		
Rasagiline	0.79 ± 0.04	9.7*	0.7*

Table 3.6: Inhibition values for MAO B specific rasagiline

Unlike MAO A, zMAO is inhibited by this inhibitor with a K_i value very similar to that for MAO B.

* Values from (Hubalek 2004)

Another MAO B specific irreversible inhibitor is L-deprenyl (selegiline). Deprenyl is an acetylenic MAO inhibitor, together with clorgyline and pargyline and has been commonly used in the treatment of Parkinson's disease (Wessel 1992). All these inhibitors target the FAD cofactor of human isoforms and form an N(5) flavocyanine adduct. Upon adduct formation, the characteristic 455 nm absorption maxima of FAD is bleached and absorption at 410 nm appears (Chuang 1974). Previously in Chapter 2, we showed that zMAO is inhibited by the MAO A-specific inhibitor clorgyline and by the MAO B-specific inhibitor deprenyl. Competitive inhibition studies showed that the K_i value for zMAO inhibition by deprenyl is 30.4 μM while it is 14 μM for MAO B. A characteristic 415 nm band for N(5) flavocyanine formation is also observed upon zMAO inhibition by deprenyl (Figure 2.5) and by clorgyline (Figure 2.6).

Hydrazines

Hydrazines are one of the first MAO inhibitors discovered and still gather attention due to their pharmacological importance (Kost, Matrenina et al. 1967; Binda 2008). Benzylhydrazine, phenylhydrazine and phenylethylhydrazines are among the well-studied hydrazine analogues and mechanism based MAO inhibitors. All of these hydrazine analogues are metabolized by MAO A or MAO B to their corresponding diazenes which then inhibit either enzyme irreversibly through N(5) adduct formations (Binda 2008). Phenylethylhydrazine inhibits either enzyme but exhibits stronger inhibition with MAO B and to date it is occasionally used in the treatment of severe depression. Studies of zMAO with hydrazine analogues are summarized in Table 3.7 and show that the enzyme is inhibited by either analogue reversibly. Benzylhydrazine inhibits zMAO 20-fold tighter than it binds to MAO B while phenylhydrazine inhibits zMAO

with a value of higher than either human isoform. The K_i value of phenylethylhydrazine inhibition is in between to that for human MAO A and B (Table 3.7)

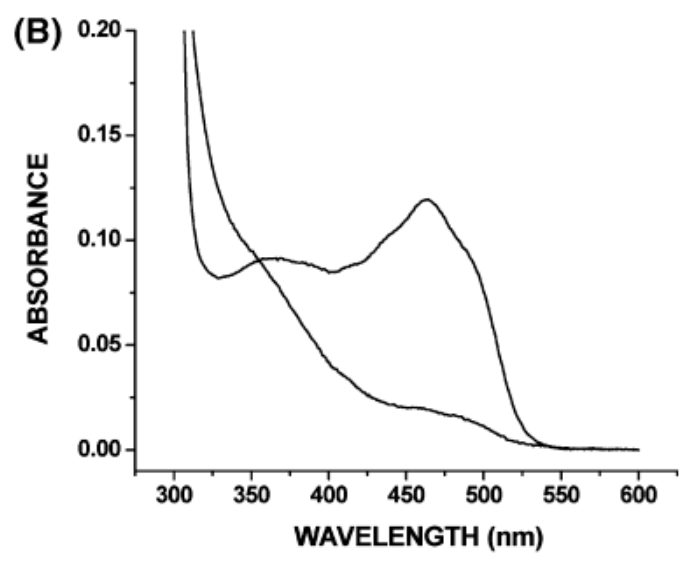
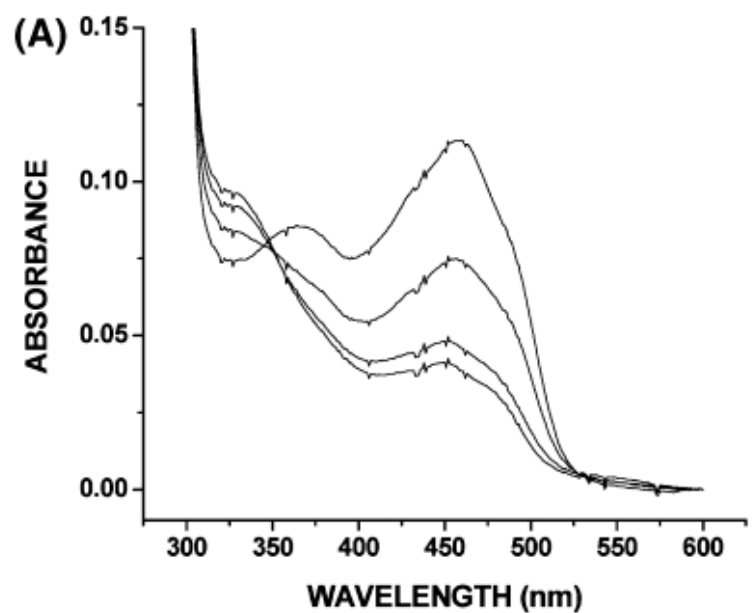
	zMAO	Human A*	Human B*
	K _i (μM)		
Benzylhydrazine	0.81 ± 0.07	2096 ± 268	26 ± 1
Phenylhydrazine	19.1 ± 2.2	205 ± 4	N.D.**
Phenylethylhydrazine	24.0 ± 3.5	47 ± 2	15 ± 2

Table 3.7: Comparison of zMAO inhibition by arylalkylhydrazines with human MAO A and B

*Data obtained from (Binda 2008).

**No detectable inhibition is observed up to 100 μM phenylhydrazine concentration. (Binda 2008)

Further spectral studies performed with zMAO inhibition suggest an alteration of the flavin, presumably through covalent adduct formation. Recently it has been shown that both human MAO isoforms form N(5) flavin adduct upon phenylethylhydrazine inhibition. Visible absorption spectral changes in human MAO A and B upon phenylethylhydrazine inhibition are shown in Figure 3.2. In comparison, zMAO exhibits a similar UV-Vis absorption spectral change on incubation with phenylethylhydrazine. These observation suggest the enzyme might be also alkylated at the N(5) flavin position, however further experiments has to performed for more precise conclusion.



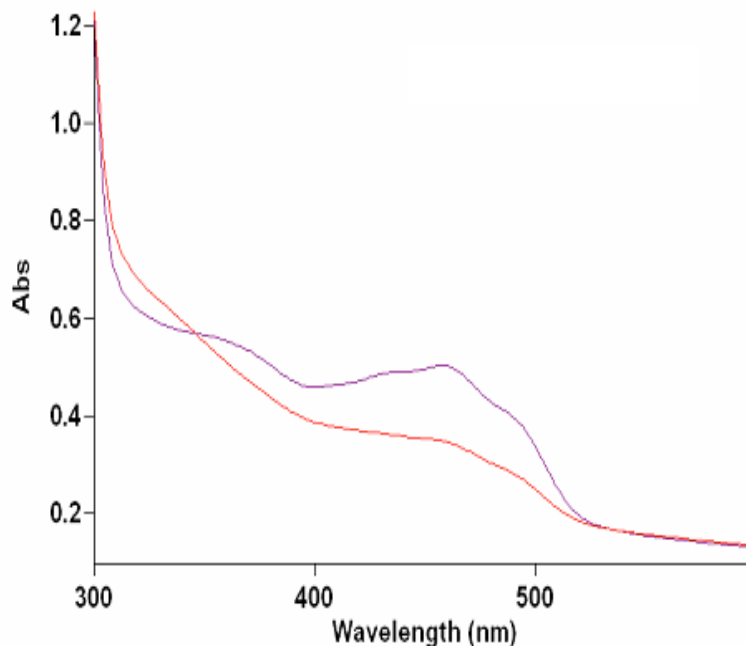


Figure 3.2. Comparison of the UV-Visible absorption spectra of human MAO A (A), human MAO B (B) and zMAO (bottom) phenylethyldiazine inhibition.

Spectral properties of zMAO resemble shows similar pattern to that human forms. This study was performed with approximately 60% functional enzyme which exhibited no detectable activity after the inhibition. Figure A and B are in part with permission from Binda 2008. Copyright 2008 American Chemical Society.

Non-Specific Inhibitors

Not all MAO inhibitors are isoform selective. Non-specific MAO inhibitors such as d-amphetamine and isatin are small inhibitors often used in pharmacological studies (Green and El Hait 1980; Sowa, Holt et al. 2004). We show that amphetamine binds to zMAO at a similar value to those for either human isoforms, while isatin binds to zMAO with a similar K_i value to that for human MAO B (Table 3.8).

	zMAO	Human A	Human B
	Ki (μM)		
Amphetamine	5.2 \pm 0.4	3.7 \pm 0.5 ^a	~4 ^a
Isatin	3.1 \pm 0.7	15 ^b	3 ^b

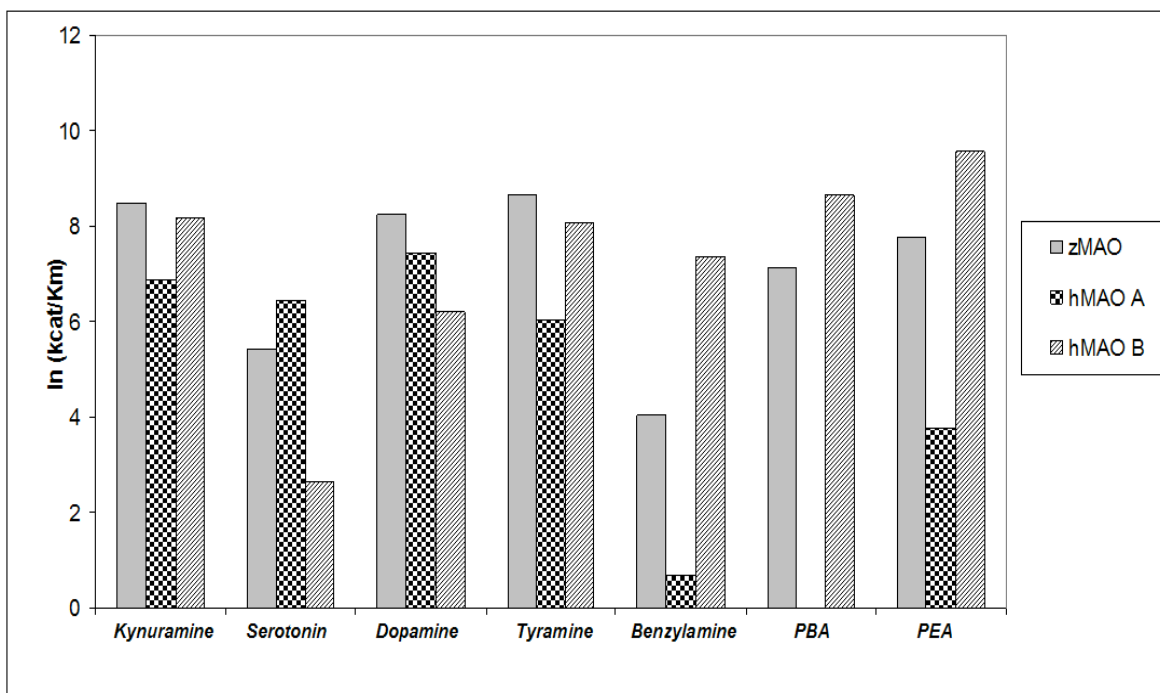
Table 3.8: Inhibition profile of zMAO with amphetamine

Values are taken from ^aJ. Wang PhD Thesis and ^b(Binda 2006)

3.3. Summary

The limited number of publications on zMAO suggests that the enzyme exhibits properties of both human MAO A and MAO B, with more similarities to human MAO A (Sallinen 2009). However, this conclusion is based on limited experimental data; which were not performed on purified zMAO. In the previous chapter we described the high-level expression and purification protocol for recombinant zMAO. To provide information on the kinetic properties of this enzyme, I performed detailed steady-state kinetic analyses and inhibition studies on this purified enzyme, as presented in this chapter. To investigate the validity of current notion on zMAO and to provide further improved comparative data with the purified enzyme, a number of human MAO A and MAO B specific substrates and inhibitors were tested. Table 3.9 summarizes the ratio of k_{cat} values for zMAO with human MAO A and human MAO B. Steady-state kinetic properties of zMAO show that the enzyme oxidizes serotonin (a MAO A-specific substrate) with a one-half the value for human MAO A and three times higher than human MAO B, and oxidizes kynuramine or dopamine at rates approximately two-fold higher than either human MAO A or MAO B. Tyramine is oxidized by zMAO with

similar values to human MAO A. In Chapter 2 we have shown that the MAO B specific substrate phenylethylamine is oxidized by zMAO at a rate nearly equivalent to that exhibited by MAO B; while another MAO B specific substrate benzylamine is oxidized by zMAO at rates approximately two-fold higher than MAO. Interestingly, phenylbutylamine which inhibits the activity of MAO A is shown to be a substrate for both zMAO and human MAO B. Overall, based on the substrate data, we confirmed that zMAO can oxidize the substrates of both human isoforms.



Ratio k_{cat}/K_m values for:	Kynuramine	Serotonin	Dopamine	Tyramine	Benzylamine	Phenylbutylamine
zMAO / hMAO A	5.20	0.37	13.1	13.0	26.3	Inhibitor
zMAO / hMAO B	1.39	16.40	7.40	1.75	0.04	0.13

Table 3.9: Comparison of $\ln(k_{cat}/K_m)$ ($\text{min}^{-1} \text{mM}^{-1}$) for zMAO and human MAO isoforms using various substrates.

PBA and PEA stands for phenylbutylamine and phenylethylamine, respectively. Note that PBA inhibits the activity of MAO A but is a substrate for MAO B and zMAO. Measurements are performed under air saturation.

Considering the importance of MAO inhibitors, the inhibition profile of zMAO is also established. Similar to the observed substrate specificities, zMAO catalytic activity is competitively inhibited by a number of MAO A and MAO B specific inhibitors (Table 3.10). While zMAO is inhibited by a number of MAO B specific inhibitors, one particular MAO B specific inhibitor, Safinamide, shows 100-fold weaker binding affinity with zMAO than with MAO B. Safinamide is one of the inhibitors that was examined in a significant study, on the importance of MAO B Ile199 (Hubalek 2005). Among safinamide, the binding of 8-(3-chlorostyryl)-caffeine, 1,4-diphenyl-2-butene, and 1,4-diphenyl-1,3-butadiene was shown to be effected by the presence of this residue. Based on the crystal structures of MAO B with these inhibitors, Ile199 was assigned as “the gate” of human MAO B binding site. Replacing Ile with a Phe (such as occurs in bovine MAO B, human MAO A and in the homologous position in zMAO) resulted in the loss of sensitivity of MAO B to these inhibitors (Hubalek 2005). As shown here, zMAO is inhibited by all these inhibitors, except for safinamide. Therefore, despite the presence of an Phe in the homologous position, the inhibition of zMAO with bulky inhibitors such as 8-(3-chlorostyryl)-caffeine, 1,4-diphenyl-2-butene, and 1,4-diphenyl-1,3-butadiene is intriguing and suggest that the high sequence identity of zMAO to MAO A in the active site residues do not necessarily reflect identical structural and functional properties.

Another set of inhibitors that reflects the promiscuity of zMAO, are the hydrazines. While benzylhydrazine has high selectivity towards MAO B and phenylhydrazine specifically inhibits MAO A, zMAO is inhibited by both hydrazines with relatively tight affinities (Table 3.11). Phenylethylhydrazine can inhibit either human isoforms, and also inhibits zMAO with similar spectral properties to the human forms, suggesting the

formation of an N(5) alkylated flavin coenzyme. The acetylenic inhibitors such as rasagiline, deprenyl and clorgyline react with zMAO to form irreversible N(5) flavocyanine adducts. The low micromolar range K_i values for these inhibitors are in agreement with values found in the literature, which showed zMAO exhibits a MAO A-like IC_{50} inhibition profile for deprenyl and a MAO B-like IC_{50} profile for clorgyline (Setini, Pierucci et al. 2005)

In conclusion, the studies presented in this chapter demonstrate that expressed and purified zMAO, exhibits functional properties in common with those of either human MAO A or MAO B with a number of catalytic properties more similar to those of human MAO A. Based on the structural and functional information it is known that human MAO A has a smaller sized catalytic site than human MAO B and the binding of bulky inhibitors such as 1,4-diphenyl-1,3-butadiene is abolished. Safinamide is the one and only bulky inhibitor that does not inhibit zMAO. Based on this functional behavior, one could propose that zMAO contains a wider binding pocket than human MAO A, despite sharing a high sequence identity. Certainly, without structural evidence, these ideas are quite speculative. Additionally, results show that an evolutionary co-ortholog of a human enzyme can function with higher functional promiscuity. Considering that zebrafish contains only one form of MAO, the high selectivity of this enzyme is reasonable. Further structural and mechanistic work on zMAO is required and should provide new insights into the molecular basis for the differing functional properties of MAO A and of MAO B.

MAO A Specific Inhibitors	Ratio K_i Values zMAO/hMAO A
Harmane	0.83
Tetrindole Mesylate	6.47
Phenylbutylamine	Substrate for zMAO
Phenylhydrazine	0.09
Phenyethylhydrazine	0.53
MAO B Specific Inhibitors	Ratio K_i Values zMAO/hMAO B
8-(3-Chlorostyryl)-caffeine	13.3
1,4-Diphenyl-1,3-Butadiene	0.14
1,4-Diphenyl-2-Butene	0.04
Farnesol	0.48
Safinamide	1.31
Mofegiline	125
Benzylhydrazine	0.03
Phenyethylhydrazine	1.67

Non-Specific Inhibitors	Ratio K_i Values zMAO/hMAO A	Ratio K_i Values zMAO/hMAO B
Amphetamine	1.35	1.30
Isatin	0.21	1.03

Table 3.10 : K_i (μM) inhibition ratio values zMAO with MAO A, MAO B and non-specific inhibitors

3.4 References

- Andreeva, N. I., Golovina S. M., Mashkovskii, M.D. (1992). "A new antidepressant tetrindole II. Experimental investigation of tetrindole tolerability." Pharmaceutical Chemistry Journal **26** (11-12): 19-22
- Anichtchik, O., Sallinen, V., Peitsaro, N., Panula, P. (2006). "Distinct structure and activity of monoamine oxidase in the brain of zebrafish (*Danio rerio*)." Journal of Comparative Neurology **498**(5): 593-610.
- Binda, C., Hubalek, F., Li, M., Castagnoli, N., Edmondson, D. E., Mattevi, A. (2006). "Structure of the human mitochondrial monoamine oxidase B - New chemical implications for neuroprotectant drug design." Neurology **67**(7): S5-S7.
- Binda, C., Hubalek, F., Li, M., Herzig, Y., Sterling, J., Edmondson, D. E., Mattevi, A. (2005). "Binding of rasagiline-related inhibitors to human monoamine oxidases. a kinetic and crystallographic analysis." Journal of Medicinal Chemistry **48**(26): 8148-8154.
- Binda, C., J. Wang, Pisani, L., Caccia, C., Carotti, A., Salvati, P., Edmondson, D.E., Mattevi, A. (2007). "Structures of human monoamine oxidase B complexes with selective noncovalent inhibitors: Saffinamide and coumarin analogs." Journal of Medicinal Chemistry **50**(23): 5848-5852.
- Binda, C., Wang, J., Li, M., Hubalek, F., Mattevi, A., Edmondson, D. E. (2008). "Structural and mechanistic studies of arylalkylhydrazine inhibition of human monoamine oxidases A and B." Biochemistry **47**(20): 5616-5625.
- Chen, K., H. F. Wu, Grimsby, J., Shih, J.C. (1994). "Cloning of a novel monoamine oxidase cDNA from trout liver." Mol Pharmacol **46**(6): 1226-33.
- Chuang, H. Y., D. R. Patek and L. Hellerman (1974). "Mitochondrial monoamine oxidase. Inactivation by pargyline. Adduct formation." J. Biol. Chem. **249**: 2381.
- De Colibus, M. L., C. Binda, A. Lustig, D. E. Edmondson, A. Mattevi (2005). Proc Natl Acad Sci U S A **102**(12684-12689).

- Edmondson, D. E., Binda, C., Wang, J., Upadhyay, A., Mattevi, A. (2009). "Molecular and Mechanistic Properties of the Membrane-Bound Mitochondrial Monoamine Oxidases." Biochemistry **48**(20): 4430-4230.
- Edmondson, D. E., DeColibus, L., Binda, C., Li, M., Mattevi, A. (2007). "New insights into the structures and functions of human monoamine oxidases A and B." Journal of Neural Transmission **114**(6): 703-705.
- Green, A. L., M. A. El Hait (1980). "p-Methoxyamphetamine, a potent reversible inhibitor of type-A monoamine oxidase in vitro and in vivo." J Pharm Pharmacol **32**(4): 262-6.
- Holt, A., Palcic, M.M. (2006). "A peroxidase-coupled continuous absorbance plate-reader assay for flavin monoamine oxidases, copper-containing amine oxidases and related enzymes " Nature Protocols **1**(5): 2498-2505.
- Holt, A., D. F. Sharman, Baker, G.B., Palcic, M.M. (1997). "A continuous spectrophotometric assay for monoamine oxidase and related enzymes in tissue homogenates." Anal Biochem **244**(2): 384-92.
- Hubalek, F., Binda, C., Khalil, A., Li, M., Mattevi, A., Castagnoli, N., Edmondson, D. E. (2005). "Demonstration of isoleucine 199 as a structural determinant for the selective inhibition of human monoamine oxidase B by specific reversible inhibitors." J Biol Chem **280**(16): 15761-15766.
- Hubalek, F., Binda, C., Li, M., Herzig, Y., Sterling, J., Youdim, M. B. H., Mattevi, A., Edmondson, D. E. (2004). "Inactivation of purified human recombinant monoamine oxidases A and B by rasagiline and its analogues." Journal of Medicinal Chemistry **47**(7): 1760-1766.
- Kost, A. N., V. L. Matrenina, Sidorkin, V.I., Smirnova, A.V., Shardurskii, K.S. (1967). "Pharmacological and biochemical properties of pyridylethylhydrazines and pyridylethylamines." Farmakologiya Toksikologiy (Moscow) **30**(2): 178-183.

- Li, M., F. Hubalek, Newton-Vinson, P., Edmondson D.E. (2002). "High-level expression of human liver monoamine oxidase A in *Pichia pastoris*: comparison with the enzyme expressed in *Saccharomyces cerevisiae*." Protein Expr Purif **24**(1): 152-62.
- Lieschke, G. J., P. D. Currie (2007). "Animal models of human disease: zebrafish swim into view." Nature Reviews Genetics **8**(5): 353-367.
- Milczek, E. M., Bonivento, D., Binda, C., Mattevi, A., McDonald, I. A., Edmondson, D. E. (2008). "Structural and Mechanistic Studies of Mofegiline Inhibition of Recombinant Human Monoamine Oxidase B." Journal of Medicinal Chemistry **51**(24): 8019-8026.
- Nandigama, R. K. and D. E. Edmondson (2000). "Structure-activity relations in the oxidation of phenethylamine analogues by recombinant human liver monoamine oxidase A." Biochemistry **39**(49): 15258-65.
- Sallinen, V., M. Sundvik, Reenilä, I., Peitsaro, N., Khrustalyov, D., Anichtchik, O., Toleikyte, G., Kaslin, J., Panula, P. (2009). "Hyperserotonergic phenotype after monoamine oxidase inhibition in larval zebrafish." Journal of Neurochemistry **109**(2): 403-415.
- Setini, A., F. Pierucci, Senatori, O., Nicotra, A. (2005). "Molecular characterization of monoamine oxidase in zebrafish (*Danio rerio*)." Comparative Biochemistry and Physiology B-Biochemistry & Molecular Biology **140**(1): 153-161.
- Sowa, B. N., A. Holt, Todd, K.G., Baker G.B. (2004). "Monoamine oxidase inhibitors, their structural analogues, and neuroprotection." Indian J Exp Biol **42**(9): 851-7.
- Stanhope, M. J., A. Lupas, M.J. Italia, K.K. Koretke, V.C. Volker, J.R. Brown (2001). "Phylogenetic analyses do not support horizontal gene transfers from bacteria to vertebrates. ." Nature **411**: 940-944.
- Upadhyay, A. K., Borbat, P.P., Wang, J., Freed, J.H., Edmondson, D.E. (2008). "Determination of the oligomeric states of human and rat monoamine oxidases in

the outer mitochondrial membrane and octyl beta-D-glucopyranoside micelles using pulsed dipolar electron spin resonance spectroscopy." Biochemistry **47**(6): 1554-1566.

Wessel (1992). "Selegiline--An overview of its role in the treatment of Parkinson's disease." Clin Invest **70**(): 459.

Zhou, M., Z. Diwu, Panchuk-Voloshina, N., Haugland, R.P. (1997). "A stable nonfluorescent derivative of resorufin for the fluorometric determination of trace hydrogen peroxide: applications in detecting the activity of phagocyte NADPH oxidase and other oxidases." Anal Biochem **253**(2): 162-8.

CHAPTER 4

COMPARATIVE STRUCTURE-ACTIVITY RELATIONSHIPS OF ZEBRAFISH MONOAMINE OXIDASE

4.1 Introduction

Previous studies in the Edmondson laboratory have investigated the structures of the substrate binding sites and the mechanism of catalysis for human MAO A and MAO B using quantitative-structure activity relationship (QSAR) analysis of kinetic data. These studies were based on measuring the turnover rates and binding affinities of MAO enzymes using a series of *para*-substituted benzylamine analogues and have shown that besides their substrate and inhibitor specificities, human MAO enzymes also exhibit differences in their QSAR properties. An increase in the size of *para*- substituent of benzylamine increases the analogue binding affinity to human MAO A; the hydrophobicity of the *para*- substituent was shown to facilitate analogue binding to human MAO B. The effect of the *para*- substituent's electron donating/withdrawing ability on the rate of flavin reduction in MAO A shows that C-H bond cleavage occurs involving proton abstraction step (Miller 1999). On the other hand, restricted orientation of the substrate's phenyl ring prevents expression of the *para* substituent's electronic effect, in MAO B (Walker 1994).

QSAR is a useful tool to understand the substrate binding site and the parameters that effect substrate binding & catalytic mechanism. The main objective of this chapter is to investigate the substrate binding site of zMAO through QSAR analysis of kinetic measurements.

Why QSAR?

The principle of QSAR approach is to establish mathematical models that relate variations of various factors with variations in responses (Gupta 1987). The factors could be structural and/or physicochemical properties of the subjected compounds and are described using quantitative molecular parameters. The idea is based on the “*similar changes in structure produce similar changes in reactivity*” view by L.P. Hammett and was initially proposed as “the electronic effect of substituents on similar reaction systems could be estimated based on the effects of substituents on the ionization of benzoic acids” (Hammett 1935). Thus, the most widely used equation in QSAR studies is the Hansch equation; a derivation from the classic Hammett equation (Hansch and Leo 1995). The parameters and their explanations are summarized in Table 4.1 and 4.2 and can be applied to proteins to understand their properties.

Equation #	Parameter	Equation Formula
1	Klinman equation	$\frac{{}^D k_{cat} - 1}{{}^D (k_{cat} / K_m) - 1} = K_m / K_d$
2	Corrected Kd Values	$K_{d(corrected)} = \frac{K_{d(observed)}}{1 + \text{anti log}(pK_a - pH)}$
3	Hammett equation	$\log k_x = \rho\sigma + \log k_H$
4	Hansch equation	$\log k(\text{or } K_d) = \rho(\sigma) + A(\pi) + B(V_w)(\text{or } E_s) + C$
5	F Value	$F_{1,n} = (n-2) \frac{r^2}{1-r^2}$

Table 4.1 Overall view of the equations used in QSAR studies (Gupta 1987; Hansch and Leo 1995)

k	Rate Constant	Rate constant for product formation & enzyme turnover, refers to k_{cat} for the presented study
K_d	Dissociation constant	Obtained from Equation 2 of Table 4.1 for steady state measurements, represents the substrate dissociation constant from all enzyme-substrate complexes
ρ	Reaction Constant	Slope of the Hammett plot, a measure of the sensitivity of a reaction to the electronic effect of the substituents
σ	Hammett Constant	Defined for <i>meta</i> and <i>para</i> substituents to represent electronic character; positive value denotes electron-withdrawing character and negative value denotes electron-donating character
π	Hydrophobic constant	$\pi = \log P_x - \log P_H$ where P_x is the partition coefficient of the substituted compound and P_H is the unsubstituted reference compound (distribution between octanol and water)
V_w	Van der Waals volume	Molar volume calculated from atomic radius
E_s	Taft steric constant	Represent the steric effect affecting intramolecular and intermolecular hindrance to the reaction or binding

Table 4.2 Explanation of the parameters in Hansch equation used in QSAR studies (Gupta 1987; Hansch and Leo 1995)

The objective of this work is to investigate the quantitative structure–activity relationships (QSAR) to predict the active site properties of zMAO and to compare these properties with the human isoforms. QSAR measurements were already performed with human MAO A using *para*- benzylamine and phenylethylamine but not with the *meta*-substituted form of the either human isoform (several *meta*- substituted benzylamine analogues were measured for bovine MAO B, previously (Husain, Edmondson et al. 1982; Walker 1994; Miller 1999; Nandigama and Edmondson 2000). Therefore the QSAR data for of *meta*- benzylamine and phenylethylamine analogues of human isoforms as well as *para*- phenylethylamines with human MAO B are also obtained. The QSAR data presented here are based on a series of *para*- and *meta*- substituted benzylamines and phenylethylamines. The parameters that correlate with kinetic data exhibited by zMAO are determined and then compared with human MAO isoforms for a detailed understanding of the differences between these co-orthologs.

4.2 Materials & Methods

4.2.1 Materials

Reduced Triton X-100 was from Fluka (Sigma-Aldrich, St. Louis, MO). Glycerol and kynuramine were purchased from Sigma-Aldrich (St. Louis, MO). All *para* substituted benzylamine analogues were synthesized previously by Dr. Richard Miller and by Dr. Mark Walker (Walker 1994, Miller and Edmondson 1999). The following phenylethylamine analogues were purchased from Sigma-Aldrich (St. Louis, MO): *p*- H, *p*- NO₂, *p*- Me, *p*- MeO, *p*-Cl. Other analogues, such as *p*- Br and *p*- CF₃ were

synthesized previously by Nandigama et al (Nandigama and Edmondson 2000). Octyl β -D-glucoside was purchased from Anatrace Inc (Maumee, OH).

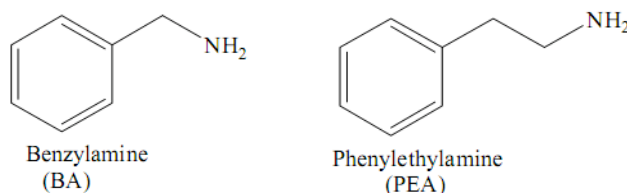


Figure 4.1: Chemical structures of MAO substrates benzylamine and phenylethylamine

4.2.2 Preparation of enzymes

Similar procedures were followed for preparation of zMAO as described in Chapter 1 and Chapter 3. Prior to use, enzyme was stored in 20 mM KPi buffer containing 0.8% (w/v) octyl β -D-glucoside and 20% glycerol (pH=7.4) on ice and dark at all times. Human MAO A and MAO B preparations were prepared by Ms. Milagros Aldeco (Edmondson's lab) and were diluted to sufficient concentrations by 50 mM potassium phosphate buffer with 20% glycerol (w/v) containing 0.8% (w/w) octyl β -D-glucoside (pH=7.2) and stored on ice and dark at all times.

4.2.3 Determination of kinetic parameters: k_{cat} , K_m and K_d

Steady state assays for direct measurement of substrate oxidation performed spectrophotometrically. k_{cat} and K_m values were determined by non-linear fits of steady state kinetic data to the Michaelis-Menten equation using Origin software (OriginLab Corporation, Northampton, MA).

4.2.4 Steady state kinetic measurements of *para*- and *meta*- substituted benzylamine analogue oxidation

All steady state kinetic measurements of *para*- and *meta*- substituted benzylamine analog oxidation with zMAO were performed in 50 mM potassium phosphate buffer (pH =7.4) containing 0.5% (w/v) reduced Triton X-100 at 25 °C. Steady state rate of *para*- and *meta*- benzylamine analogue oxidation to its corresponding aldehyde was measured spectrophotometrically. Wavelength and molar absorption extinction coefficients for each aldehyde are shown in Table 4.3. For benzylamine analogues such as *p*-Me-BA, *p*-MeO-BA, *p*-H-BA and their α,α -[²H]benzylamine analogs, as well as *m*-Me-BA, *m*-MeO-BA and their α,α -[²H]benzylamine analogs, an amplex-red peroxidase coupled assay was used for an increased detection sensitivity ($\epsilon_{m560} = 54,000 \text{ M}^{-1}\text{cm}^{-1}$). For measurements that required saturated oxygen conditions, the dissolved oxygen concentrations in the reaction buffers were adjusted by passing pure oxygen to give a concentration of 960 μM , in the reaction buffer using an air sparger. The concentrations of the dissolved oxygen in the reaction buffers were measured polarographically before the measurements.

Benzylamine Substituent	Wavelength of Maximal Absorbance Change	Δ Extinction Coefficient ($M^{-1} cm^{-1}$)
p-H	250	15,600
p-MeO	281	12,600
p-Me	259	12,800
p-F	250	14,200
p-Cl	257	21,800
p-Br	264	21,700
p-CF ₃	243	11,800
m-MeO	253	11,900
m-Me	252	15,700
m-Cl	247	16,300
m-CF ₃	252	15,700
m-Cl	247	16,300

Table 4.3 Extinction coefficients for *para*- and *meta*- substituted benzylamine substrates

Values were determined previously by Walker through direct comparison of the rates of oxygen consumption with the rates of changes in absorbance during the oxidation of substituted benzylamine substrates (Walker 1994).

4.2.5 Steady state kinetic measurements of *para*- and *meta*- substituted phenylethylamine analogue oxidation

An amplex red peroxidase coupled assay was used to determine the steady state values of phenylethylamine analogues ($\epsilon_{m560} = 54,000 \text{ M}^{-1}\text{cm}^{-1}$) as described in Chapter 3. All steady state kinetic measurements of *para*- and *meta*- substituted benzylamine analogue oxidation with zebrafish MAO, human MAO A and B were performed in 50 mM KPi buffer (pH =7.4) containing 0.5% (v/v) reduced Triton X-100 at 25 °C.

4.2.6 Data analysis

K_d values were calculated from steady state deuterium kinetic isotope effect data as previously described by Klinman and Matthews (Klinman and Matthews 1985). Apparent K_d values were corrected to reflect the concentration of deprotonated amine in solution which is specifically bound (McEwen, Sasaki et al. 1969), (McEwen, Sasaki et al. 1968). Substituent parameter values (σ , π , and E_s) were obtained from Hansch (Hansch and Leo 1995) . Values for V_w (Van der waals) values were calculated as described by Bondi (Bondi 1964). Multi-component statistical analyses of correlations were performed using StatView software (Abacus Concepts, Piscataway, NJ).

4.3 Results

4.3.1 Steady state kinetic measurements with *para*-substituted benzylamine analogues and the effects of isotopic substitution

A major difference in the catalytic behaviors of human MAO A and MAO B is the influence of *para*- substituents in the oxidation of benzylamine analogues. MAO A demonstrates a strong electronic contribution ($\rho=+1.8$) (Miller and Edmondson 1999) but no electronic effect is observed with MAO B (Walker and Edmondson 1994). Given the similarities of zMAO to MAO A, the influence of *para*- substitution on the steady state rate of benzylamine oxidation was determined for seven analogues. The kinetic data are shown in Table 4.4.

In agreement with published data on human MAO A (Newton-Vinson, Hubalek et al. 2000), and MAO B (Li, Hubalek et al. 2002), Shown in Table 4.4, $^Dk_{cat}$ and $^Dk_{cat}/K_m$ kinetic isotope effects with α,α -[D₂]benzylamine analogues range in values from 4 to 8, demonstrating that the α -C-H bond cleavage kinetic step is rate limiting in catalysis as found in MAO A and B from various mammalian sources.

Substituent	k_{cat} (H) (min ⁻¹)	K_m (H) (μ M)	k_{cat} (D) (min ⁻¹)	K_m (D) (μ M)	$^Dk_{cat}$ (min ⁻¹)	$^D(V/K)$	Calculated Kd (corrected) (μ M)
<i>p</i> -MeO	8.30 ±0.7	55.5 ±4.1	1.42 ±0.05	77.1 ±8.2	5.9 ±0.7	8.3 ±0.5	0.61
<i>p</i> -Me	6.92 ±0.13	67.8 ±4.1	1.08 ±0.02	64.4 ±4.3	6.4 ±0.2	6.0 ±0.2	0.61
<i>p</i> -H	4.71 ±0.14	82.2 ±9.0	2.34 ±0.20	153 ±32	2.0 ±0.2	3.8 ±0.3	3.3
<i>p</i> -F	14.91 ±0.28	161.1 ±8.1	2.23 ±0.05	85.8 ±6.2	6.7 ±0.2	3.5 ±0.1	1.2
<i>p</i> -Br	40.03 ±3.05	102.8 ±20.1	4.88 ±0.17	75.3 ±7.9	8.2 ±0.7	6.0 ±0.4	1.8
<i>p</i> -Cl	34.6 ±1.1	94 ±10	5.9 ±0.17	126.8 ±8.7	5.9 ±0.2	8.0 ±0.4	3.4
<i>p</i> -CF ₃	93.7 ±6.8	115 ±36	22.5 ±1.5	140 ±20	4.2 ±0.3	5.1 ±0.4	7.2
<i>p</i> - <i>t</i> -butyl	6.9 ±0.2	48 ±6	3.4 ±0.2	102.2 ±16.1	2.0 ±0.1	4.4 ±0.2	1.3

Table 4.4 Effect of *para*-substitution on the kinetic properties of zMAO oxidation by various benzylamine analogues

4.3.5 Steady state kinetic measurements with meta-substituted benzylamine analogues and the effects of isotopic substitution

A series of *meta*-substituted benzylamine was previously synthesized in our lab to determine the steady-state properties of bovine MAO B (Walker 1994). In this study, we determined the catalytic properties of zMAO, human MAO A and B with six different *meta*-substituted benzylamine analogues to provide an accurate comparison. The observed k_{cat} values are shown in Table 4.5.

It was observed that zMAO exhibits turnover rates similar to human MAO A. Both human MAO A and zMAO have a rate increase with the CF_3 as *meta*- substituent compare the *meta*-H substituent (~20 fold and ~5 fold respectively) while there is not a large change in the rates of human MAO B with either substituent. The kinetic isotope effect values of human MAO A were too difficult to detect with the standard catalytic assay due to the slow rates and even slower rates when α,α -deuterated *meta*-benzylamine analogues are used as substrates. Human MAO B exhibits detectable rates with α,α -deuterated *meta*- benzylamines with Dk_{cat} values ranging from 3.06 to 5.31.

The values of Dk_{cat} with human MAO B are similar to those observed for bovine MAO B (Walker 1994). The magnitude of bovine MAO B Dk_{cat} value (ranging from 10.9 – 14.1) exceeds those observed for human MAO B (Table 4.6).

Human MAO A			
Meta-Substituent	k_{cat} (H) (min⁻¹)	K_m(H) (μM)	log^H(V/K) (min⁻¹μM⁻¹)
1. H	2.5 \pm 0.1	1250 \pm 50	-2.70
2. F	2.7 \pm 0.1	575 \pm 26	-2.33
3. Cl	3.2 \pm 0.2	59.6 \pm 7.6	-1.27
4. CF3	52 \pm 6	26 \pm 1	0.30
5. Me	2.0 \pm 0.1	88 \pm 12	-1.64
6. MeO	3.5 \pm 0.2	189.4 \pm 17.0	-1.73
Human MAO B			
1. H	246 \pm 10	157 \pm 7	0.20
2. F	335 \pm 22	115.3 \pm 5.9	0.46
3. Cl	353 \pm 21	65.5 \pm 3.3	0.37
4. CF3	325.8 \pm 21.5	112.8 \pm 7.6	-0.27
5. Me	349.1 \pm 20.0	35.2 \pm 5.1	0.63
6. MeO	308.7 \pm 12.2	58.1 \pm 6.2	0.27
Zebrafish MAO			
1. H	4.36 \pm 0.14	82.0 \pm 4.1	-1.27
2. F	2.78 \pm 0.14	164.6 \pm 18.2	-1.77
3. Cl	8.81 \pm 2.05	60.5 \pm 4.5	-0.84
4. CF3	9.57 \pm 0.57	61.3 \pm 4.2	-0.81
5. Me	2.79 \pm 0.14	54.3 \pm 2.7	-1.29

Table 4.5: Comparison of the steady-state rates of hMAO A, hMAO B and zMAO catalyzed α,α -¹H]-*m*-substituted benzylamines. α,α -²H] rates were not detectable for hMAO A and zMAO.

Substituent	k_{cat} (D) (min ⁻¹)	K_m (D) (μ M)	$^Dk_{cat}$	$^D(V/K)$	K_d (μ M)	Corrected log K_d (μ M)
1. Cl	66.5 ± 3.4	88.4 ± 4.4	4.1 ± 0.2	3.06 ± 0.15	58.7 ± 2.9	1.77
2. H	51.3 ± 2.7	450.0 ± 22.5	4.7 ± 0.2	4.5 ± 0.2	425.6 ± 21.3	2.63
3. CF ₃	80.05 ± 4.00	89.0 ± 4.6	4.1 ± 0.2	3.23 ± 0.17	64.6 ± 3.3	1.81
4. MeO	102.5 ± 5.2	112.1 ± 5.6	3.4 ± 0.2	3.12 ± 0.13	98.9 ± 4.9	2.00
5. Me	115.5 ± 5.7	129.2 ± 6.5	3.0 ± 0.2	5.13 ± 0.19	264.2 ± 13.2	2.42

Table 4.6: Steady-state kinetic constants for the human MAO B catalyzed oxidation of *m*-substituted benzylamine analogues

4.3.7 Steady state kinetic measurements of *para*-substituted phenylethylamine analogues

For further QSAR analysis, the steady state kinetic parameters for the zMAO and human MAO B catalyzed oxidation of seven *para*-substituted phenylethylamine analogues were determined and compared with the previously determined human MAO A (Nandigama and Edmondson 2000). The values for enzyme turnover and kinetic isotope effects are shown in Tables 4.7-4.9 for zMAO, human MAO A and B, respectively. The highest k_{cat} value of zMAO is achieved with the *para*-H substituent, among the other substituents the k_{cat} value ranges from a minimum 63.69 min⁻¹ for the *para*-Me analogue and to maximum of 72.2 min⁻¹ for *para*-Br analogue.

Substituent	k_{cat} (H) (min ⁻¹)	K_m (H) (μ M)	k_{cat} (D) (min ⁻¹)	K_m (D) (μ M)	$^Dk_{cat}$	$^D(V/K)$	K_d (μ M)
1. Me	63.69 ±2.52	173.20 ±6.92	14.16 ±0.56	319.86 ±12.76	4.50 ±0.27	9.19	405.3
2. Cl	71.4 ±3.2	74.40 ±3.4	22.15 ±1.5	239.60 ±19.58	3.22 ±0.16	10.5	318.4
3. Br	72.2 ±3.2	104.50 ±6.4	23.4 ±1.6	352.69	3.09 ±0.15	10.4	470
4. H	203 ±15	86.00 ±6.0	16.8 ±0.7	80.0 ±15.5	12.1 ±0.6	11.3	79.8
5. F	69.01 ±2.95	234.13 ±10.7	17.99 ±0.7	138.39 ±12.45	3.84 ±0.19	2.3	218.5
6. CF ₃	71.86 ±4.00	409.00 ±20.4	20.7 ±4.9	350.1 ±17.5	3.48 ±0.17	3.0	329.8
7. NO ₂	65.32 ±3.3	205.15 ±10.26	21.73 ±1.09	298.45 ±14.93	3.09 ±0.16	4.36	329.8

Table 4.7: Steady-state kinetic constants for the zMAO catalyzed oxidation of *p*-substituted phenylethylamine analogues

Substituent	k_{cat} (H) (min ⁻¹)	K_m (H) (μ M)	^H (k_{cat}/K_m) (min ⁻¹ / μ M)	k_{cat} (D) (min ⁻¹)	K_m (D) (μ M)	^D k_{cat} (min ⁻¹)	^D (V/K)	K_d (μ M)
1. Me	156.1 ±9.4	6.45 ±0.39	24.20 ±1.45	129.9 ±7.8	9.86 ±0.59	1.22 ± 0.07	1.76 ±0.1	24.8
2. Cl	142.1 ±9.9	7.45 ±0.45	19.07 ±1.14	110.4 ±6.6	7.64 ±0.46	1.29 ±0.07	1.33 ±0.08	8.46
3. Br	144.0 ±11.5	7.67 ±0.53	18.77 ±1.50	114.4 ±9.2	7.95 ±0.64	1.26 ±0.10	1.30 ±0.11	8.66
4. H	228.9 ±11.4	16.00 ±0.80	14.31 ±0.72	134.6 ±6.7	24.00 ±1.20	1.70 ±0.08	2.55 ±0.13	35.4
5. F	176.6 ±7.1	6.50 ±0.26	27.17 ±1.09	124.2 ±4.9	7.12 ±0.36	1.39 ±0.06	1.52 ±0.06	43.3
6. CF ₃	135.9 ±9.5	10.54 ±0.74	12.89 ±0.64	96.7 ±3.9	8.62 ±0.35	1.40 ±0.06	1.14 ±0.05	3.68
7. NO ₂	47.90 ±2.10	14.47 ±1.1	2.31 ±0.11	28.0 ±1.6	11.90 ±1.1	1.71 ±0.07	1.39 ±0.05	7.95

Table 4.8: Steady-state kinetic constants for the human MAO B catalyzed oxidation of *p*-substituted phenylethylamine analogues. Both *z*MAO and *h*MAO B kinetic assays were determined at air saturation (240 μ M) at 25°C using a peroxidase-coupled assay.

Measurements with α,α -[D₂]phenylethylamine analogues showed Dk_{cat} values for zMAO between 3.09 – 4.50 for the six of the substituents, suggesting that α -C-H bond cleavage is the rate limiting step for zMAO, as seen for human MAO A. Overall, both zMAO and human MAO A exhibit kinetic isotope effects with *para*- substituted α,α -[D₂]phenylethylamine analogues while human MAO B does not.

4.3.9 Steady state kinetic measurements with *meta*-substituted phenylethylamine analogues

Steady state kinetic rates of zebrafish MAO, human MAO A and human MAO B oxidation by 5 different *meta*- substituted phenylethylamine analogues were determined and compared. The rates for enzyme turnover (k_{cat}), kinetic isotope effects and the binding constants (K_d) are determined as described previously and are listed in Tables 4.10-4.12. There is no considerable change on the rate of zMAO turnover among the various *meta*-phenylethylamine analogues. Overall, zMAO exhibits faster rates with these analogues than either hMAO A and B do. The deuterium kinetic isotope effect values (Dk_{cat}) on enzyme turnover are large for both zMAO and human MAO A for all the *meta*- substituted phenylethylamine analogues tested and range from 7.09-12.8 for zMAO and 4.0-9.57 for human MAO A . In contrast, human MAO B does not exhibit large kinetic isotope effects with these substrate analogues.

Substituent	k_{cat} (H) (min ⁻¹)	K_m (H) (μ M)	k_{cat} (D) (min ⁻¹)	K_m (D) (μ M)	$^Dk_{cat}$ (min ⁻¹)	$^D(V/K)$	K_d (μ M)
1. H	203.8 ± 10.2	86.0 ± 4.3	16.8 ± 0.84	80.0 ± 4.0	12.1 ± 0.6	11.24	79.03
2. F	212.2 ± 10.6	67.9 ± 3.2	19.0 ± 0.91	77.8 ± 3.9	11.2 ± 0.6	12.80	78.55
3. Cl	245.4 ± 11.7	72.0 ± 3.9	31.5 ± 1.8	78.0 ± 3.4	7.79 ± 0.4	8.43	78.79
4. Br	272.3 ± 13.6	85.1 ± 4.6	30.4 ± 1.5	93.2 ± 4.7	8.96 ± 0.46	9.79	93.97
5. CF ₃	285.0 ± 14.2	109.0 ± 5.4	31.0 ± 1.6	84.1 ± 4.2	9.19 ± 0.46	7.09	81.05

Table 4.10: Steady-state kinetic constants for the zMAO catalyzed oxidation of *m*-substituted phenylethylamine analogues

Substituent	k_{cat} (H) (min ⁻¹)	K_m (H) (μ M)	k_{cat} (D) (min ⁻¹)	K_m (D) (μ M)	$^Dk_{cat}$ (min ⁻¹)	$^D(V/K)$	K_d (μ M)
1. F	83.7 ± 4.2	85.21 ± 4.4	19.2 ± 0.9	77.8 ± 3.2	4.41 ± 0.18	4.03	84.9
2. Cl	166.1 ± 8.3	10.01 ± 0.50	35.7 ± 1.8	10.7 ± 0.5	4.64 ± 0.23	4.98	79.9
3. Br	176 ± 7	34.03 ± 2.38	34.4 ± 1.72	42.2 ± 2.1	5.12 ± 0.26	6.32	82.1
4. CF ₃	205.0 ± 9.2	26.2 ± 1.31	49.2 ± 2.2	55.0 ± 2.5	4.16 ± 0.21	8.70	119.4

Table 4.11: Steady-state kinetic constants for the hMAO A catalyzed oxidation of *m*-substituted phenylethylamine analogues

Substituent	k_{cat} (H) (min ⁻¹)	K_m (H) (μ M)	k_{cat} (D) (min ⁻¹)	K_m (D) (μ M)	$^Dk_{cat}$ (min ⁻¹)	$^D(V/K)$	K_d (μ M)
1. F	83.7 ±3.7	11.40 ± 0.52	74.7 ±3.4	17.2 ±0.8	1.12 ±0.05	1.69 ±0.08	23.4
2. Cl	62.1 ±3.4	4.70 ±0.26	48.2 ±2.6	10.7 ±0.59	1.29 ±0.06	2.93 ±15	31.3
3. Br	71.0 ±3.6	5.67 ±0.28	62 ±3	8.5 ±0.4	1.45 ±0.07	1.71 ±0.09	29.9
4. CF ₃	47 ±3	77.0 ±3.8	38.4 ±1.9	78.9 ±3.9	1.22 ±0.08	1.25 ±0.08	87.5

Table 4.12: Steady-state kinetic constants for the hMAO B catalyzed oxidation of *m*-substituted phenylethylamine analogues

4.3. Quantitative Structural Activity Relationships Describing zMAO Catalysis

4.3.1 QSAR in *para*- and *meta*- substituted benzylamine analogues binding to zMAO

✦ *para*-benzylamines:

Correlations of k_{cat} with various electronic, steric and hydrophobicity parameters of the *para* substituents show the electronic parameter σ to exhibit a major contribution. Figure 4.2 show that zMAO exhibits a linear correlation $\log k_{cat}$ with σ ; a property also seen with human MAO A (Miller and Edmondson 1999) but not with MAO B (Walker 1994).

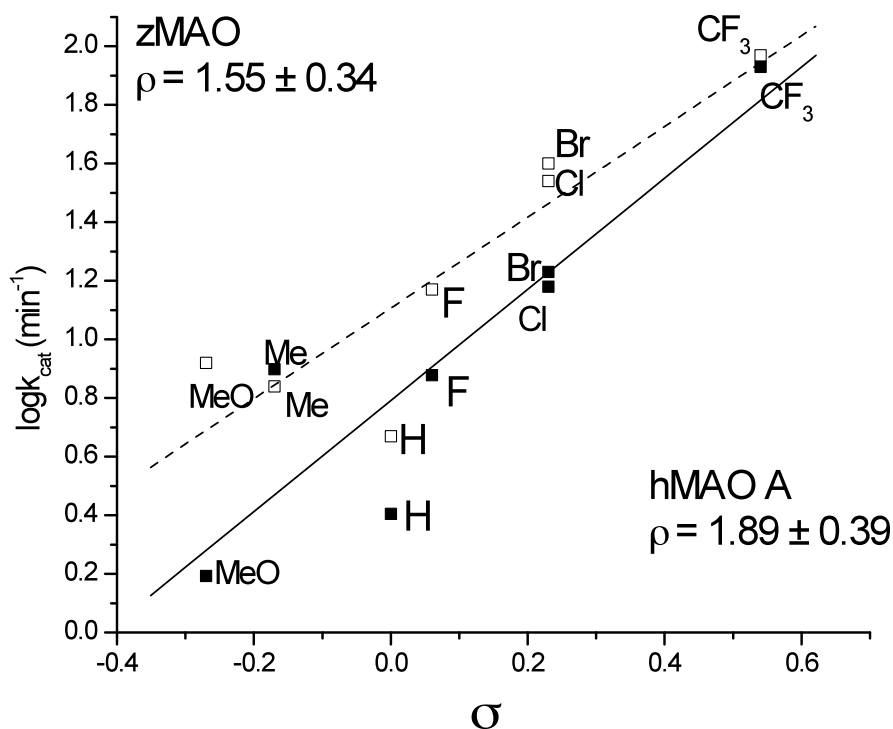


Figure 4.2: Correlation of steady state rates of zMAO (dashed line) and human MAO A (solid line) k_{cat} values with the substituent electronic parameter (σ).

The linear relation for zMAO is best described by the equation:

$$\text{Log } k_{cat} = 1.55 (\pm 0.34) \sigma + 1.1 (\pm 0.09) \quad (F_{1,6}=20; p=0.006) \quad (\text{Equation 4.1})$$

Analyses using additional substituent parameters such as van der Waals volume or hydrophobicity do not improve the correlation. As the equation (4.1) shows, the rate of turnover increases with increases in electron withdrawing power of the *para*-substituent as shown previously with human MAO A. The calculated ρ value for zMAO (+1.55) is close to that observed (+1.89) for human MAO A (Miller and Edmondson 1999). These

data demonstrate that the catalytic behavior of zMAO is more similar to that of human MAO A than to that of MAO B.

The calculated binding affinities of deprotonated *para*-substituted benzylamines for zMAO were analyzed to determine whether correlations with steric substituent parameters are observed as found with human MAO A (Miller and Edmondson 1999). Surprisingly, no correlations are observed with steric or hydrophobicity parameters. A reasonable correlation is observed for $\log K_d$ with the electronic contribution (σ) which differs from those correlations previously observed with either MAO A or with MAO B (Figure 4.3). It should be noted here that σ effect on amine pKa value is taken into consideration by correcting K_d for amount of deprotonated amine. The observed ρ value (+1.3) shows electron withdrawing groups on the benzylamine substrate analogue increase the binding affinity to zMAO. The correlation is represented by the following equation:

$$\mathbf{\log K_{d(corr)} = 1.29 (\pm 0.31) \sigma + 5.86 (\pm 0.08) \quad (F_{1,6} = 17.1; p = 0.009) \quad (\text{Equation 4.2})}$$

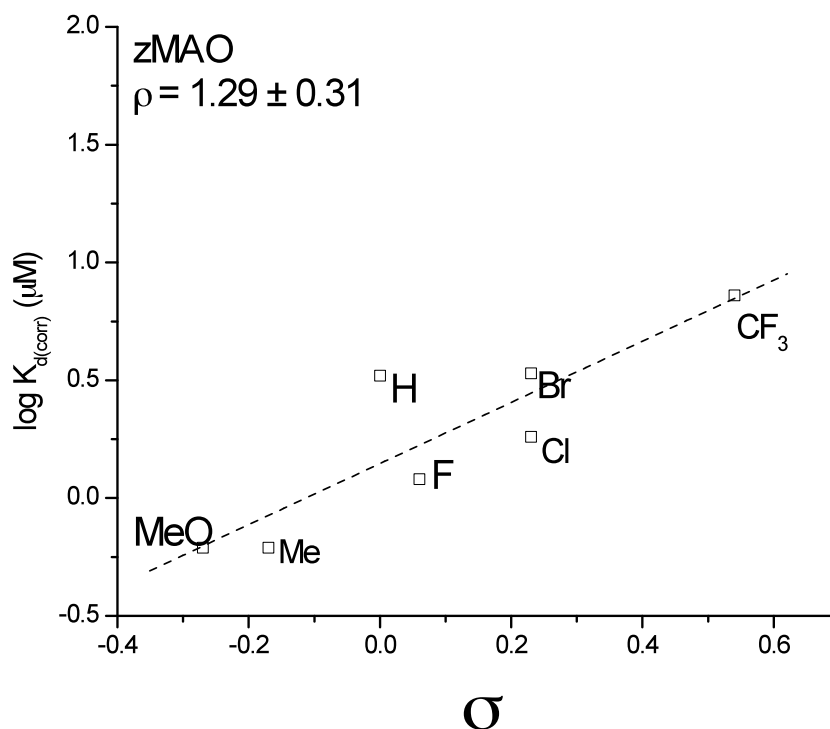


Figure 4.3: Correlation of calculated binding affinities of *p*-benzylamine analogues for zMAO and the substituent electronic parameter (σ). Neither MAO A nor MAO B shows correlation of binding affinity with electronic effect, thus this is a unique property for zMAO.

Correlation analysis with two components did not improve the statistics even with the addition of two more substituents ($-\text{NO}_2$ and $-\text{COO}^-$). This correlation shows electron withdrawing groups facilitate benzylamine binding to the active site of zMAO. The molecular basis for this effect on binding is currently unknown but suggests a site where an electron-deficient aromatic ring is favored. Despite the high sequence similarity with MAO A in the substrate-binding region, zMAO appears to exhibit its own unique substrate binding site.

One major difference among zMAO, human MAO A and MAO B are their $K_m(O_2)$ values. As indicated in the previous chapters of this thesis, human MAO A proceeds at V_{max} under air-saturation, human MAO B and zMAO do not. So then, the next question is, how does the enzyme behave under conditions of saturated oxygen concentration? Does it conserve the the rate-determining step, and does it exhibit the same QSAR properties? Therefore, to determine whether the correlation is also conserved under saturated oxygen conditions we performed another set of steady-state kinetics studies with four different *para*-benzylamine substituents and performed further QSAR analyses. The kinetic data for zMAO is shown in Table 4.13. The quantitative structure activity relationships describing the binding of *para*-benzylamines under saturated oxygen are shown in Figure 4.5.

Substituent	k_{cat} (H) (min^{-1})	k_{cat} (D) (min^{-1})	$D(V/K)$	$^Dk_{cat}$ (min^{-1})	Kd (μM)	Calculated Kd (corrected) (μM)
1. H	9.56 ± 0.57	2.68 ± 0.16	4.81 ± 0.29	3.57 ± 0.21	93.4 ± 5.6	0.91
2. F	19 ± 1	5.7 ± 0.4	3.83 ± 0.27	3.33 ± 0.23	23.7 ± 1.7	0.3
3. Br	48.0 ± 2.4	11.0 ± 0.6	5.22 ± 0.26	4.36 ± 0.22	172.1 ± 8.6	4.41
4. CF_3	115 ± 6.6	28.8 ± 1.8	4.45 ± 0.27	3.99 ± 0.19	50.6 ± 2.5	2.69

Table 4.13: Effects of *para*-substitution on the kinetic properties of zMAO oxidation by various benzylamine analogues under saturated oxygen ($\sim 940 \mu\text{M}$)

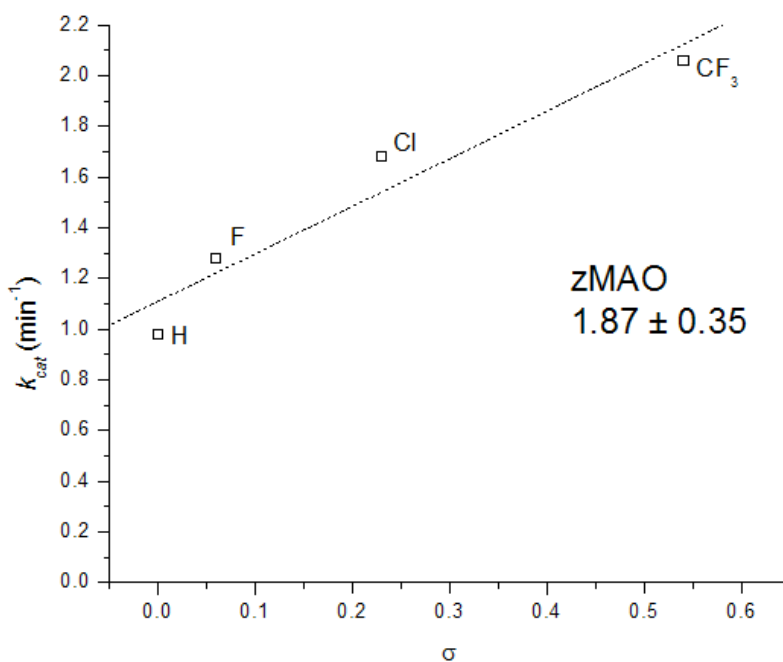


Figure 4.4: Quantitative structure activity relationships describing the turnover rate of *para*-substituted benzylamine analogues under saturated oxygen. Similar ρ value to correlation under air saturation is observed.

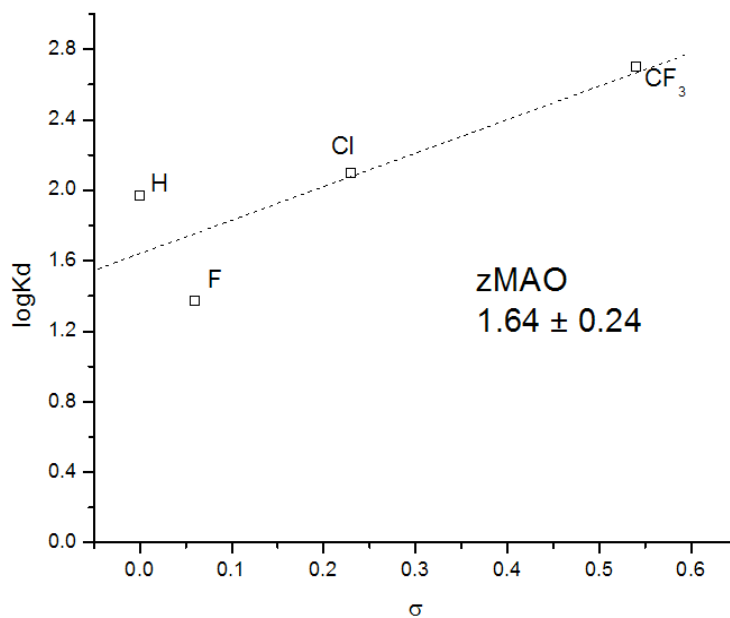


Figure 4.5: Quantitative structure activity relationships describing the binding of *para*-substituted benzylamine analogues and the effects of isotopic substitution under saturated oxygen. Values show similar ρ value to correlation under air saturation.

★ *meta*-benzylamines:

Linear regression analysis of the $\log k_{cat}$ as a function of substituent parameter was measured using six substrate analogues. The analysis showed a positive correlation with π (slope = 0.71 ± 0.21 , correlation coefficient (F) 11.2, Table 4.14). On the other hand, neither human MAO A nor B showed any correlation with $\log k_{cat}$ as a function of substituent with any parameter. Since Dk_{cat} values are not available, it is hard to predict which step is rate determining is catalysis. The equation of zMAO is shown as the following:

$$\log k_{cat} = (0.71 \pm 0.21) \pi + (0.49 \pm 0.09) \quad F=(11.2) \text{ (Equation 4.3)}$$

parameter	correlation	y-intercept	correlation coefficient	F value	significance
σ	-0.25 ± 0.75	0.73 ± 0.17	0.76	0.12	0.025
V_w	0.096 ± 0.25	0.59 ± 0.28	0.72	0.15	0.13
E_s	-0.39 ± 0.22	0.44 ± 0.17	0.18	3.09	0.82
π	0.71 ± 0.21	0.49 ± 0.09	0.49	11.2	0.01
π	0.74 ± 0.27	0.53 ± 0.16	0.19	4.1	0.08
V_w	-0.05 ± 0.15				0.75
π	0.77 ± 0.14	0.55 ± 0.06	0.05	16.6	0.14
σ	-0.53 ± 0.23				0.30

Table 4.14: Correlation Analysis of $\log k_{cat}$ with Hydrophobic, Steric and Electronic Parameters in the Interaction of *meta*-substituted benzylamine analogues with zMAO

Linear regression analysis of the $\log k_{cat}$ as a function of substituent parameter was measured using the same substrate analogues were performed for human MAO A and B, as well. Both human MAO A and B reaction rates, show a weak correlation with electronic effect parameter (σ) ($F=2.4$ and 1.3 , respectively) (Table 4.15). Moreover, the similar regression analysis for the binding constant values of human MAO B demonstrates that the enzyme exhibits a very weak correlation with the electronic parameter ($F=3.2$) when it comes to binding, as well (Table 4.16-17). Overall, none of the enzymes show a significant correlation with any of the QSAR parameters tested.

parameter	correlation	y-intercept	correlation coefficient	F value	significance
σ	1.55 ± 0.61	0.34 ± 0.27	0.19	2.4	0.119
V_w	-0.29 ± 0.44	0.92 ± 0.47	0.54	0.45	0.12
Es	-0.44 ± 0.51	0.33 ± 0.43	0.43	0.77	0.49
π	0.83 ± 0.57	0.33 ± 0.29	0.22	2.15	0.032
σ	1.45 ± 1.15	0.52 ± 0.54	0.41	1.04	0.029
V_w	-0.16 ± 0.43				

Table 4.15: Correlation Analysis of $\log k_{cat}$ with Hydrophobic, Steric and Electronic Parameters in the Interaction of *meta*-substituted benzylamine analogues with human MAO A

parameter	correlation	y-intercept	Correlation coefficient	F value	significance
σ	-2.91 ± 1.62	2.83 ± 0.72	0.32	0.013	0.32
π	-0.28 ± 1.67	2.35 ± 0.85	0.88	0.028	0.05
V_w	0.97 ± 1.01	1.33 ± 1.06	0.38	0.95	0.38
Es	-0.61 ± 0.66	1.81 ± 1.09	0.66	0.24	0.67
σ π	-0.36 ± 0.85 0.67 ± 1.89	2.69 ± 0.99	0.61	0.57	0.36

Table 4.16: Correlation Analysis of $\log k_{cat}$ with Hydrophobic, Steric and Electronic Parameters in the Interaction of *meta*-substituted benzylamine analogues with human MAO B

parameter	correlation	y-intercept	Correlation coefficient	F value	significance
σ	-0.93 ± 0.53	4.45 ± 0.14	0.506	3.2	0.1778
π	-0.04 ± 0.42	4.39 ± 0.23	0.002	0.007	0.9369
V_w	-0.14 ± 0.27	4.52 ± 0.31	0.635	2.1	0.085
Es	0.04 ± 0.33	4.40 ± 0.29	0.00026	0.0008	0.9935

Table 4.17: Correlation Analysis of $\log K_d$ with Hydrophobic, Steric and Electronic Parameters in the Interaction of *meta*-substituted benzylamine analogues with human MAO B

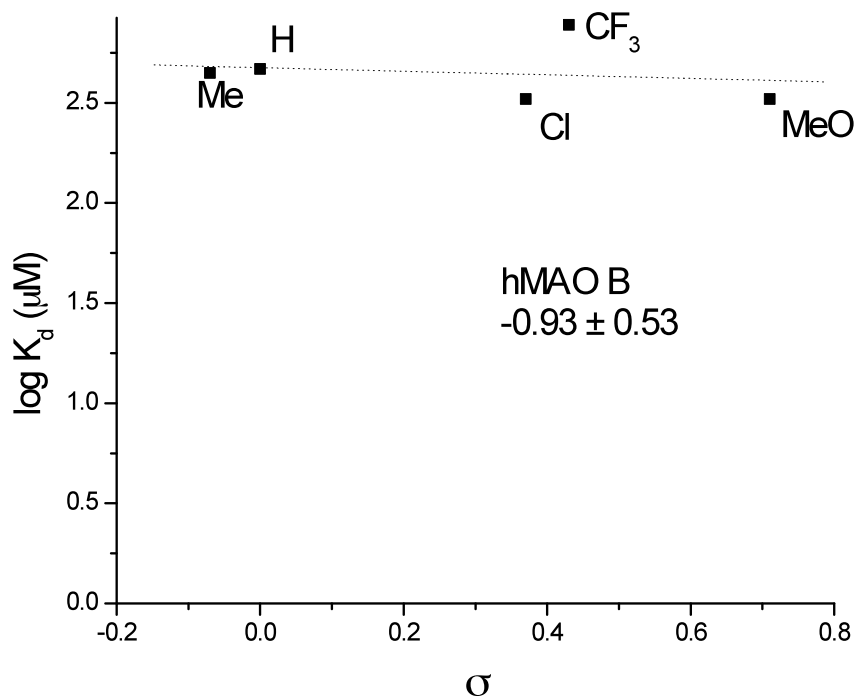


Figure 4.6: Quantitative structure activity relationships describing the binding of *meta*-substituted benzylamine analogues are shown for human MAO B

4.3.2 QSAR with *meta*- and *para*- substituted phenylethylamine analogues binding to zMAO

✦ *para*-phenylethylamines

Previously, the QSAR properties of human MAO A were determined for the phenylethylamine class of substrates (Nandigama and Edmondson 2000). Here we performed the QSAR studies with human MAO B and zMAO to understand how rate and binding constants (shown in Table 4.18) correlate with the QSAR parameters. Using the approach outlined previously, we first established the single correlation with zMAO $\log k_{cat}$ and then included a second parameter to see if the fit is improved. The best fit was obtained by this second attempt, and is seen with steric effect (E_s) and electronic effect (σ) as follows:

$$\log k_{cat} = (-0.21 \pm 0.11) E_s - (0.08 \pm 0.02) \sigma + (1.82 \pm 0.08) \quad F=(11.2) \quad (\text{Equation 4.5})$$

parameter	coefficient	y-intercept	correlation coefficient	F value	significance
V_w	-0.18 ± 0.11	2.13 ± 0.14	0.41	2.77	0.171
σ	-0.16 ± 0.24	1.94 ± 0.09	0.082	0.44	0.533
E_s	-0.03 ± 0.03	1.82 ± 0.02	0.36	1.68	0.280
π	-0.33 ± 0.19	2.09 ± 0.12	0.42	2.88	0.167
E_s	-0.21 ± 0.11	1.82 ± 0.08	0.918	11.2	0.818
σ	0.08 ± 0.02				

Table 4.18: Correlation Analysis of $\log k_{cat}$ with Hydrophobic, Steric and Electronic Parameters in the Interaction of *para*-substituted phenylethylamine analogues with zMAO

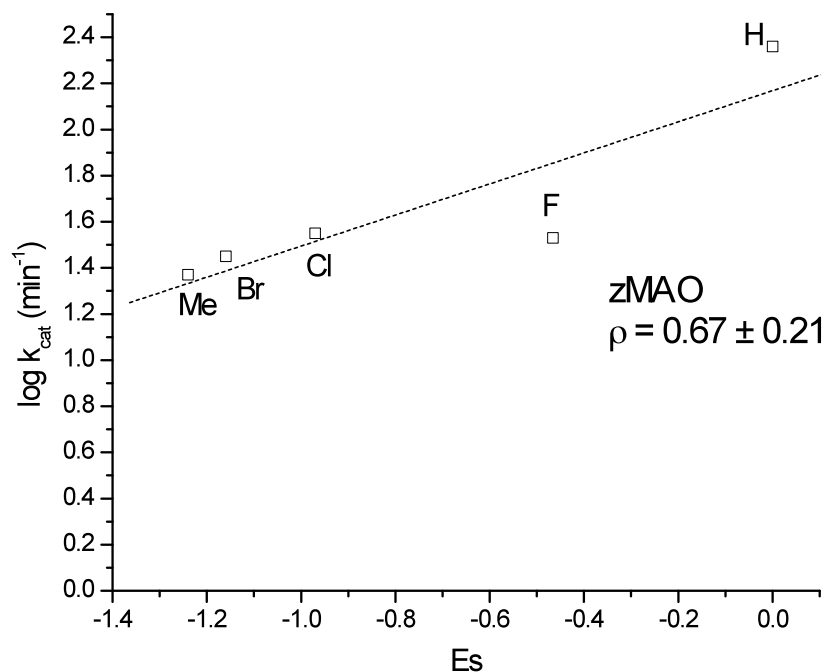


Figure 4.7: Quantitative structure activity relationships describing the steady state turnover rates of *para*-substituted phenylethylamine analogues with zMAO

Furthermore, the binding constants of *para*-phenylethylamine analogues were correlated with either single or multiple parameters outlined in Table 4.19. Of the single parameters, the best fit for zMAO binding constants, is the hydrophobic effect (π) with a relatively low F value ($F=8.22$) (Figure 4.8, Equation 4.6). The multiple parameter analysis did not improve any correlation (not shown).

$$\log K_d = (0.61 \pm 0.21) \pi + (2.11 \pm 0.13) \quad F=(8.22) \quad (\text{Equation 4.6})$$

parameter	coefficient	y-intercept	correlation coefficient	F value	significance
π	0.61 ± 0.21	2.11 ± 0.13	0.670	8.22	0.0456
V_w	0.32 ± 0.13	2.06 ± 0.17	0.586	5.70	0.0759
Es	0.09 ± 0.12	2.59 ± 0.09	0.163	0.58	0.5007
σ	0.01 ± 0.34	2.39 ± 0.13	0.564	0.38	0.5643

Table 4.19: Correlation Analysis of $\log K_d$ with Hydrophobic, Steric and Electronic Parameters in the Interaction of *para*-substituted phenylethylamine analogues with zMAO. The *F* values for σ and Es are 0.38 and 0.58, respectively.

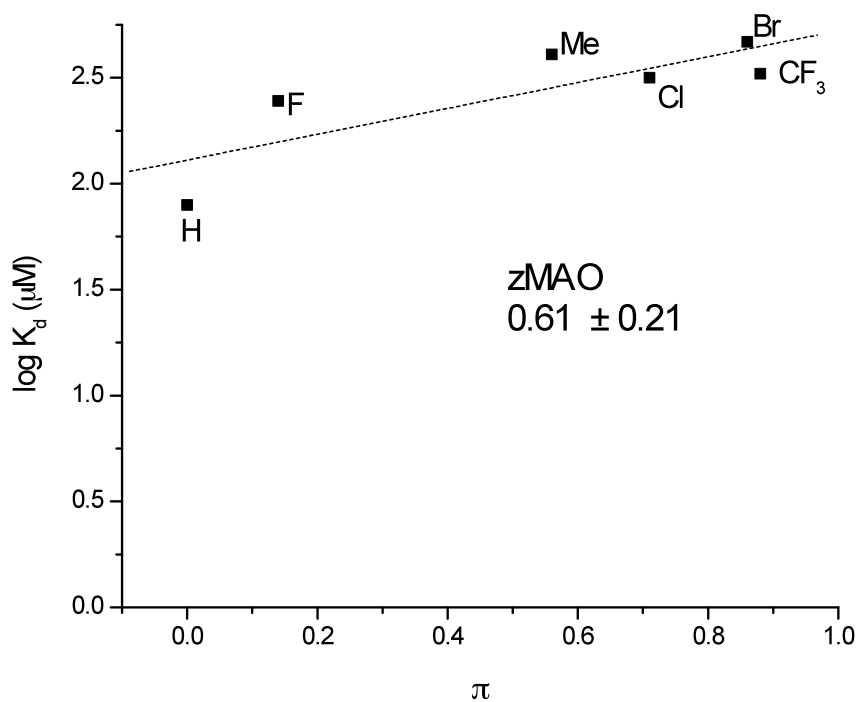


Figure 4.8: Quantitative structure activity relationships describing the binding of *para*-substituted phenylethylamine analogues to zMAO

On the other hand, unlike zMAO, human MAO B exhibits a correlation of hydrophobicity constant (π) both with turnover rate ($\log k_{cat}$) and binding constant (K_d) as represented by the following equations:

$$\log k_{cat} = (-0.21 \pm 0.04) \pi + (2.31 \pm 0.03) \quad F=(25.7) \quad (\text{Equation 4.7})$$

$$\log K_d = (-1.09 \pm 0.25) \pi + (1.70 \pm 0.16) \quad F=(16.9) \quad (\text{Equation 4.8})$$

parameter	correlation	y-intercept	correlation coefficient	F value	significance
π	-0.21 ± 0.04	2.31 ± 0.03	0.865	25.67	0.0071
V_w	0.12 ± 0.28	2.36 ± 0.37	0.798	15.76	0.016
σ	-0.54 ± 0.17	2.26 ± 0.07	0.670	10.36	0.0235
E_s	-0.23 ± 0.06	2.01 ± 0.05	0.755	12.30	0.247
σ	-0.29 ± 0.11	2.19 ± 0.91	0.923	18.80	0.0212
E_s	-0.16 ± 0.05				

Table 4.20: Correlation Analysis of $\log k_{cat}$ with Hydrophobic, Steric and Electronic Parameters in the Interaction of *para*-substituted phenylethylamine analogues with human MAO B. The graph representing the correlation is shown in Figure 4.9.

Previous data by Nandigama show that human MAO A binding parameters correlate with steric effect (E_s or V_w) (Nandigama and Edmondson 2000). In this aspect, zMAO is exhibiting relatively similar properties to human MAO B than to MAO A.

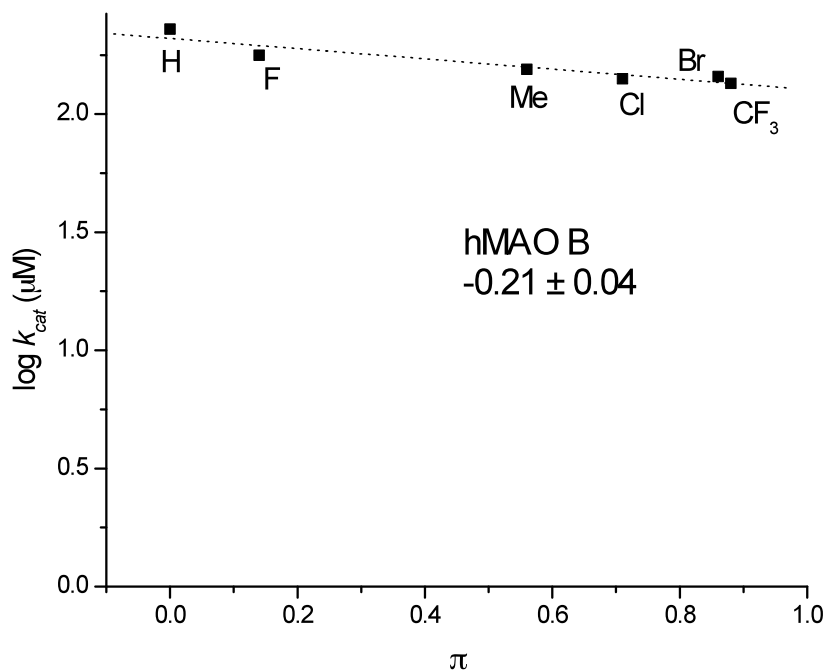


Figure 4.9: Quantitative structure activity relationships describing the binding of *para*-substituted phenylethylamine analogues to **human MAO B**

parameter	coefficient	y-intercept	correlation coefficient	F value	significance
π	-1.09 ± 0.25	1.70 ± 0.16	0.808	16.84	0.0148
V_w	-0.55 ± 0.15	1.82 ± 0.19	0.774	13.67	0.209
σ	-0.92 ± 0.36	1.35 ± 0.14	0.569	6.6	0.501
V_w σ	-0.35 ± 0.14 -0.87 ± 0.37	1.71 ± 0.15	0.921	17.5	0.921

Table 4.21: Correlation Analysis of **logK_d** with Hydrophobic, Steric and Electronic Parameters in the Interaction of **para-substituted phenylethylamine** analogues with **human MAO B**. The graph representing the correlation is shown in Figure 4.9.

✦ *meta*-phenylethylamines

In addition to *para*- substituted phenylethylamines, the analysis of turnover rates and the binding constant data of *meta*- phenylethylamine analogues to zMAO, hMAO A and B are performed. As the single parameters correlations in Table 4.22 demonstrate, zMAO k_{cat} correlates with hydrophobic constant (π) with an F value of 73.4. The correlation using two parameters also shows the relationship of zMAO k_{cat} with hydrophobic (π) as well as steric (V_w) constants (Equation 4.9, 4.10); in contrast no correlation is observed on the binding constants of zMAO.

$$\log k_{cat} = (0.16 \pm 0.02) \pi + (2.30 \pm 0.01) \quad F=(73.4) \quad \text{(Equation 4.9)}$$

$$\log k_{cat} = (0.086 \pm 0.012) (0.1x V_w) + (2.28 \pm 0.02) \quad F=(48.2) \quad \text{(Equation 4.10)}$$

parameter	coefficient	y-intercept	correlation coefficient	F value	significance
σ	0.31 ± 0.13	2.28 ± 0.044	0.650	5.58	0.099
V_w	0.086 ± 0.012	2.28 ± 0.02	0.941	48.2	0.0061
Es	-0.065 ± 0.019	2.32 ± 0.02	0.801	12.1	0.042
π	0.155 ± 0.018	2.30 ± 0.01	0.961	73.4	0.0033
V_w	0.079 ± 0.240	2.28 ± 0.022	0.946	17.4	0.0544
σ	0.046 ± 0.102				
π	0.093 ± 0.044	2.29 ± 0.012	0.982	53.4	0.0184
V_w	0.037 ± 0.025				

Table 4.22: Correlation analysis of $\log k_{cat}$ with hydrophobic, steric and electronic parameters in the interaction of *meta*-substituent phenylethylamine analogues with zebrafish MAO. The enzyme shows no correlation with *meta*-phenylethylamines in binding.

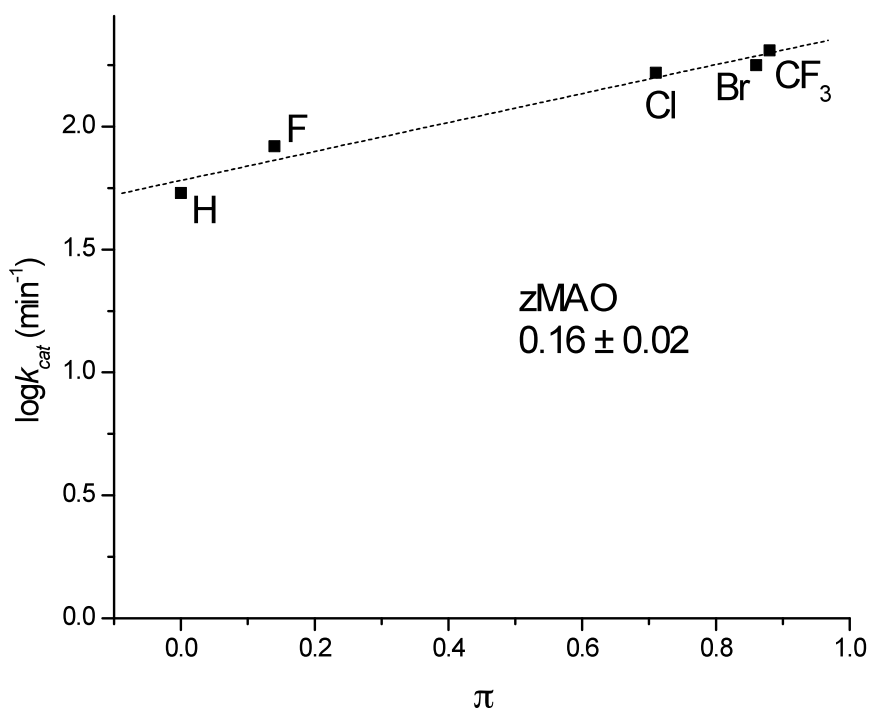


Figure 4.10: Quantitative structure activity relationships describing the rate of *meta*-substituted phenylethylamine analogues with zMAO

Unlike zMAO, the single correlation analysis of the binding and rate data for the *meta*-phenylethylamine analogues to human MAO A showed both the rate and binding of MAO A best fits with steric (V_w) values (Table 4.23-4.24) (Equation 4.11, 4.12). The linear plots representing the correlation is shown in Figures 4.11 as well.

$$\log k_{cat} = (0.55 \pm 0.13) (0.1x V_w) + (1.55 \pm 0.09) \quad F=(18.1) \quad (\text{Equation 4.11})$$

$$\log K_d = (1.50 \pm 0.23) (0.1x V_w) + (3.45 \pm 0.38) \quad F=(16.2) \quad (\text{Equation 4.12})$$

parameter	correlation	y-intercept	correlation coefficient	F value	significance
σ	0.31 ± 0.01	-0.30 ± 0.08	0.62	0.32	0.07
π	0.49 ± 1.22	-0.49 ± 2.34	0.73	0.16	0.85
V_w	0.55 ± 0.13	1.55 ± 0.09	0.05	18.1	3×10^{-3}
Es	-0.72 ± 1.49	-0.71 ± 2.85	0.68	0.23	0.83

Table 4.23: Correlation analysis of $\log k_{cat}$ with hydrophobic, steric and electronic parameters in the interaction of *meta*-substituted phenylethylamine analogues with human MAO A

parameter	correlation	y-intercept	correlation coefficient	F value	significance
V_w	1.5 ± 0.23	3.45 ± 0.38	0.06	16.2	0.0012

Table 4.24: Correlation analysis of $\log K_d$ with hydrophobic, steric and electronic parameters in the interaction of *meta*-substituted phenylethylamine analogues with human MAO A

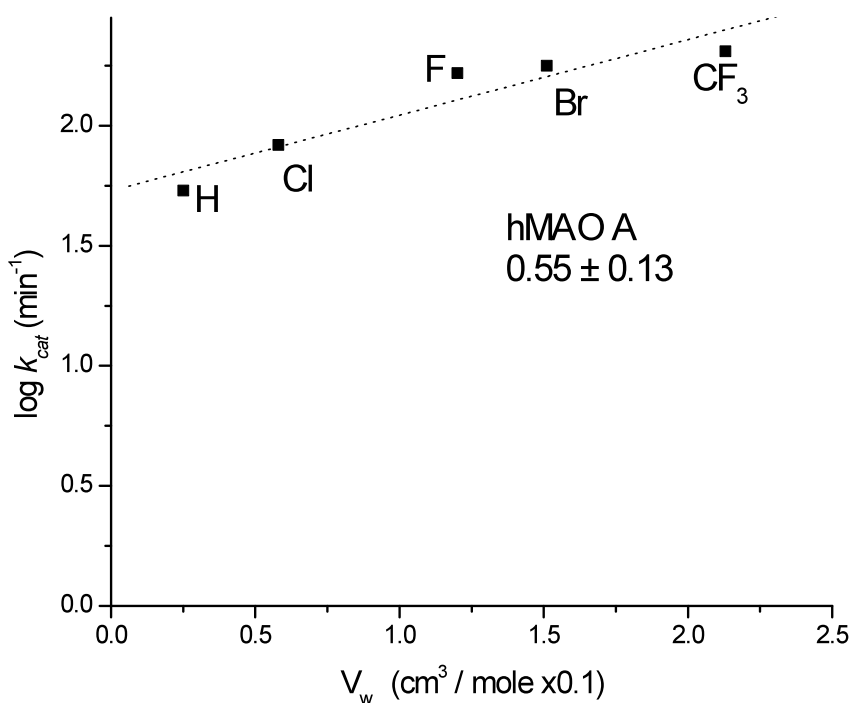


Figure 4.11: Quantitative structure activity relationships describing the binding of *meta*-substituted phenylethylamine analogues to human MAO A

While human MAO A turnover rate best fits with the steric parameter (V_w), human MAO B exhibit a correlation with the electronic parameter (σ) with *meta*-substituted phenylethylamine analogues tested. Similarly, both steric and electronic parameters contribute to the correlation of hMAO B binding constant with QSAR parameters are shown in Table 4.25 and are summarized in the equations below:

$$\log k_{cat} = (-1.48 \pm 0.18) \sigma + (2.37 \pm 0.06) \quad F=(70.8) \text{ (Equation 4.13)}$$

$$\log k_{cat} = (-1.22 \pm 0.21) \sigma + (0.07 \pm 0.04) Es \quad F=(56.7) \text{ (Equation 4.14)}$$

$$\log K_d = (-3.55 \pm 0.67) \sigma + (0.56 \pm 0.16) (0.1x V_w) \quad F=(14.4) \text{ (Equation 4.15)}$$

parameter	correlation	y-intercept	correlation coefficient	F value	significance
σ	-1.48 ± 0.18	2.37 ± 0.06	0.959	70.8	0.0035
π	-0.53 ± 0.21	2.19 ± 0.13	0.698	6.9	0.078
V_w	-0.30 ± 0.12	2.26 ± 0.14	0.731	8.15	0.0649
σ V_w	-1.23 ± 0.27 -0.076 ± 0.062	2.38 ± 0.06	0.977	42.1	0.023
σ π	-1.302 ± 0.309 -0.095 ± 0.133	2.36 ± 0.067	0.968	29.8	0.0324
σ Es	-1.22 ± 0.21 0.067 ± 0.041	2.36 ± 0.049	0.983	56.71	0.0173

Table 4.25: Correlation analysis of $\log k_{cat}$ with hydrophobic, steric and electronic parameters in the interaction of *meta*-substituted phenylethylamine analogues with human MAO B

parameter	correlation	y-intercept	correlation coefficient	F value	significance
σ	-1.67 ± 0.91	2.23 ± 0.34	0.531	3.39	0.1629
σ	-3.55 ± 0.67	2.18 ± 0.15	0.935	14.4	0.0651
V_w	0.56 ± 0.16				

Table 4.26: Correlation analysis of $\log K_d$ with hydrophobic, steric and electronic parameters in the interaction of *meta*-substituted phenylethylamine analogues with human MAO B

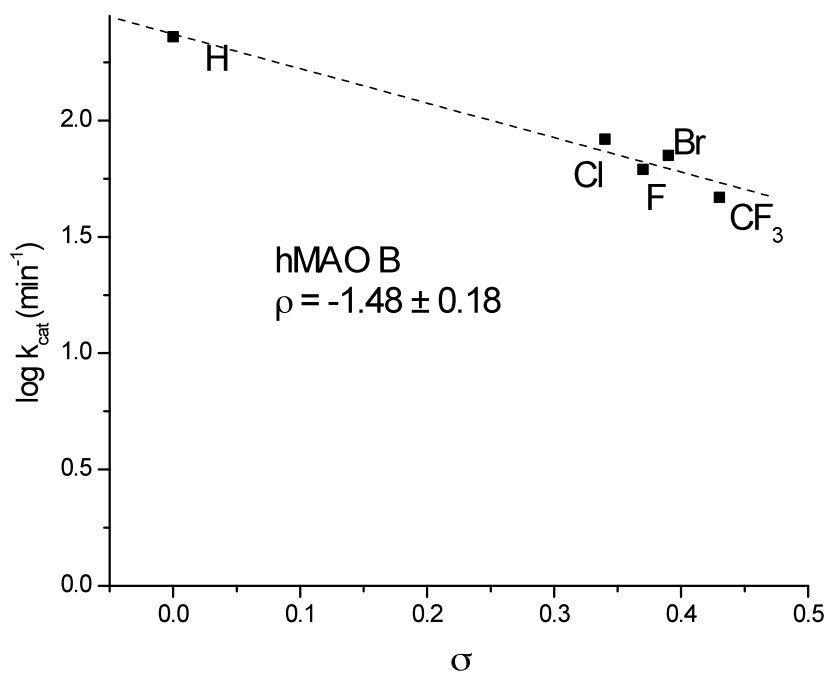


Figure 4.12: Quantitative structure activity relationships describing the binding of *meta*-substituted phenylethylamine analogues to human MAO B

4.4 Discussion

4.4.1 Overview of the QSAR Data

Human MAO A and B are known to exhibit different properties when it comes to structure-activity relationships during the oxidation of benzylamine and phenylethylamine analogues (Walker 1994; Miller 1999; Nandigama and Edmondson 2000). Previously, QSAR properties of the oxidation of *para*-phenylethylamine and benzylamine analogues by human MAO A and oxidation of *para*- and *meta*-benzylamines by bovine MAO B were established. The main objective of this study was to determine the properties of zebrafish MAO; therefore we obtained steady-state kinetic data and the corresponding structure-activity correlations, in comparison to human MAO isoforms.

Furthermore, we completed the structure-activity data for human MAO B with *meta*- and *para*-phenylethylamine analogues as well as with *meta*- and *para*-benzylamine analogues and human MAO A with *meta*-phenylethylamines. The structure-activity analyses of benzylamine and phenylethylamine analogues used similar approaches used previously, using the general equation:

$$\log k_{cat} \text{ (or } K_d) = \rho (\sigma) + A (\pi) + B (V_w) \text{ (or } E_s) + C \text{ (Hansch equation)}$$

where σ is the electronic (electron-withdrawing or -donating) contribution of the substituent, π is the hydrophobicity parameter (Hansch 1995), V_w is the van der Waals volume of the substituent, also referred as the steric parameter, which is also modeled by other parameters such as E_s (Bondi 1964; Hansch 1995). The outcomes of the analyses

for zMAO, human MAO A and B are summarized in Table 4.27 and 4.28 and further discussed herein.

<i>Substrate</i> →	Benzylamine				Phenylethylamine			
<i>Substituent</i> →	<i>meta</i>		<i>para</i>		<i>meta</i>		<i>para</i>	
Enzyme	Correlation		Correlation		Correlation		Correlation	
	$\log k_{cat}$	$\log K_d$	$\log k_{cat}$	$\log K_d$	$\log k_{cat}$	$\log K_d$	$\log k_{cat}$	$\log K_d$
zMAO	$\pi, \pi + \sigma$	-	σ	σ	$\pi, \pi + V_w$	-	Es, σ	π
hMAO A	-	-	σ	V_w	V_w	V_w	V_w	V_w
hMAO B	-	-	-	π	$\sigma, \sigma + Es$	$\sigma + V_w$	π, V_w	π, V_w

Table 4.27: Summary of QSAR parameters effective on zMAO, hMAO A and hMAO B.

The reaction rates and the binding affinities of 9 *para*-substituted benzylamine analogues with zMAO were determined by steady-state kinetic experiments. $^D k_{cat}$ kinetic isotope effects with α, α -[D₂]benzylamines are similar for each substrate analogue and range in values from 4-8 with $^D k_{cat}/K_m$ values again ranging from 4-8. These data demonstrate that α -C-H bond cleavage is the rate-limiting step in catalysis as found in both human and rat MAO A and B. The *para*-substituent on benzylamine exhibits a strong electronic effect on zMAO k_{cat} values with an observed ρ value of ~ 1.6 . This property demonstrates a more similar functional character of zMAO with human or rat MAO A than with MAO B. Overall, these data demonstrate that zMAO exhibits functional properties intermediate

between those observed for MAO A and those observed for MAO B when it comes to catalysis of *para*-benzylamine analogues.

The interaction of *meta*- benzylamine analogues with zMAO is governed by the hydrophobicity (π) of the substituent (slope =0.71). The addition of a second parameter to the hydrophobicity parameter does not improve the F value over that is observed with a single parameter fit. While the correlation is poor ($F=11$), no correlation of single QSAR parameters are observed with either human isoforms. The case for human MAO B is surprising considering that bovine MAO B shows a decreasing binding affinity with the van der waals (V_w) of the substituent (the larger the meta-substituent, the weaker the binding affinity) (Walker and Edmondson 1994). No such effect is observed with either human isoform, together with no observable influence on the substituent σ , π or E_s parameters.

It was already known that human isoforms behave in a different way when reacting with benzylamines and phenylethylamines. Such as with phenylethylamines, human MAO B does not exhibit any kinetic isotope effect while exhibiting a Dk_{cat} of 4.7 in oxidation of benzylamines. On the other hand, human MAO A shows kinetic isotope effect with either substrate, indicating that the rate limiting step is the α -C-H bond cleavage in the reaction catalysis. We have already established and presented earlier in this thesis that zMAO reacts with both benzylamine and phenylethylamine, and with Dk_{cat} values of 2.7 and 12.1; hence is closer to human MAO A. Using various *meta* and *para* phenylethylamine analogues did not change this property. Both zMAO and human MAO A exhibit kinetic isotope effect with high Dk_{cat} values for either analogue, while the values for human

MAO B range from 1.1 to 2.5, indicating none (or very small) kinetic isotope effects. The structure- activity relationships correlating these data to specific parameters are different for each protein, however. For *meta*-phenylethylamines, a weak correlation between hydrophobicity (π) and k_{cat} is shown for zMAO (slope =0.16), and both reaction rate and binding affinity of hMAO A is affected by van der Waals volume (slope =0.55 and slope =1.5). On the other hand, both k_{cat} and binding affinity of human MAO B exhibit a strong correlation with the electronic parameter (σ).

Substrate	Structure	Properties of <i>para</i> substituent group			Properties of <i>meta</i> substituent group			k_{cat} (min ⁻¹)	Enzyme
		σ	Es	π	σ	π	V _w		
BA		+1.55	-	-	+0.53	0.71	-	4.71	zMAO
		+1.86	-	-	+1.55	-	-	2.5	hMAO A
		-	-	-	-2.91	-	-	246	hMAO B
PEA		+0.08	-0.21	-	-	0.16	0.086	203.8	zMAO
		-	-	-0.22	-	-	0.55	53.8	hMAO A
		-	-	-	-1.48	-	-	228.9	hMAO B

Table 4.28: Correlation of QSAR parameters and their constants for zebrafish MAO and human MAO isoforms to k_{cat}

Substrate	Structure	Properties of <i>para</i> substituent group		Properties of <i>meta</i> substituent group		$D(V/K)$	K_d (μ M)	Enzyme
		σ	π	σ	V _w			
BA		1.29	-	-	-	4.1	209.5	zMAO
		-	-	-	-	12.1	1099	hMAO A
		-	-1.1	-0.93	0.21	4.5	225.6	hMAO B
PEA		-	0.61	-	-	11.4	80.5	zMAO
		-	-	-	1.5	9.6	1433	hMAO A
		-	-1.09	-1.48	-	2.5	35.4	hMAO B

Table 4.29: Correlation of QSAR parameters and their constants for zebrafish MAO and human MAO isoforms to binding constant.

The correlations for *para*-phenylethylamines are different for human isoforms and zMAO, as well. While zMAO's reaction rate (k_{cat}) correlates with electronic (σ) and steric (E_s) parameters in a double correlation analysis, (slope =0.08 and -0.21 respectively), human MAO A is shown to be effected mostly by steric (V_w) parameter, only (Nandigama and Edmondson 2000). The reaction rate of human MAO B weakly correlates with hydrophobicity (π) (slope =0.21) On the other hand, binding of *para*-phenylethylamine to zMAO and human MAO B correlates with hydrophobic parameter (π), and to human MAO A correlates with steric parameter (V_w). In summary, when it comes to phenylethylamines, zMAO shows similar properties to human MAO A in kinetic parameters for both *para*- and *meta*-phenylethylamines and does not show any strong similarity to either human isoforms in structure-activity relationships.

4.4.1 Mechanistic and Structural Interpretation

Previous studies on the comparison of human MAO A and MAO B QSAR properties using *para*- substituted benzylamines showed that the two isoforms are influenced differently by the *para* substitution. In the case of substrate turnover, MAO A prefers analogues with strong electron-withdrawing group as *para*- substituents while MAO B is affected by the hydrophobicity of *para* substituent. On the other hand, MAO A prefers larger *para* substituents for substrate binding, while MAO B prefers smaller *para*-substituents. These properties were interpreted as MAO A containing a larger binding pocket while MAO B containing a smaller hydrophobic binding pocket. The crystal structures confirmed this proposal and revealed that human MAO A and B differ in their binding pocket sizes (Binda, Li et al. 2003; De Colibus 2005; Son 2008). Another

proposed notion was on the binding mechanism of *para*- benzylamine analogues; it was predicted that while the hydrophobic environment of MAO B substrate binding site is the reason of the hydrophobic substrate attraction into the MAO B active site, the configuration of the benzylamine substrate determines the electronic effect on catalysis of the substrate analogue to either human isoform (Miller and Edmondson 1999). The orientation of the aromatic ring influences the alignment of α -C-H carbon orbitals to allow the electronic effect of substituent to α -carbon in the case of human MAO A; while, the smaller binding pocket of MAO B does not permit such a coplanar orientation (Figure 1.13). The electronic effect on the α - carbon is important, because during the rate determining step in MAO A catalyzed benzylamine, the α -proton abstraction step is affected by the electron withdrawing character of the *para* substituent. Such occurrence does not exist in MAO B. The steady-state measurements and the subsequent analyses of zMAO with *para* benzylamines show that rate of zMAO with these analogues are influenced by the electronic property of the substituent as well. Increase in electron withdrawing group increases k_{cat} in zMAO, as seen in human MAO A. Moreover, α -C-H bond cleavage is the rate-determining step in zMAO catalysis, such as in human MAO A and B.

In addition, binding of *para*- benzylamine analogues to zMAO is influenced by electronic properties as well. Neither MAO A, nor MAO B shows contributions of electronic effects to binding affinity of benzylamine, this correlation appears to be a unique property for zMAO. Overall, zMAO exhibits similar properties to human MAO A and suggestively contains a large binding pocket like human MAO A.

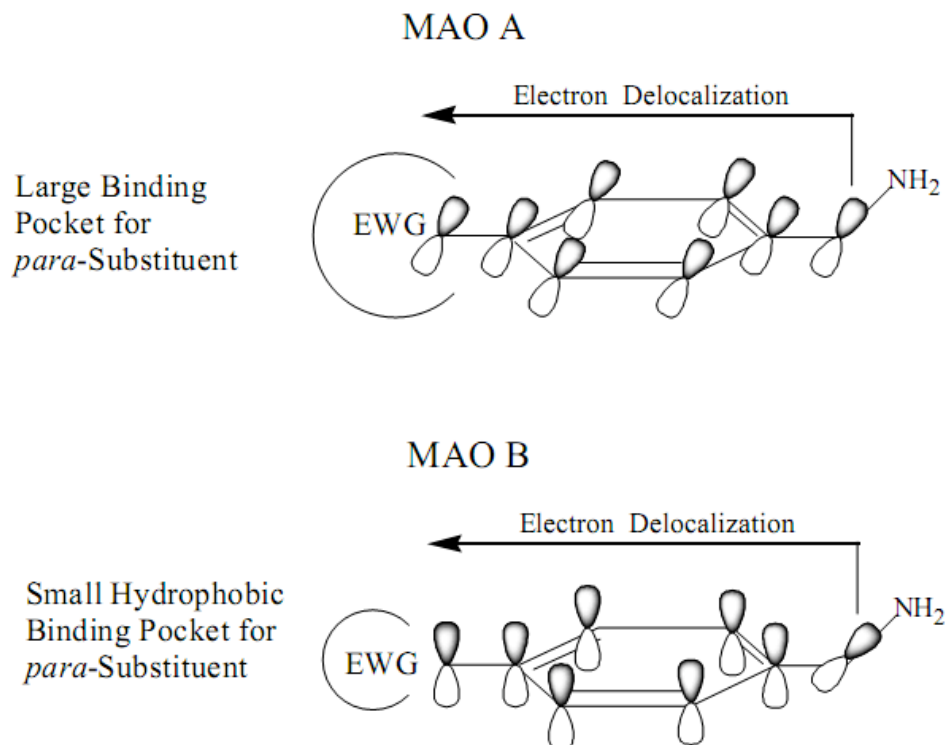


Figure 4.13 Model representation of the relative conformations of *para*-substituted benzylamine analogues bound to MAO A and MAO B, taken from reference (Miller and Edmondson 1999).

In case of *meta* substituted benzylamines, none of the analogues influence the turnover rate of zMAO. Similarly, the rates for human MAO A and MAO B turnover are not highly dependent on the nature of the *meta* substituted benzylamine analogue either. The linear correlations of zMAO k_{cat} values observed with the electronic parameter (σ) and hydrophobicity parameter (π) are thus very weak and are not considered as a major effect (Table 4.28). Likewise, human MAO A and MAO B exhibit weak correlations of k_{cat} with the electronic parameter (σ). The rate of hMAO A slightly increases with the increasing σ and the rate of hMAO B slightly decreases with the increasing σ . Complete

analysis of human MAO B with *meta* α,α -[H₂]-benzylamines shows the presence of kinetic isotope effects for MAO B oxidation of benzylamines. Preliminary data with human MAO A and zMAO also suggests a kinetic isotope effect with *meta* α,α -[H₂]-benzylamines (not shown). Linear analysis of the binding affinity of human MAO B show an inverse correlation with V_w of the substituent (a similar property to bovine MAO B, but the correlation for hMAO B is weaker). These data demonstrate that the electronic parameter of the substituent in the *meta*-benzylamine analogues is not a large factor as it is for *para*-benzylamine analogues for zMAO turnover rate as well as human MAO A and hMAO B. Taken as a whole, both zebrafish and both human MAO isoforms exhibit similar properties with *meta*-substituted benzylamines.

While QSAR studies provide a direct evidence for proton abstraction in the α -C-H bond cleavage in human MAO A and zMAO catalysis in *para* benzylamines (and potentially in *meta* benzylamines), the factors are rather different for phenylethylamines. The phenylethylamine oxidation by human MAO A was previously described as the α -C-H bond cleavage step being rate limiting in catalysis and with oxygen reacting with the reduced enzyme-imine complex (Nandigama and Edmondson 2000). On the other hand, a detectable kinetic isotope effect was not observed for hMAO B in the α -C-H bond cleavage step and the oxygen was determined to react with the free reduced enzyme (Husain, Edmondson et al. 1982; Ramsay 1991; Ramsay, Tan et al. 1994). Consistently, as our measurements show, hMAO B does not show any detectable kinetic isotope effect with the *para*- substituted phenylethylamine analogues, whereas both human MAO A and zMAO do. Linear correlation analysis demonstrates the steric effect (E_s) and electronic effect (σ) on the rate of zMAO. The most determinant parameters on the rate of human

MAO A is π and for human MAO B is both π and V_w . For binding affinity, steric and hydrophobic parameters correlate for both zMAO and human isoforms. Therefore, the rate of zMAO with *para*-substituted phenylethylamine analogues is essentially dependent on the hydrophobicity and the steric orientation of the substituent. Either MAO form is dependent on these parameters for the facilitation of the binding. However, it has to be mentioned that while human MAO A is functioning at V_{max} at air saturation, human MAO B and zMAO do not (Ramsay, Tan et al. 1994), (Chapter 2). The studies here are conducted under air saturation and further measurements under saturated oxygen conditions are required for more precise conclusion.

We observe that parameters that influence the interaction of zMAO and human isoforms with *meta*-substituted phenylethylamines are similar to those with *para*-phenylethylamines. Both zMAO and human MAO A exhibit Dk_{cat} values in the range of 4-9, providing direct evidence for C-H cleavage as being rate limiting in catalysis. QSAR results show that the rate of *meta*-phenylethylamine analogues with zMAO is highly favored by the hydrophobicity of the substituent, whereas human MAO A is more affected by steric (V_w) parameter. The major difference between zMAO and hMAO A is the correlation of binding affinity. While zMAO binding does not correlate with any of the parameters, binding of *meta*-phenylethylamines to human MAO A is facilitated by the increase of the steric (V_w) parameter of the substituent.

Human MAO B, that does not show any detectable kinetic isotope effect with these analogues, -such like other phenylethylamine analogues discussed above- shows a negative correlation between rate to electronic parameter of the *meta*-substituent (increase in electronegativity results as decrease in rate), and a binding which is mostly

facilitated by the steric (V_w) and electronic parameters (σ) as shown by linear correlation (Table 4.29). Another difference between human MAO B and zMAO is observed with their differential interactions with *para*-phenylbutylamine. This arylalkylamine functions as a competitive inhibitor for human MAO B, but is a substrate for human MAO A and for zMAO. This differential behavior is also observed using *p*-carboxybenzylamine which is a substrate for zMAO and for MAO A, but is neither a substrate nor a competitive inhibitor for MAO B. These observations provide additional support for the MAO A –type behavior of zMAO. By the data with *para*-benzylamines, it was already proposed that human MAO A has a large binding pocket (bigger than human MAO B) (Nandigama and Edmondson 2000) therefore the influence of the steric parameter is not unexpected. This data shows that the major determinant of zMAO turnover with a bulkier substrate like phenylethylamine is the hydrophobicity of the environment. Through *para*-benzylamine data, we proposed that zMAO might have a larger binding pocket as observed in human MAO A, the data with *meta* and *para* phenylethylamines further suggest that this binding pocket is strongly hydrophobic. Further X-ray crystallography data is required for definitive conclusions.

References:

- Binda, C., Li, M., Hubalek, F., Restelli, N., Edmondson, D.E., Mattevi, A. (2003). "Insights into the mode of inhibition of human mitochondrial monoamine oxidase B from high-resolution crystal structures." Proc Natl Acad Sci U S A **100**(17): 9750-5.
- Bondi, A. (1964). J Phys Chem **68**: 441-451.
- Bondi, A. (1964). "Van der Waals volumes and radii." J Phys Chem **68**: 441-451.
- De Colibus, L., Li, M., Binda, C., Lustig, A., Edmondson, D. E., Mattevi, A. (2005). "Three-dimensional structure of human monoamine oxidase A (MAO A): Relation to the structures of rat MAO A and human MAO B." Proceedings of the National Academy of Sciences of the United States of America **102**(36): 12684-12689.
- Gupta, S. P. (1987). "QSAR studies on enzyme inhibitors." Chemical reviews **87**: 1183-1253.
- Hammett, L. P. (1935). Chemical reviews **17**: 125.
- Hansch, C., Leo, A., Hoekman, D. (1995). Exploring QSAR Hydrophobic, electronic, and steric constants. Washington, DC, American Chemical Society.
- Husain, M., D. E. Edmondson (1982). "Kinetic studies on the catalytic mechanism of liver monoamine oxidase." Biochemistry **21**(3): 595-600.
- Klinman, J. P., R. G. Matthews (1985). "Calculation of Substrate Dissociation-Constants from Steady-State Isotope Effects in Enzyme-Catalyzed Reactions." Journal of the American Chemical Society **107**(4): 1058-1060.
- Li, M., F. Hubalek, Newton-Vinson, P., Edmondson, D.E. (2002). "High-level expression of human liver monoamine oxidase A in *Pichia pastoris*: comparison with the enzyme expressed in *Saccharomyces cerevisiae*." Protein Expr Purif **24**(1): 152-62.

- McEwen, C. M., G. Sasaki, Jones, D. (1969). "Human Liver Mitochondrial Monoamine Oxidase .2. Determinants of Substrate and Inhibitor Specificities." Biochemistry **8**(10): 3952-3962.
- McEwen, C. M., G. Sasaki, Jones, D. (1968). "Human Liver Mitochondrial Monoamine Oxidase .I. Kinetic Studies of Model Interactions." J Biol Chem **243**(20): 5217-5225.
- Miller, J. R., D. E. Edmondson (1999). "Influence of flavin analogue structure on the catalytic activities and flavinylation reactions of recombinant human liver monoamine oxidases A and B." J Biol Chem **274**(33): 23515-25.
- Miller, J. R., D. E. Edmondson (1999). "Structure-activity relationships in the oxidation of para-substituted benzylamine analogues by recombinant human liver monoamine oxidase A." Biochemistry **38**(41): 13670-83.
- Nandigama, R. K., D. E. Edmondson (2000). "Structure-activity relations in the oxidation of phenethylamine analogues by recombinant human liver monoamine oxidase A." Biochemistry **39**(49): 15258-65.
- Newton-Vinson, P., F. Hubalek, Edmondson, D.E. (2000). "High-level expression of human liver monoamine oxidase B in *Pichia pastoris*." Protein Expr Purif **20**(2): 334-45.
- Ramsay, R. R. (1991). "Kinetic mechanism of monoamine oxidase A." Biochemistry **30**(18): 4624-9.
- Ramsay, R. R., A. K. Tan (1994). "Kinetic properties of cloned human liver monoamine oxidase A." J Neural Transm Suppl **41**: 17-26.
- Son, S.-Y., Ma, Jichun., Youhei, Kondou., Masato, Yoshimura., Eiki, Yamashita., Tomitake, Tsukihara. (2008). "Structure of human monoamine oxidase A at 2.2-Å resolution: The control of opening the entry for substrates/inhibitors." Proc Natl Acad Sci U S A **105**(15): 5739-5744.

Walker, M. C., D. E. Edmondson (1994). "Structure-activity relationships in the oxidation of benzylamine analogues by bovine liver mitochondrial monoamine oxidase B." Biochemistry **33**(23): 7088-98.

Walker, M. C., Edmondson, D. E. (1994). "Structure-activity relationships in the oxidation of benzylamine analogues by bovine liver mitochondrial monoamine oxidase B." Biochemistry **33**(23): 7088-98.

CHAPTER 5

CONCLUSIONS

“-Would you tell me, please, which way I ought to go from here?”

- That depends a good deal on where you want to get to...”

Lewis Carroll, Alice in Wonderland

5.1 Summary of the Results

Investigating the properties of monoamine oxidase (MAO) has been the interest of many studies from various fields, such as chemistry, genetics and psychiatry for over three decades (Youdim, Edmondson et al. 2006; Edmondson 2009; Mc Dermott Rose 2009; Natalie Weder 2009). Certainly this interest is due to the importance of MAO in a variety of disciplines. Out of the many studies that are available in the literature, there is very limited information on the ancestry roots and the evolution of these two enzymes. One proposed idea is that on the basis that the two enzymes have shared a single common ancestor and then diversified through a gene duplication event. It was shown that this proposed gene duplication event potentially took place not so long ago in evolutionary timeline and suggested that unlike many other mammalian enzymes and molecules, MAO enzymes did not follow the horizontal gene transfer pattern (Stanhope 2001). A single gene is conserved from organism to organism and during the transition to mammals, have duplicated (Stanhope 2001). Additional studies has identified a teleost MAO from the

organism, zebrafish (*Danio rerio*) and vastly showed that this form of MAO, zMAO, behaves more like MAO A (Chen K. 1994; Setini, Pierucci et al. 2005; Anichtchik 2006).

Based on all these information, we simply asked the question: why? Why do humans have two forms of MAO that share such high sequence identity yet functioning to each it's own? What makes MAO so special that it was conserved among many organisms, for so long in the molecular history of life? Besides, what benefits does the gene duplication event have – in other words, what properties this single form not have that is found in two mammalian MAO's?

There are many properties that distinguish MAO A and MAO B and these characteristics have been outlined extensively in the Chapter 1 of this thesis. We structured our functional analysis of single MAO from zebrafish based on these similarities and differences. The reasoning for organism choice is also discussed in this chapter.

Briefly, the promising features of zebrafish in the field of drug development make zebrafish MAO a pharmacologically significant target. The work in this thesis presents the first detailed identification and characterization of a teleost monoamine oxidase. As a first step, my approach was to take a closer look at this single form of MAO. Being developed highly efficient expression and purification systems for many other MAO forms (Newton-Vinson, Hubalek et al. 2000; Li, Hubalek et al. 2002; Upadhyay, Wang et al. 2008), to obtain high levels of purified form of this single MAO and then extensively analyze its properties in comparison to the two human isoforms was aimed.

The expression, purification and characterization of the zMAO using the methylotropic yeast *Pichia pastoris* expression system is described in Chapter 2 of this dissertation. A 0.5 L culture of *Pichia pastoris* expresses 235 mg zMAO with 400 U of total activity. The enzyme is purified in a 30% yield and is a homogenous single species with a M_r of ~60,000 on SDS-PAGE and a mass of 58,525 (\pm 0.029) Da from MALDI-TOF measurements. The purified zMAO preparation contains one mole of covalent FAD cofactor that shows properties of an 8 α -S-cysteinyl linkage per mole of enzyme. Despite a ~70% sequence identity to either human MAO A or MAO B, zMAO exhibits no immuno-chemical cross-reactivity with anti-sera raised against human MAO A. As found previously with human MAO A and MAO B, expressed zMAO is membrane bound in the mitochondrial fraction isolated from *Pichia* cells. The $K_m(O_2)$ of zMAO (108 μ M) is intermediate to the values exhibited by human MAO B (240 μ M) or human MAO A (~12 μ M) demonstrating that zMAO exhibits functional properties intermediate between those observed for MAO A and for MAO B.

Chapter 3 of this thesis describes the functional analysis of zMAO using a variety of human MAO A and MAO B specific substrates and inhibitors. K_i values with MAO A-specific indole inhibitors are 6-7 fold weaker with zMAO than with human MAO A, while observed K_i values with harmaline are similar. The MAO B specific inhibitors chlorostyrylcaffeine, 1,4-diphenylbutene, 1,4-diphenyl-1,3-butadiene, and rasagiline inhibit zMAO with similar or tighter K_i values than human MAO B. Safinamide, another MAO B specific inhibitor exhibits a 100-fold weaker affinity for zMAO than for human MAO B. When it comes to substrate turnover, zMAO oxidizes serotonin with a k_{cat} value

one half that of human MAO A, but oxidizes dopamine with a 3-fold higher k_{cat} than either human enzyme. In conclusion, zMAO exhibits functional properties intermediate between those observed for MAO A and those observed for MAO B

Chapter 4 describes the quantitative and structural analysis relationships (QSAR) of zMAO with *meta* and *para* substituted benzylamines and phenylethylamines. The most intriguing results were obtained with *para*-substituted benzylamine analogues. A known difference in catalytic behavior of human MAO A and MAO B is that the oxidation of *para*-substituted benzylamine analogues exhibit a strong electronic effect in the A form ($\rho=1.8$) but not in the B form. The reaction rates and the binding affinities of 9 *para*-substituted benzylamine analogues with zMAO were determined by steady-state kinetic experiments. $^{\text{D}}k_{\text{cat}}$ kinetic isotope effects with $\alpha,\alpha\text{-[D}_2\text{]}$ benzylamines are similar for each substrate analogue and range in values from 4-8 with $^{\text{D}}k_{\text{cat}}/K_{\text{m}}$ values again ranging from 4-8, demonstrating that $\alpha\text{-C-H}$ bond cleavage is the rate-limiting step in catalysis as found in both human and rat MAOA and B. The *para*-substituent on benzylamine exhibits a strong electronic effect on zMAO k_{cat} values with an observed ρ value of ~ 1.6 . Overall, these data indicate the intermediate functional properties of zMAO between those observed for MAO A and those observed for MAO B, with some properties closer to those of human MAO A. It will therefore be of interest to determine the structural basis of these diverse properties. The information obtained on zMAO should be of interest in drug development studies that use this organism as a model system.

5.2 Reflections and Future Work

The studies presented in this dissertation show that zMAO is a protein with properties of both hMAO A and hMAO B, with some properties closer to hMAO A. These findings emerge new insights on the diversification of human MAO enzymes supporting the view of zMAO indeed being the co-ortholog of human isoforms.

There are numerous reviews on the gene duplication, diversification and specification of enzymes in the literature. Recently, Shelley Copley and colleagues stated that “*evolution of new enzymatic activities is believed to require a period of gene sharing in which a single enzyme must serve both its original function and a new function that has become advantageous to organism*” (McLoughlin S.Y. 2008). In contrast, it was also suggested that a new activity of an enzyme, before gene duplication, is inhibited since the need to maintain the original activity is the primary requirement and through gene duplication the original function is maintained in the in one copy, while the other copy diverges to adopt another function (Ohno 1970; Hughes 1994; Lynch 2004). In this aspect, the critical point is the notion of how/what mutations that enhance a new activity and do not affect the original activity, arise. Given that both zMAO and human MAO isoforms share high sequence identity; one can predict that mutations that gave rise to the second form somehow allowed the ancestor to compromise the original activity which was not eliminated by natural selection. It is feasible to suggest that zMAO exhibits closer functional properties and resembles the ancestor protein more than human isoforms do. Together with the information of zMAO exhibiting promiscuous activities and being closer to hMAO A, as provided in this thesis, we propose that hMAO B is the second form that diverged from the single original ancestor.

Another striking aspect is the shared properties of zMAO to hMAO B in substrate and inhibitor selectivity despite the high active site sequence similarity (~90%) between zMAO and hMAO A. This characteristic, leads to several remarks; first of all, the substrate/inhibitor selectivity of the protein is not completely dependent on the active site sequence identity. This is a remarkable finding on understanding the evolutionary trajectory of similar enzymes to MAO; since the current consensus is that active site mutations are the main dominators in the emergence of new enzymes with new functions. Therefore, for the case of MAO, there might be other parameters in charge, such as several specific structural and mechanistic features that results in new activity without a substantial compromise on the actual protein function. Secondly, the literature mainly shows examples on how new enzymatic activities evolve from a specific to more promiscuous function. In contrast, here, evolution of MAO is shown to be through an opposite direction; a protein with promiscuous activity evolves into more enzymes with more specific activities, while conserving the main original activity. To understand the structural insights of zMAO is crucial and is still under investigation by our lab and by our collaborator, the Andrea Mattevi laboratory at the University of Pavia, Italy. Surely the crystal structure of this protein will be very helpful to understand the structural differences of this ancestor protein. One other way to understand the steps that MAO took its in evolutionary path in depth is to construct the single common ancestor. Advanced phylogeny methods now allow this type of construction (Thorthon 2004; Gaucher 2008) Such study would lead to i) more significant comparison of the properties of ancestor MAO with that of teleosts' and humans' and ii) deeper understanding of the concept of gene duplication in this particular significant enzyme. The significance of

MAO enzymes on human behavior, neurotransmitter regulation and neurodegenerative diseases make these investigations very important. In conclusion, the results presented in this thesis set the framework of new studies on understanding molecular mechanisms, gene duplication, evolution and properties of a novel single enzyme for the first time and are the most important contributions of this dissertation to the field.

5.3 References

- Anichtchik, O., Sallinen, V., Peitsaro, N., Panula, P. (2006). "Distinct structure and activity of monoamine oxidase in the brain of zebrafish (*Danio rerio*)." Journal of Comparative Neurology **498**(5): 593-610.
- Caspi A, M. J., Moffitt T, Mill J, Martin J, Craig I, Taylor A, Poulton R (2002). "Role of genotype in the cycle of violence in maltreated children." Science **297**(5582): 851-4.
- Chen, J. J., Swope, D. M. (2007). "Pharmacotherapy for Parkinson's disease. ." Pharmacotherapy **27**(161-173).
- Chen K., W. H., Grimsby J., Shih JC (1994). "Cloning of a novel monoamine oxidase cDNA from trout liver." Mol. Pharmacol. **46**(6): 1226-33.
- Edmondson, D. E., Binda, C., Wang, J., Upadhyay, A., Mattevi, A. (2009). "Molecular and Mechanistic Properties of the Membrane-Bound Mitochondrial Monoamine Oxidases." Biochemistry **48**(20): 4430-4230.
- Gaucher, E. A., Govindarajan, S., Ganesh O.K (2008). "Palaeotemperature trend for Precambrian life inferred from resurrected proteins." Nature **451**: 704-707.
- Holschneider, D. P., K. Chen, Seif, I., Shih, J.C. (2001). "Biochemical, behavioral, physiologic, and neurodevelopmental changes in mice deficient in monoamine oxidase A or B." Brain Res Bull **56**(5): 453-62.
- Hughes, A. L. (1994). "The evolution of functionally novel proteins after gene duplication." Proc. R. Soc. Lond. B.: 1190124.
- Li, M., F. Hubalek, Newton-Vinson, P., Edmondson, D.E. (2002). "High-level expression of human liver monoamine oxidase A in *Pichia pastoris*: comparison with the enzyme expressed in *Saccharomyces cerevisiae*." Protein Expr Purif **24**(1): 152-62.

- Lynch, M., Katju, V. (2004). "The altered evolutionary trajectories of gene duplicates." Trends Genet **20**(544-549).
- Mc Dermott Rose, T. D., Cowden, J., Frazzetto G., Johnson D.P. (2009). "Monoamine oxidase A gene (MAOA) predicts behavioral aggression following provocation." Proc Natl Acad Sci U S A **106**(7): 2118-2123.
- McLoughlin S.Y., Copley, S.D. (2008). "A compromise required by gene sharing enables survival: Implications for evolution of new enzyme activities" Proc Natl Acad Sci U S A **105**(36): 13497-13502.
- Natalie Weder, B. Z. Y., Heather Douglas-Palumberi, Johari Massey, John H Krystal, Joel Gelernter, Joan Kaufman (2009). "MAOA Genotype, Maltreatment, and Aggressive Behavior: The Changing Impact of Genotype at Varying Levels of Trauma." Biol Psychiat **65**(5): 417-42.
- Newton-Vinson, P., F. Hubalek, Edmondson, D.E. (2000). "High-level expression of human liver monoamine oxidase B in *Pichia pastoris*." Protein Expr Purif **20**(2): 334-45.
- Ohno, S. (1970). Evolution by Gene Duplication. New York, Springer.
- Setini, A., F. Pierucci, et al. (2005). "Molecular characterization of monoamine oxidase in zebrafish (*Danio rerio*)." Comparative Biochemistry and Physiology B-Biochemistry & Molecular Biology **140**(1): 153-161.
- Shih, J. C., K. Chen, Ridd, M.J. (1999). "Monoamine oxidase: from genes to behavior." Annu Rev Neurosci **22**: 197-217.
- Stanhope, M., Andrei, Lupas, Michael J. Italia, Kristin K. Koretke, Craig Volker, James R. Brown (2001). "Phylogenetic analyses do not support horizontal gene transfers from bacteria to vertebrates." Science **2001**: 940-944.
- Thorthon, J. W. (2004). "Resurrecting ancient genes: experimental analysis of extinct molecules." Nat. Rev. Genet. **5**: 366-375.

Upadhyay, A. K., J. Wang, Edmondson, D.E. (2008). "Comparison of the structural properties of the active site cavities of human and rat monoamine oxidase a and B in their soluble and membrane-bound forms." Biochemistry **47**(2): 526-536.

Youdim, M. B. H., D. Edmondson, Tipton, K. (2006). "The therapeutic potential of monoamine oxidase inhibitors." Nature Reviews Neuroscience **7**(4): 295-309.